Neuro-robotic interfaces

Silvestro Micera

Natural control of movement

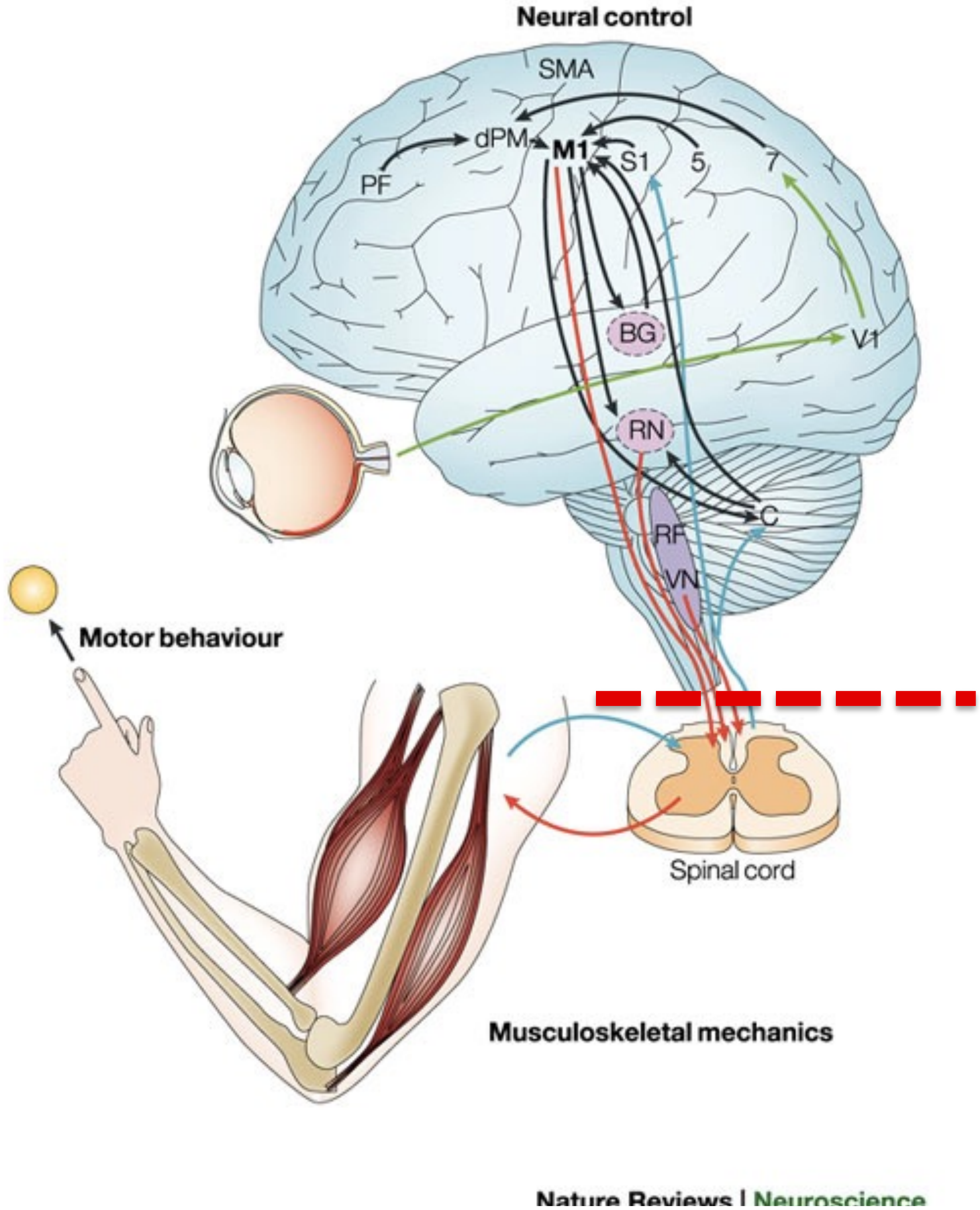

A spinal cord injury creates a GAP between brain commands and muscle movement generation

Brain to machine interfaces (BMIs)

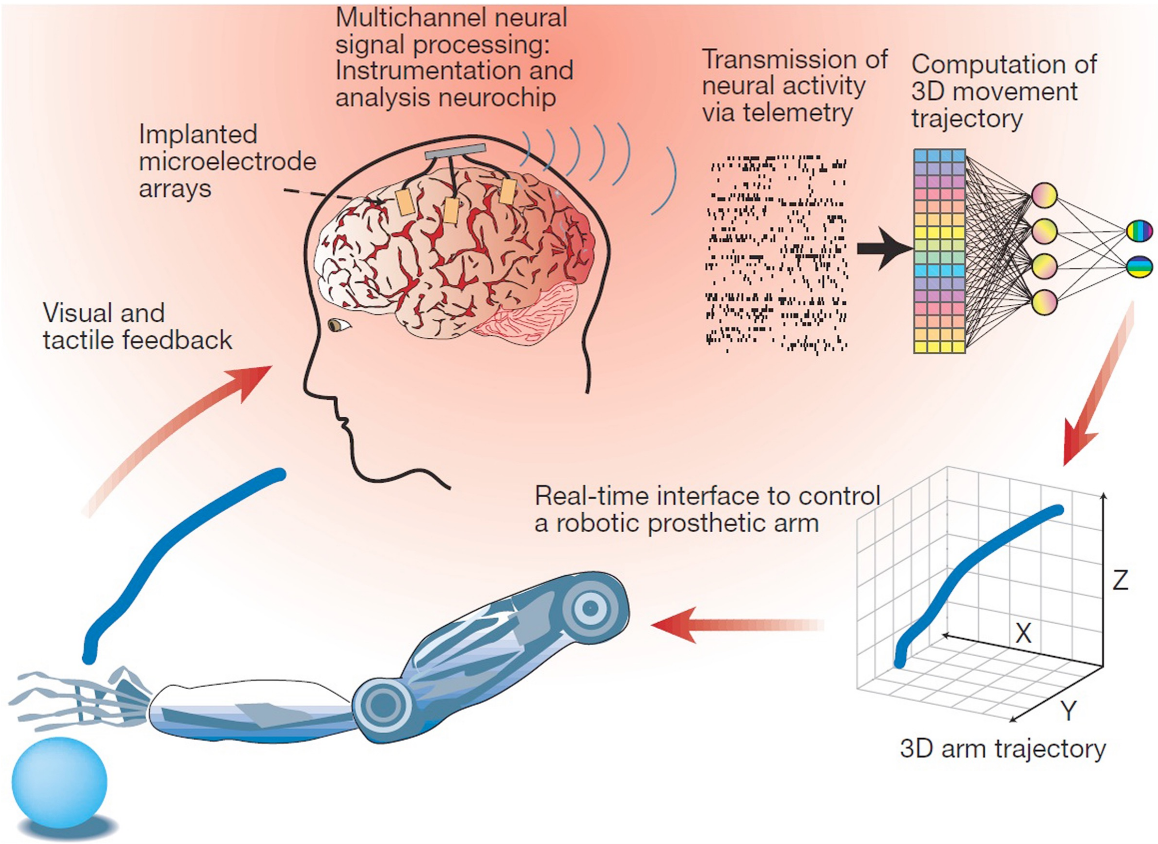

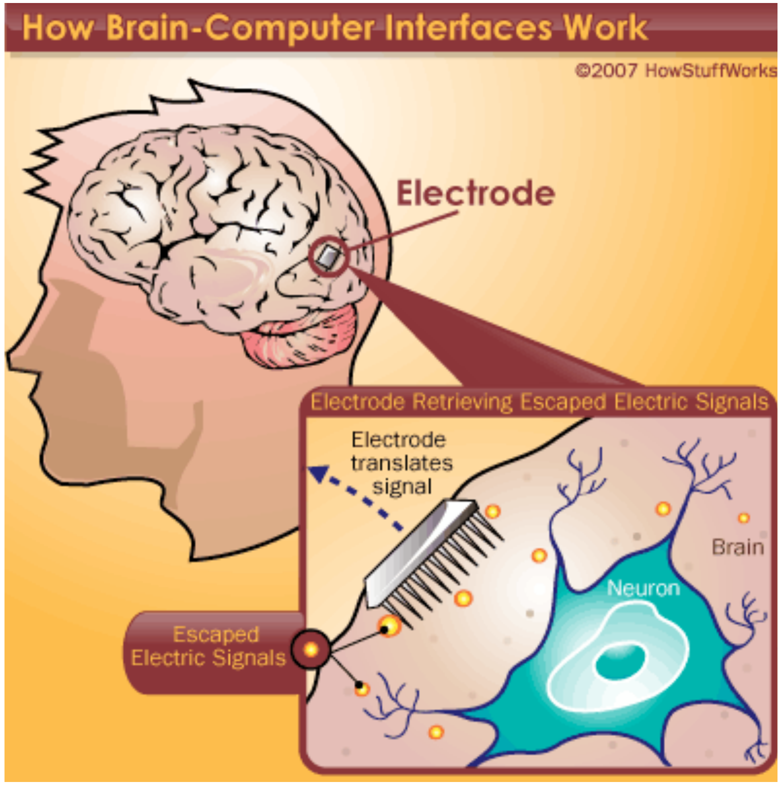

Sensing the Brain

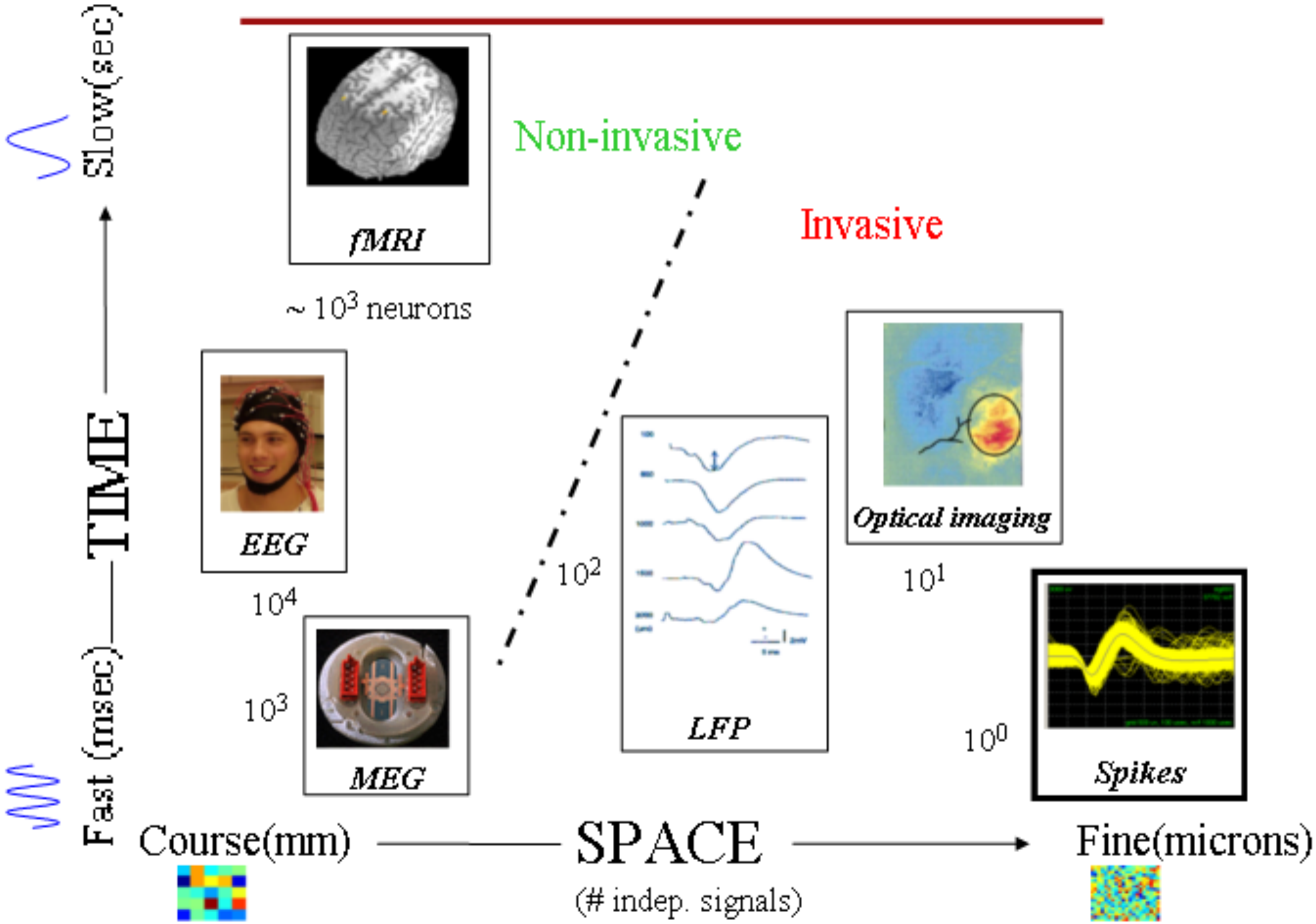

Sensing technologies that can be used to observe neural activity, divided by non-invasive vs. invasive, spatial and temporal resolution.

Neural Signals - ECoG

- Electrical activity on the surface of the brain resulting from volume conduction of coherent collective neural activity through the brain
- Recorded via surface (disk) electrodes
- Amplitude as high as 5 mV and frequency content up to 200 Hz

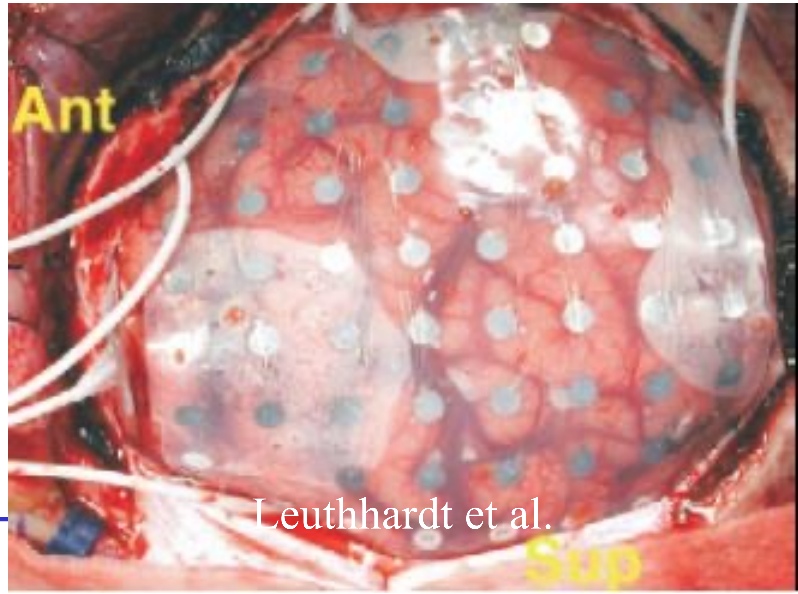

Leuthhardt et al.

Neural Signals - LFP

- Summation of pre and postsynaptic activities from a population of neurons around the electrode tip
- Recorded via microelectrodes or lower impedance electrodes
- Amplitude as high as 1 mV and frequency content up to 200 Hz

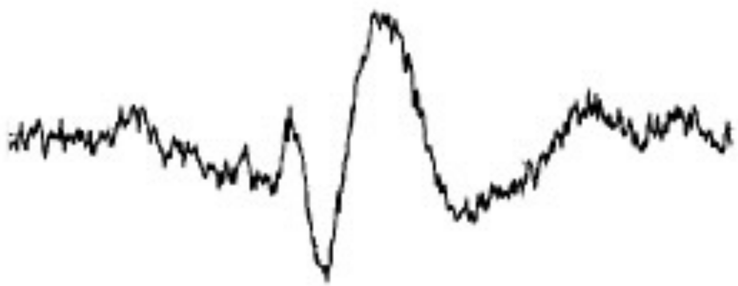

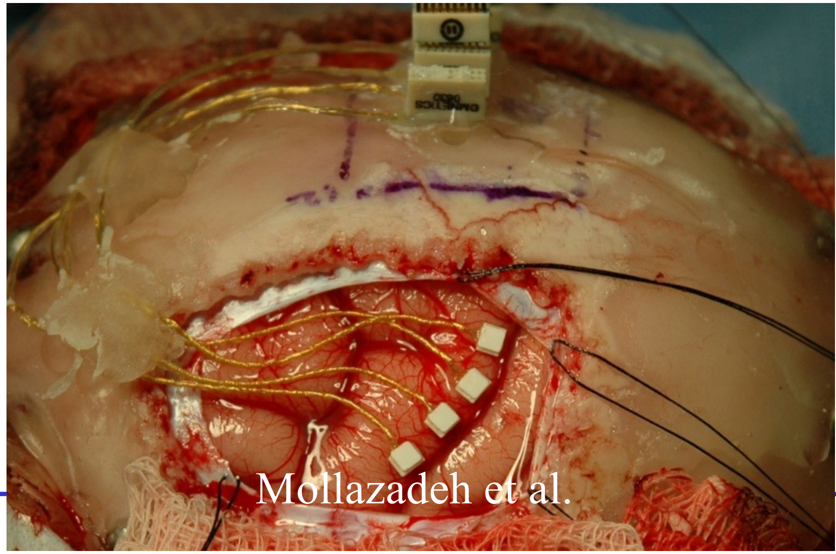

Mollazadeh et al.

Neural Signals - Spike

- Single unit firings
- Recorded via microelectrodes placed close to the neuron cell body
- Amplitude as high as 500 μV and frequency content up to 7 kHz

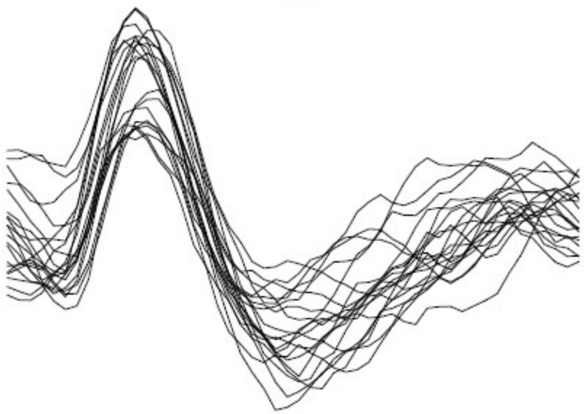

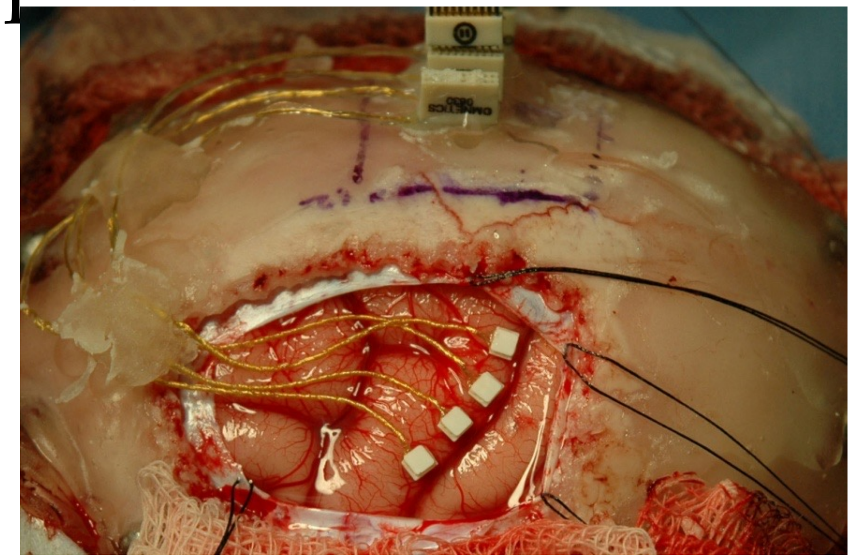

Pre-motor and motor area of the cortex

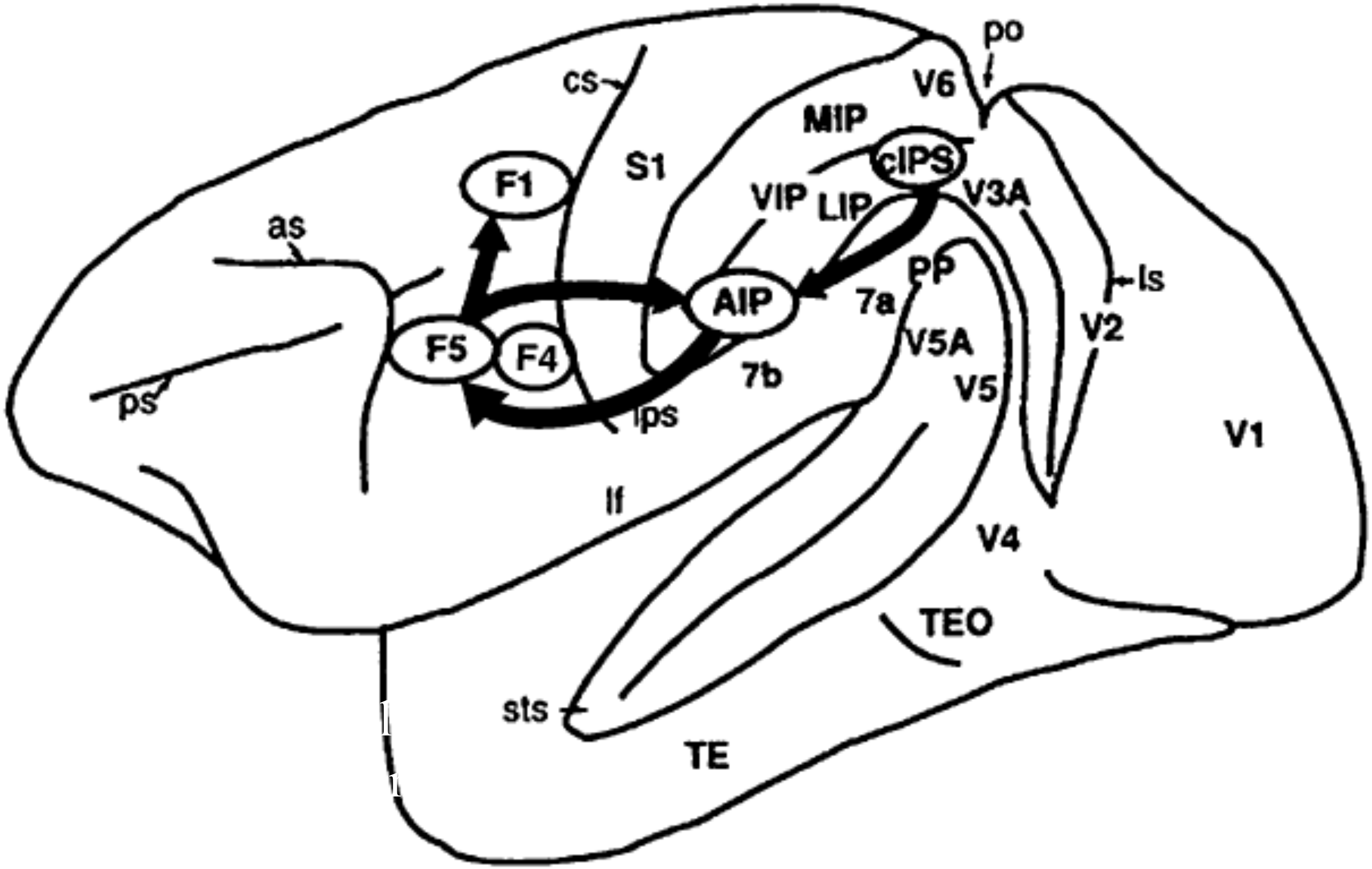

Extraction of 2D movements from M1

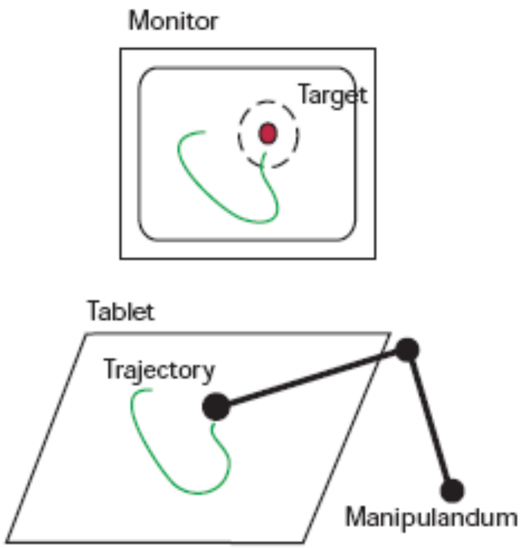

Extraction of 2D movements from M1

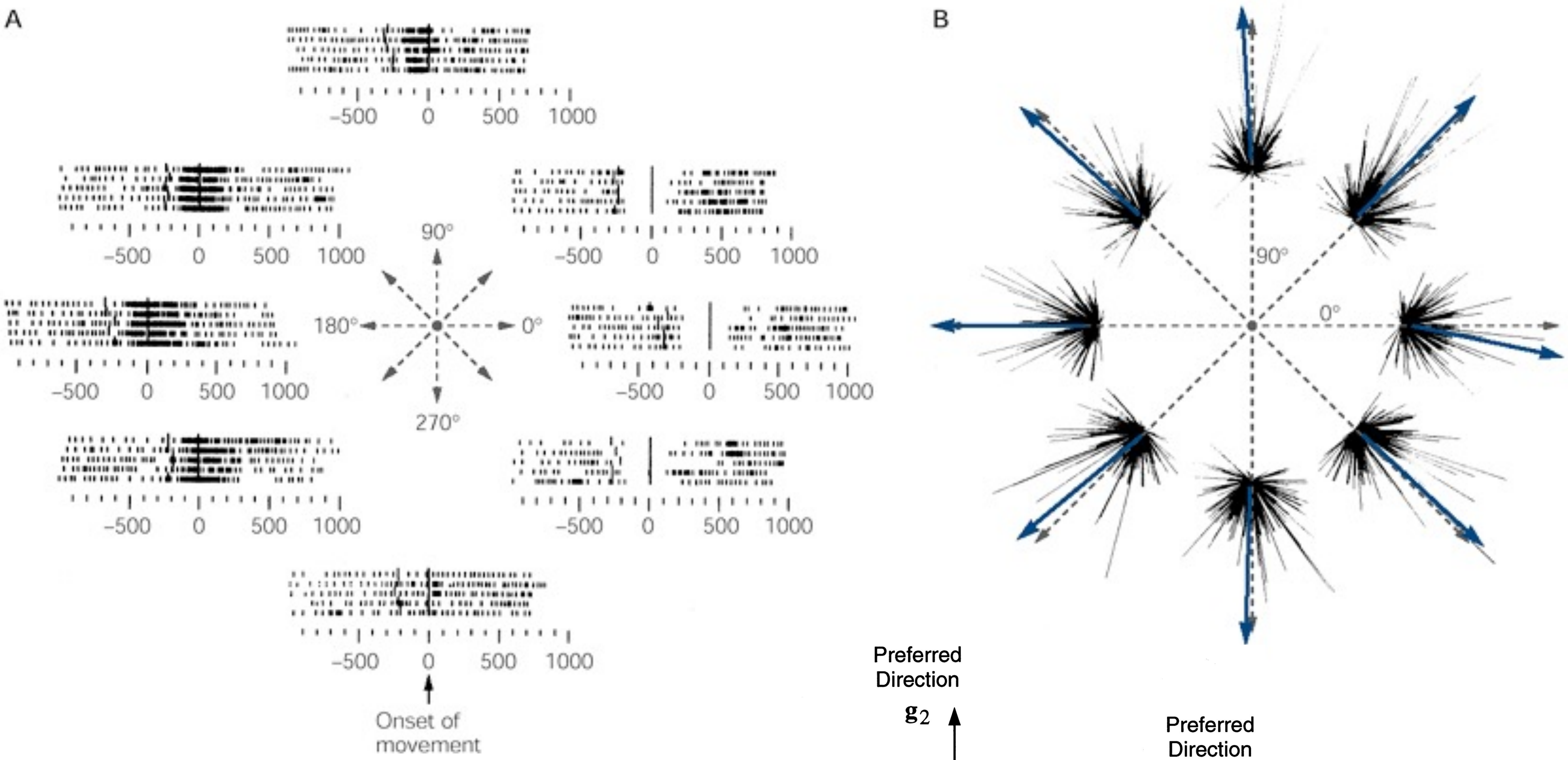

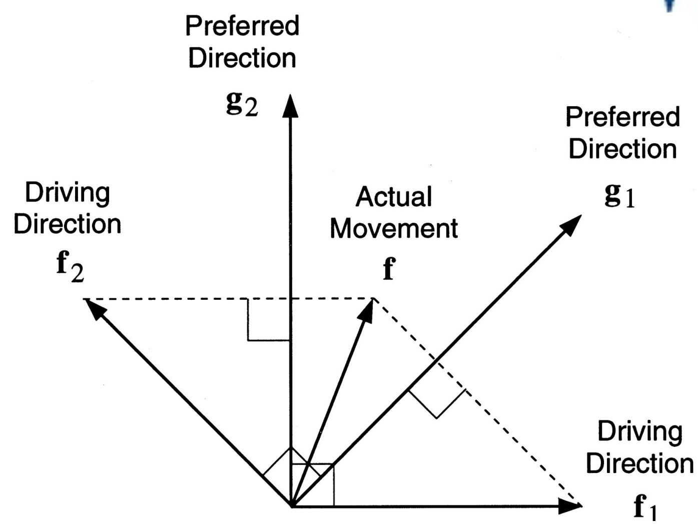

Extraction of movements from M1

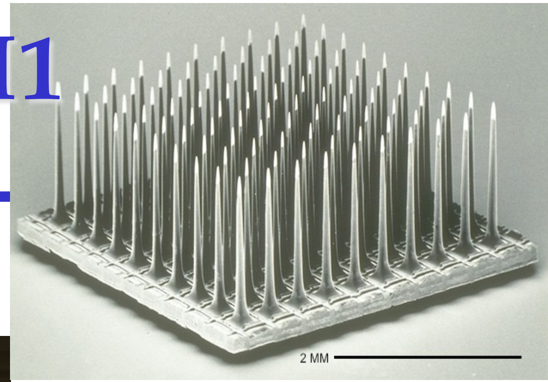

Utah Array, Cyberkinetics LTD

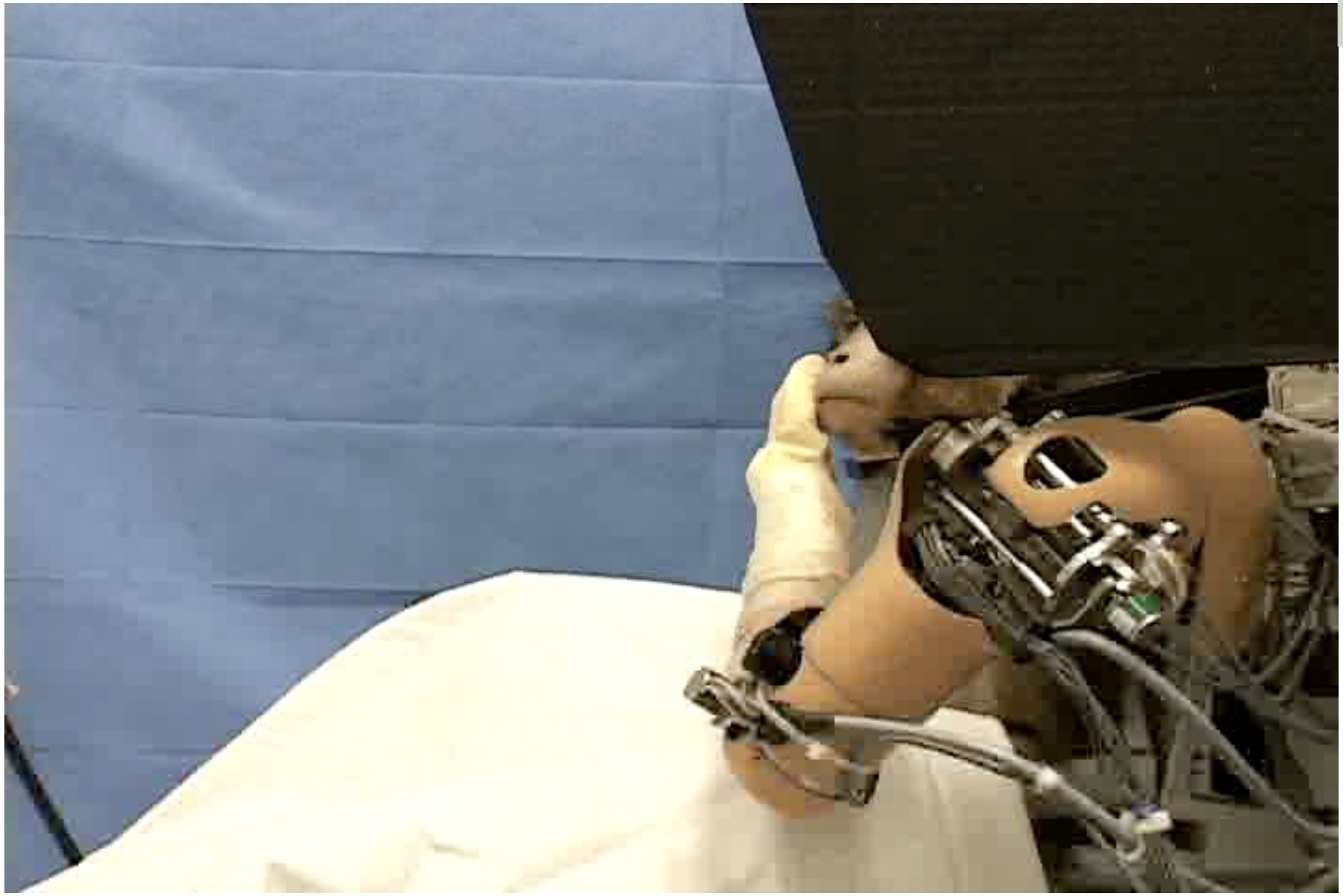

Schwartz and colleagues

Cortical control of robotic systems

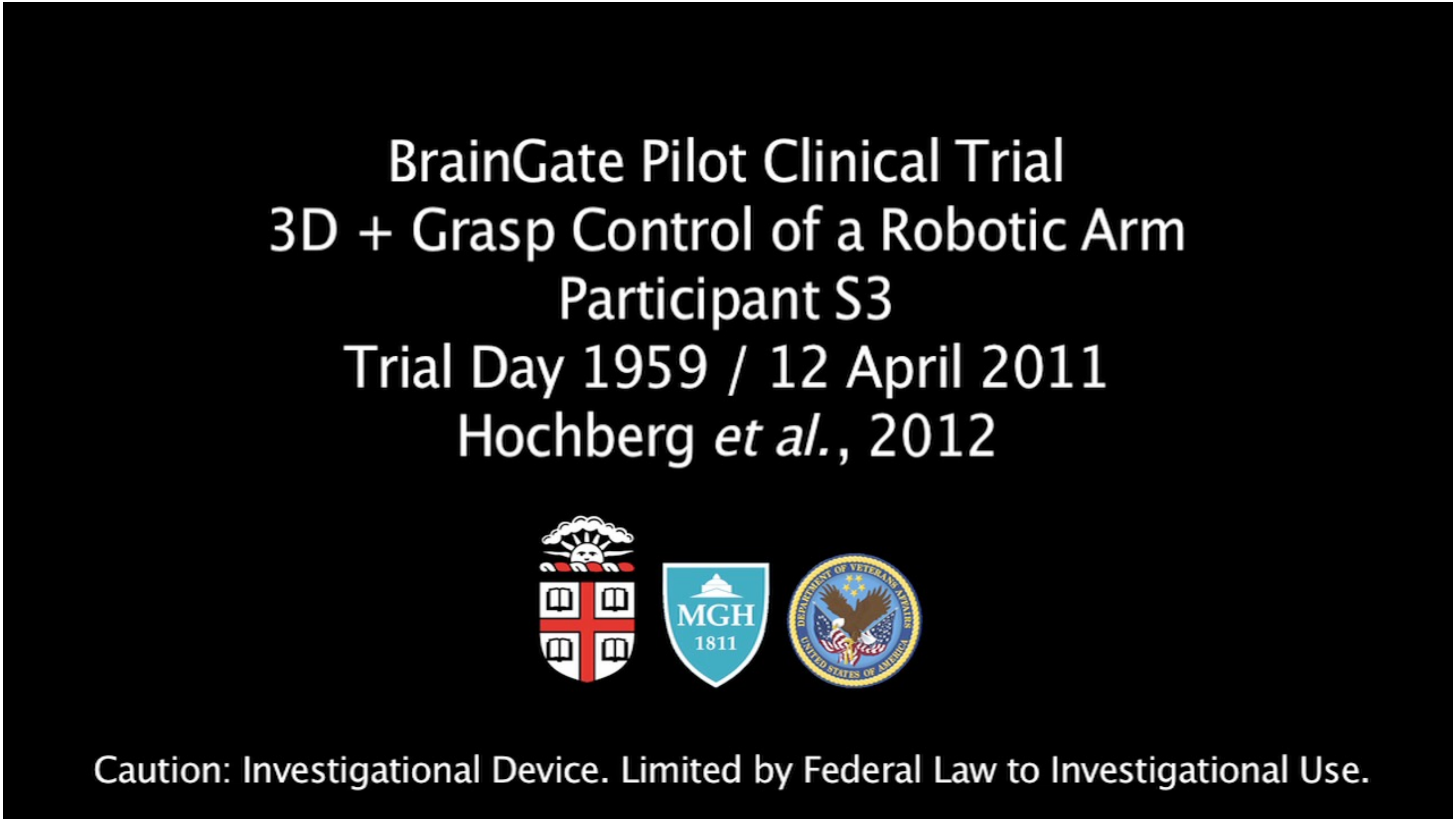

High-level CNP

- Recordings were made at points along a major pathway for visually guided movement which begins in the extrastriate visual cortex and passes through the parietal reach region (PRR) and area 5 to the dorsal premotor cortex (PMd) and then to the primary motor cortex
- Although PRR is specialized for reaching movements, it represents the goals of the reach in visual coordinates

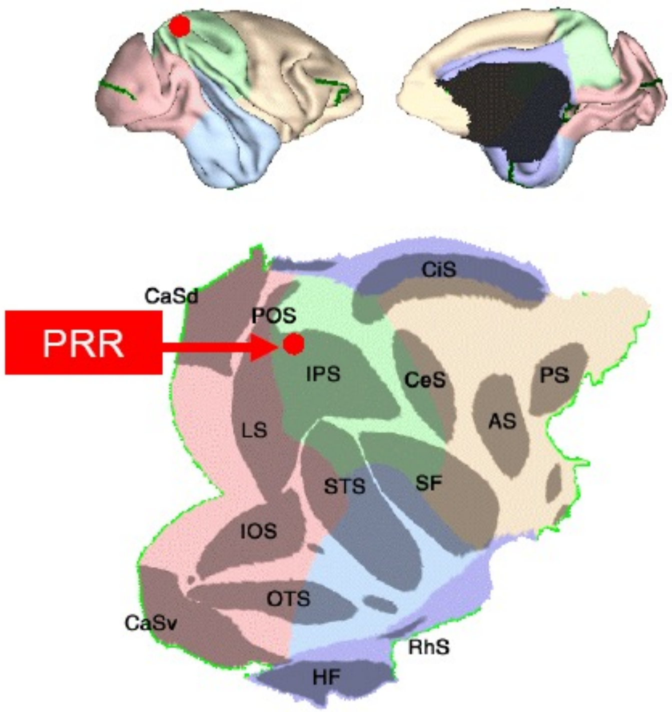

D. Van Essen, H. Drury (1998)

High-level CNP

Estimating the Planned Reach Direction

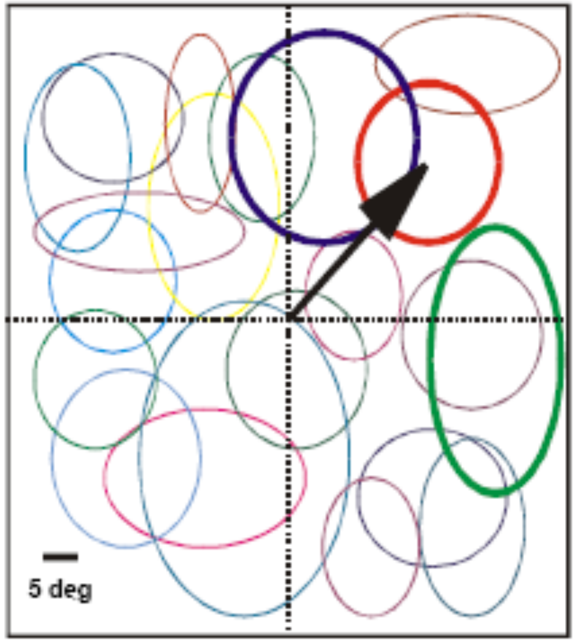

PRR receptive fields span workspace.

Complete set of reaches: P(n|x)

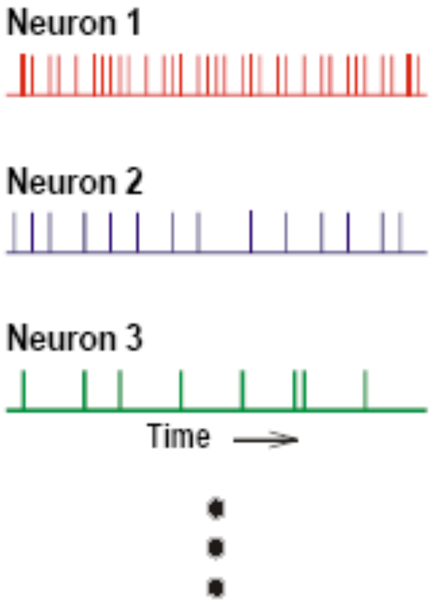

For any given reach...

... measure spike trains: n

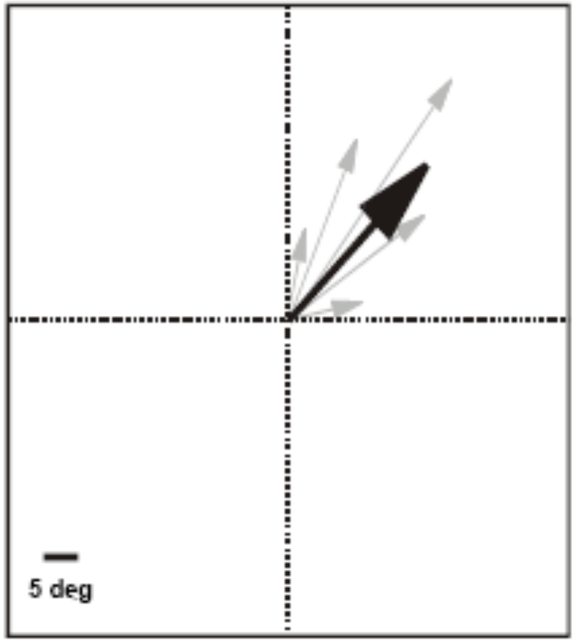

Calculate probability of all reaches:

P(x|n) P(n) = P(n|x) P(x)

Select most probable: max (P(x|n))

High-level CNP

Potential Advantages of PRR Neurons for Prosthetic Systems

PRR neurons encode:

- The plan to reach to a target
- The plan for the upcoming reach
- The plan with respect to the eyes

PRR neurons may:

- not encode muscle forces
- reorganize little following injury
- adapt quickly to calibrate the system

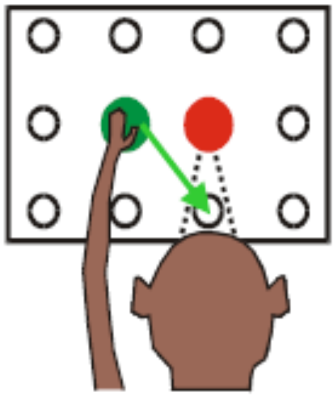

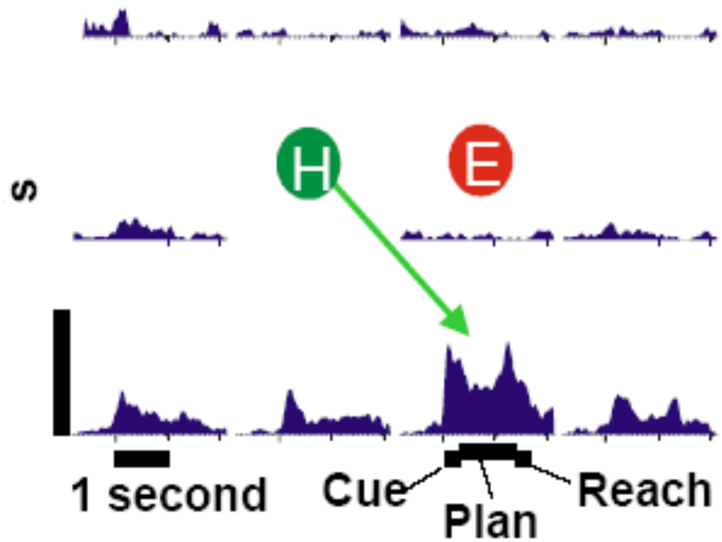

Batista, Buneo, Snyder, Andersen (1999) *Science* 285.

High-level CNP

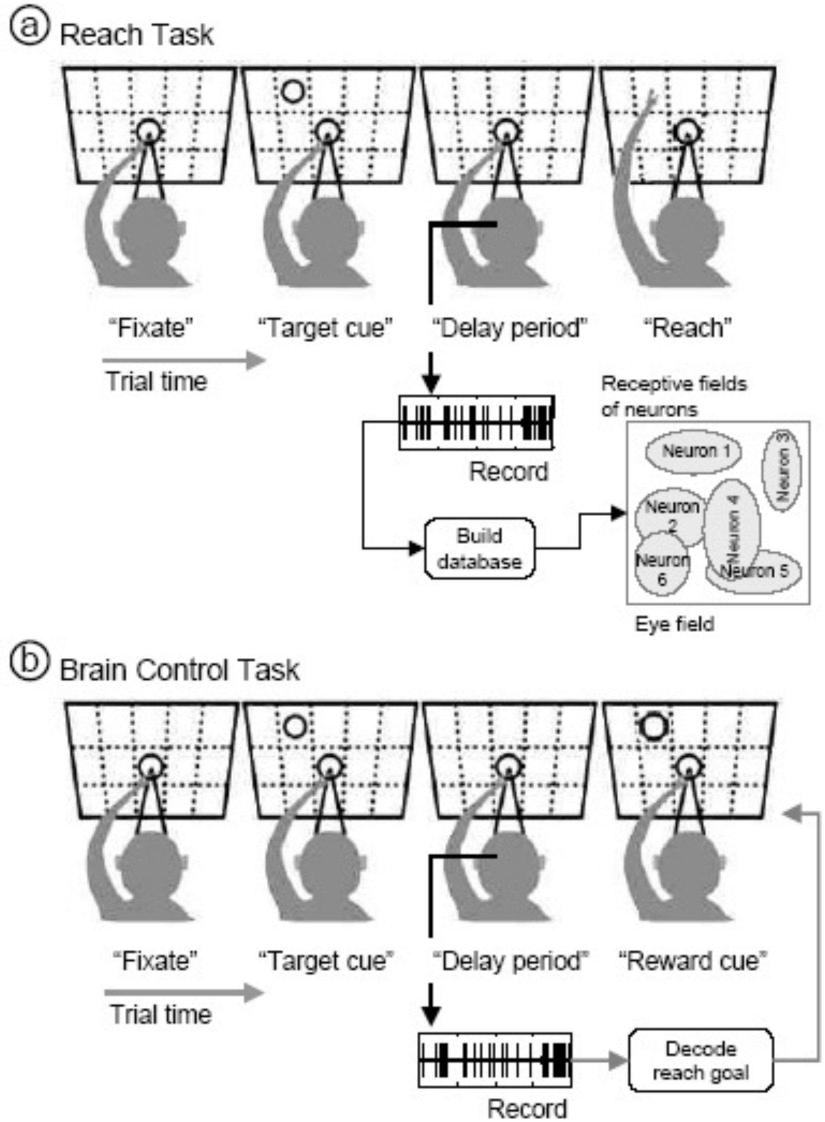

High-level CNP

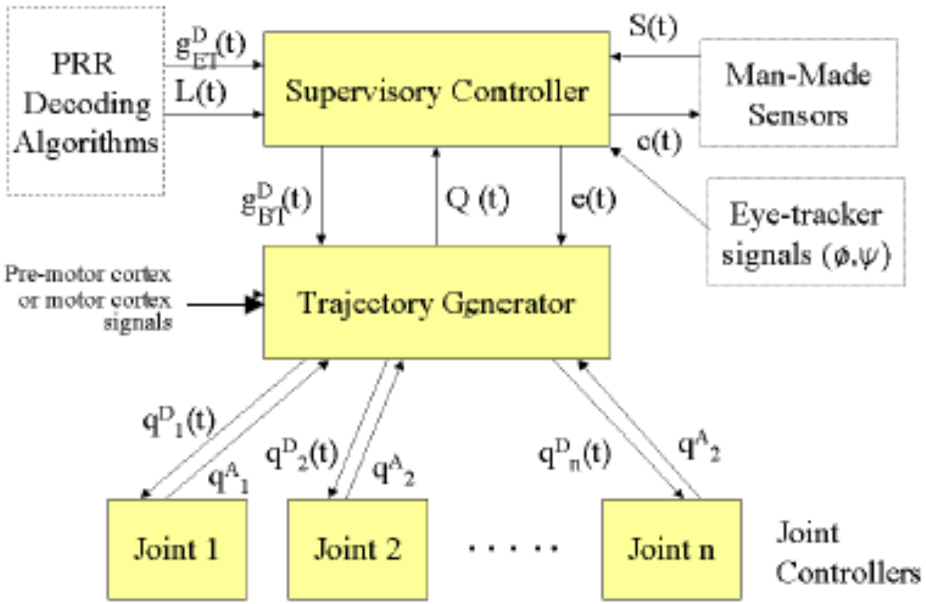

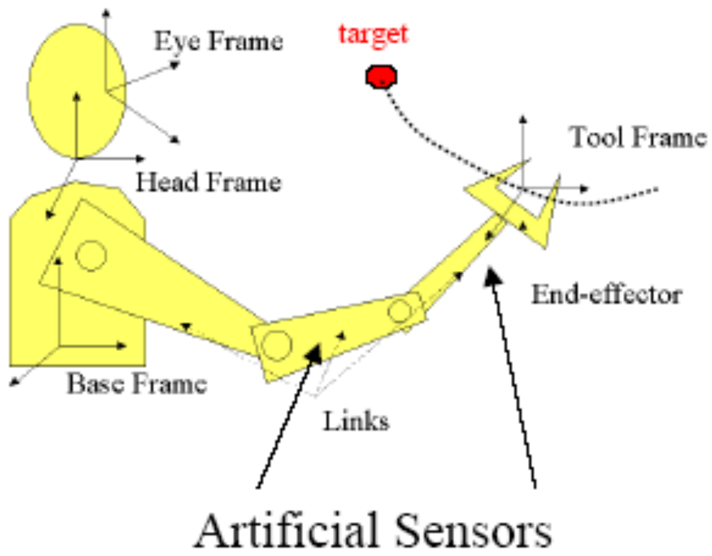

Key variables

- intended reach location
- intentional and cognitive mind state
- external sensor variables

Voluntary control of grasping after cervical spinal cord injury

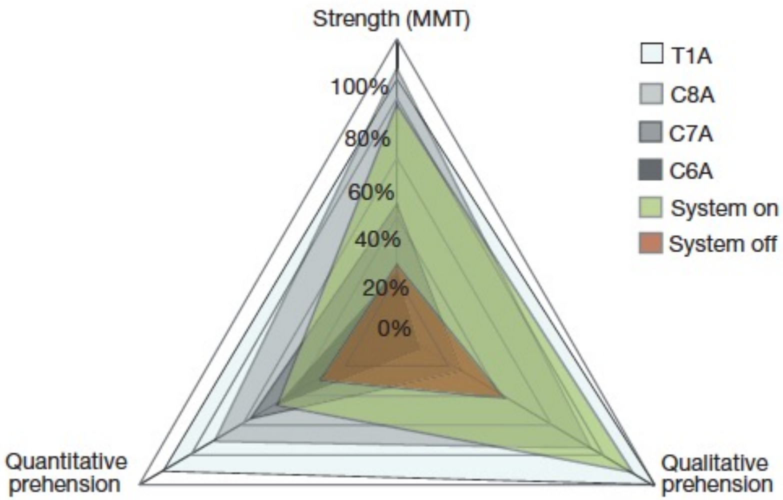

Restoring cortical control of functional movement in a human with quadriplegia

Chad E. Bouton[1]†, Ammar Shaikhouni[2,3], Nicholas V. Annetta[1], Marcia A. Bockbrader[2,4], David A. Friedenberg[5], Dylan M. Nielson[2,3], Gaurav Sharma[1], Per B. Sederberg[2,6], Bradley C. Glenn[7], W. Jerry Mysiw[2,4], Austin G. Morgan[1], Milind Deogaonkar[2,3] & Ali R. Rezai[2,3]

Brain-to-machine-to-brain interface

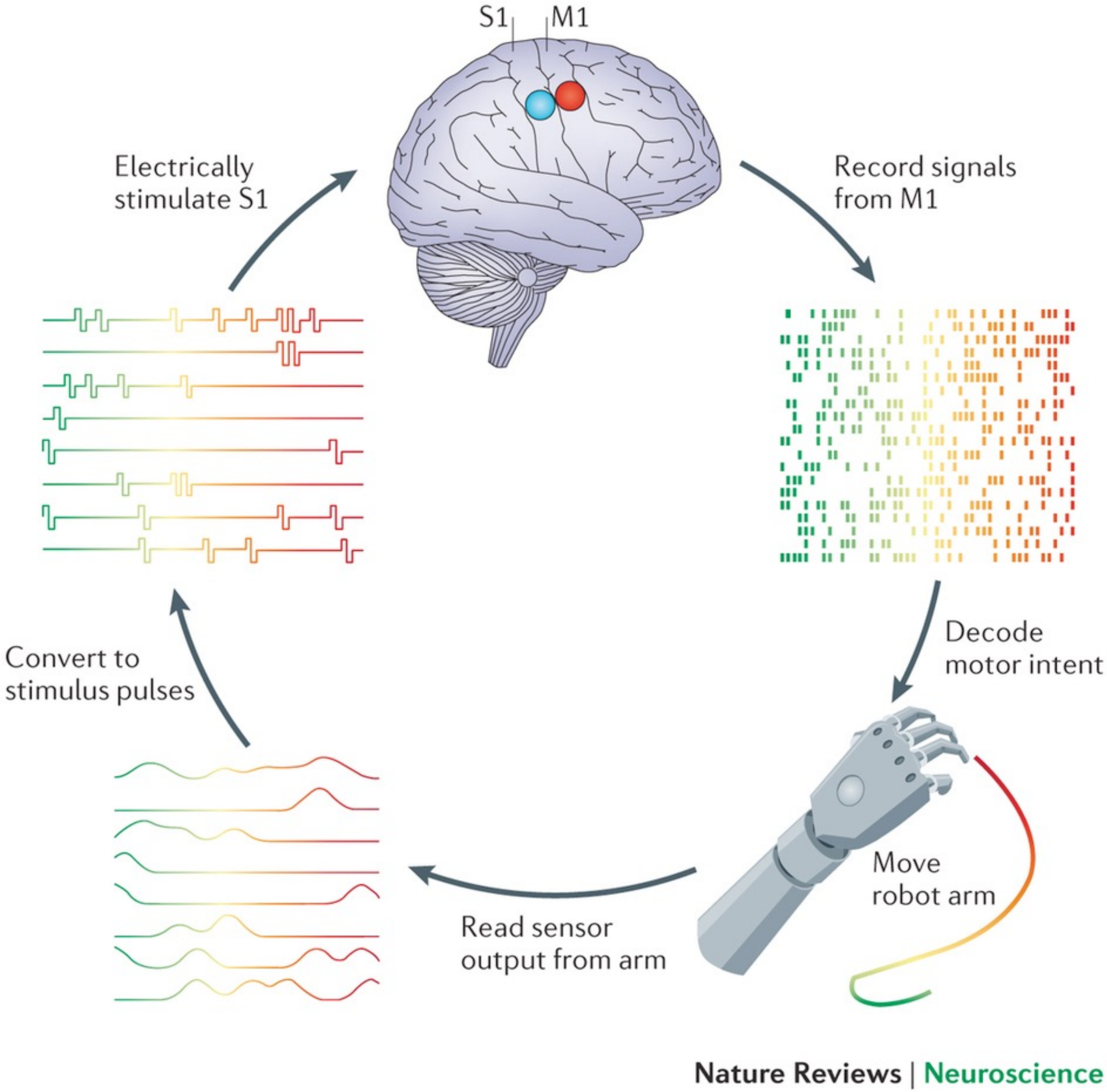

Intracortical sensory feedback

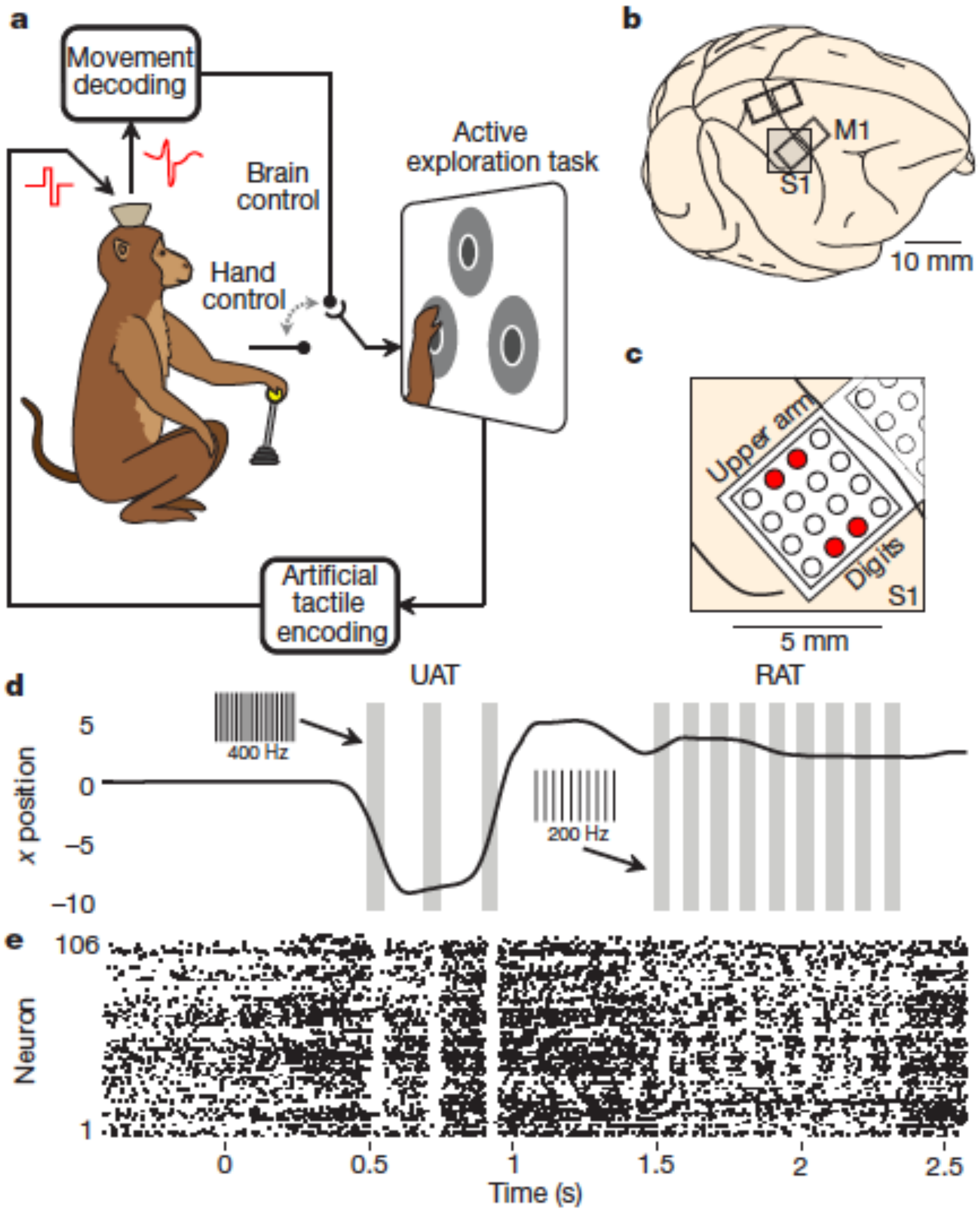

Intracortical sensory feedback is possible but the performance are still limited

O'Doherty et al., 2011

Brain-to-machine-to-brain interface in a quadriplegic subject

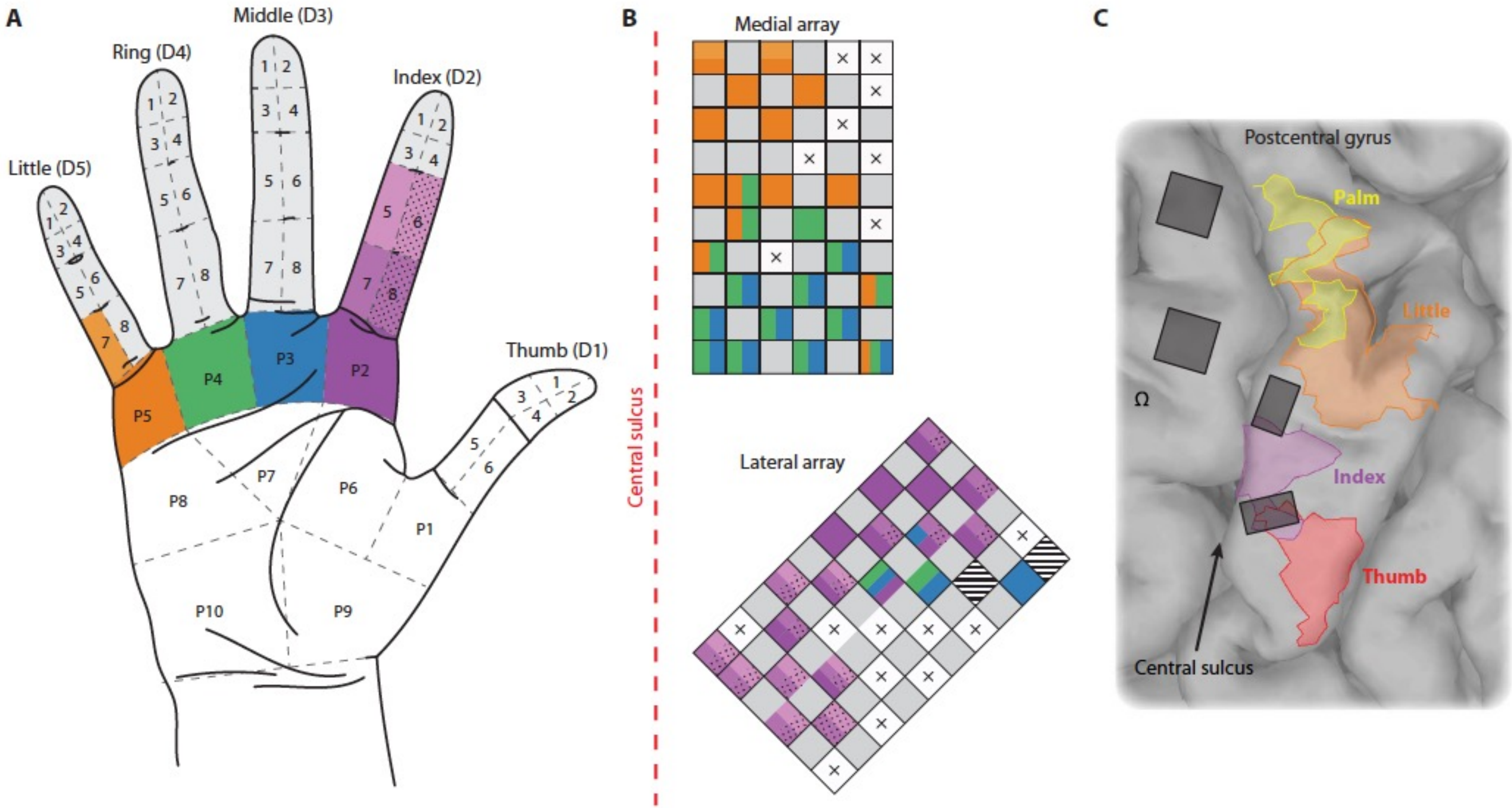

Brain-to-machine-to-brain interface in a quadriplegic subject

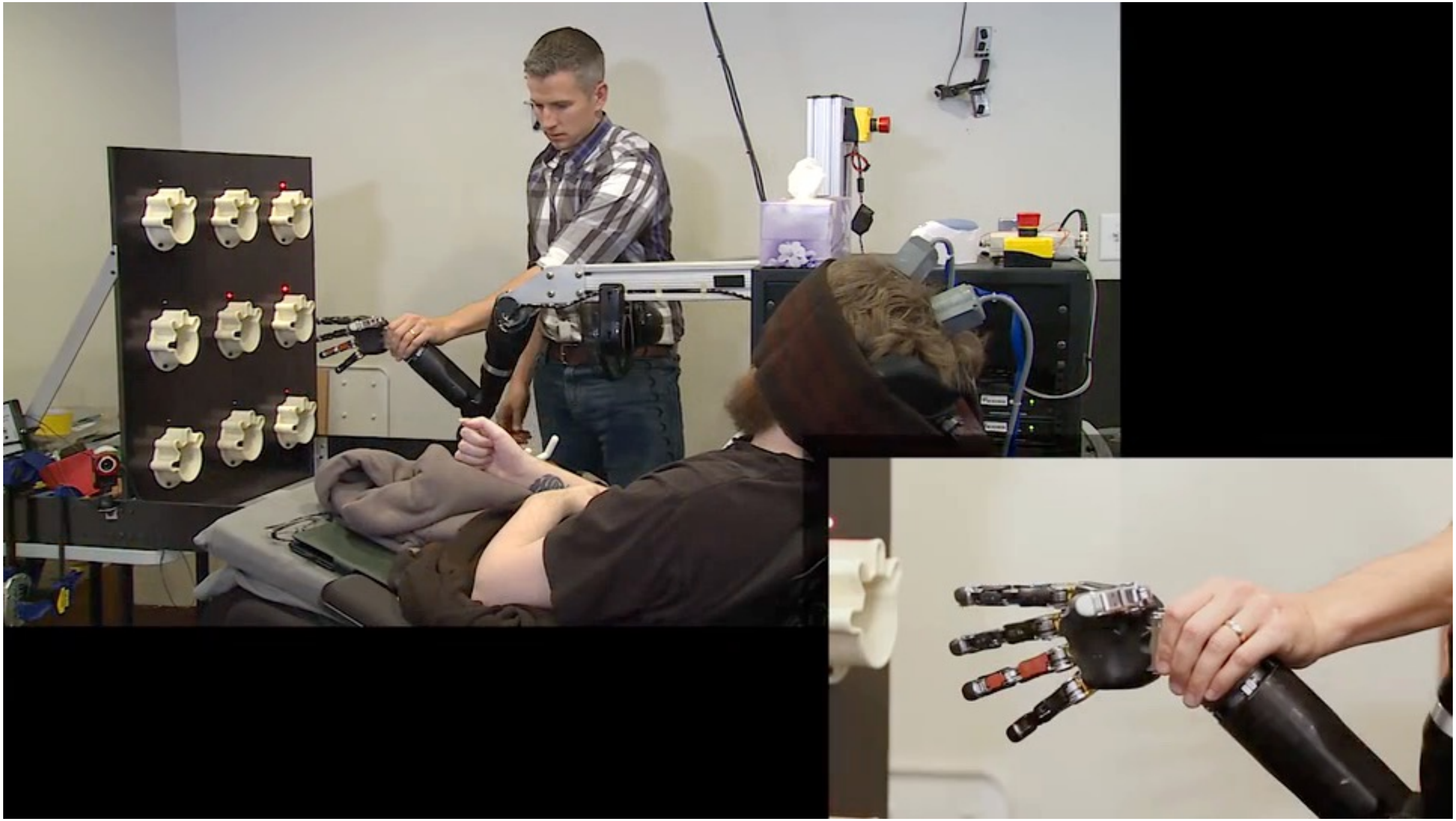

Hand prosthesese - Motivation

The loss of the upper limb is a traumatic event that changes the **quality of life** radically

Reduction of

- Ability in **reaching, grasping and manipulation**
- Ability in **sensing** through the sense of touch
- **Gesture** (communication)

Statistics

38% Transhumeral

31% Transradial

14% Partial hand

5% Fingers

…

…

1.7 million total number of amputees living in the U.S

65,000 upper limb amputations in the U.S. each year

27,000 hand amputation below the wrist in the U.S. each year

400 hand amputation below the wrist in Italy each year

Consequences

Few innovations in the past 50 years

Actual prostheses **do not satisfy** amputees' requirements and are very different from the natural model

What can an amputee get today?

Hand Prosthesis

- Prosthetic Hands
  - Passive
    - Cosmetic
  - Active
    - Body-powered
    - Myoelectric

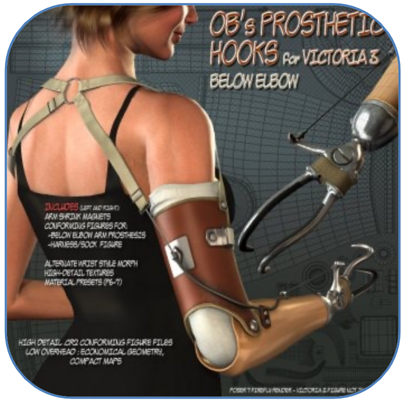

Mechatronic
Design issues: adaptability

Problem: It's an hard task to **design, actuate, and control** a self-contained artificial hand with a number of degrees of freedom (DoF) equal or close to those in the biological human hand!

22 muscles … + 18

Adaptation also improves **grasp stability** as it increases the **contact areas** while grasping

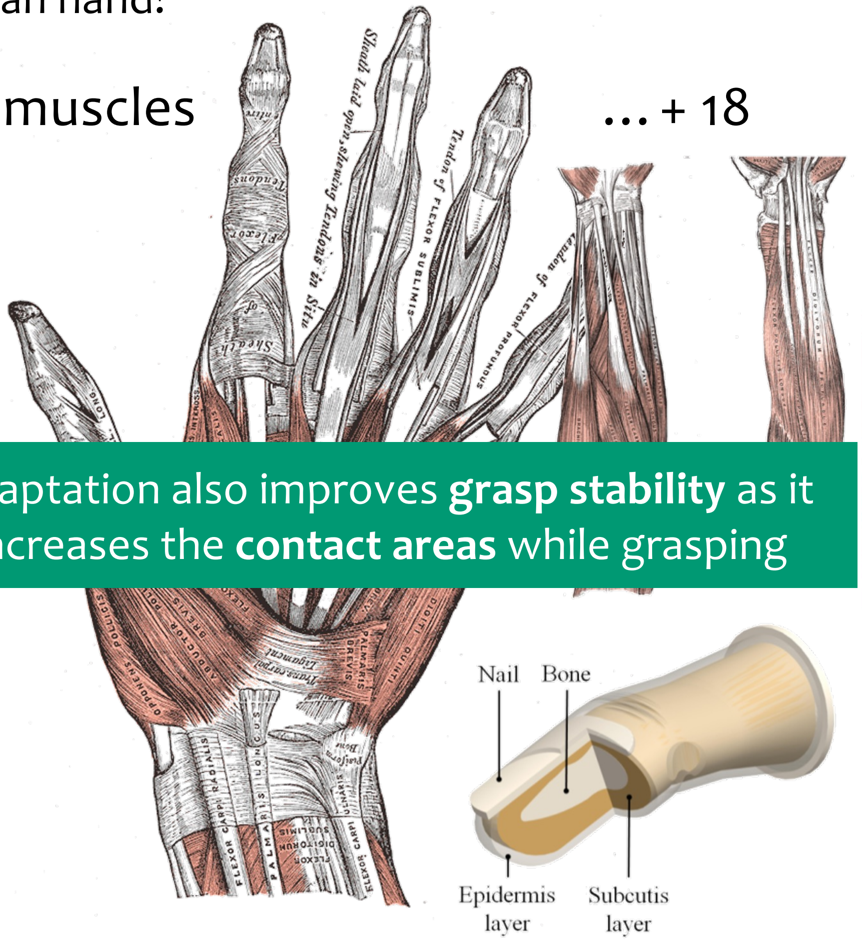

Phalanx adaptation mechanisms

Possible solutions (to simplify the problem):

- Cut DoFs; Rigidly couple DoFs;
- Implement adaptable mechanisms.

Hand adaptation mechanisms

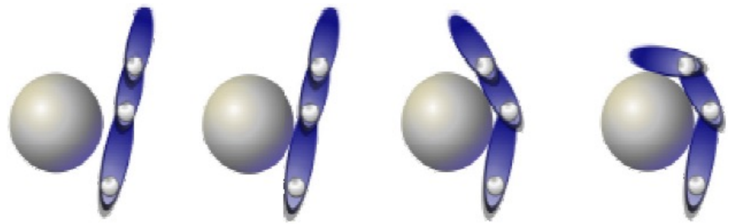

Finger adaptation mechanisms

Underactuated mechanisms

Mechatronic
Design issues: non back drivability

Mechanisms wherein motions generated by the input (motor) drive are transmitted to the output (i.e. fingers) and wherein motions originated from the output are blocked

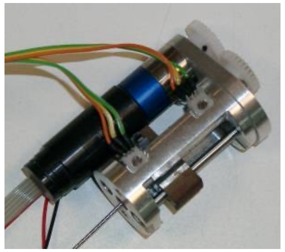

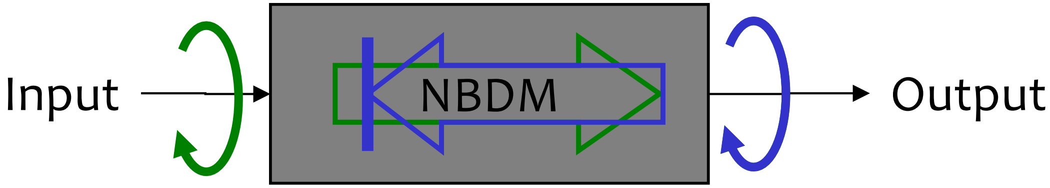

In a prosthesis it allows to maintain the grasp once the power supply is switched off

Non back drivable transmission = Power saving!= key in prosthetics!

Lead Screw

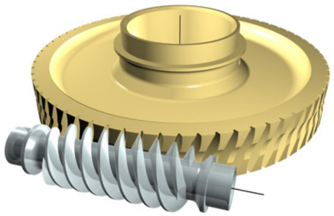

Worm Gear

Gear heads with high reduction rate

Brakes/ clutches

Case Study

The SmartHand prototype

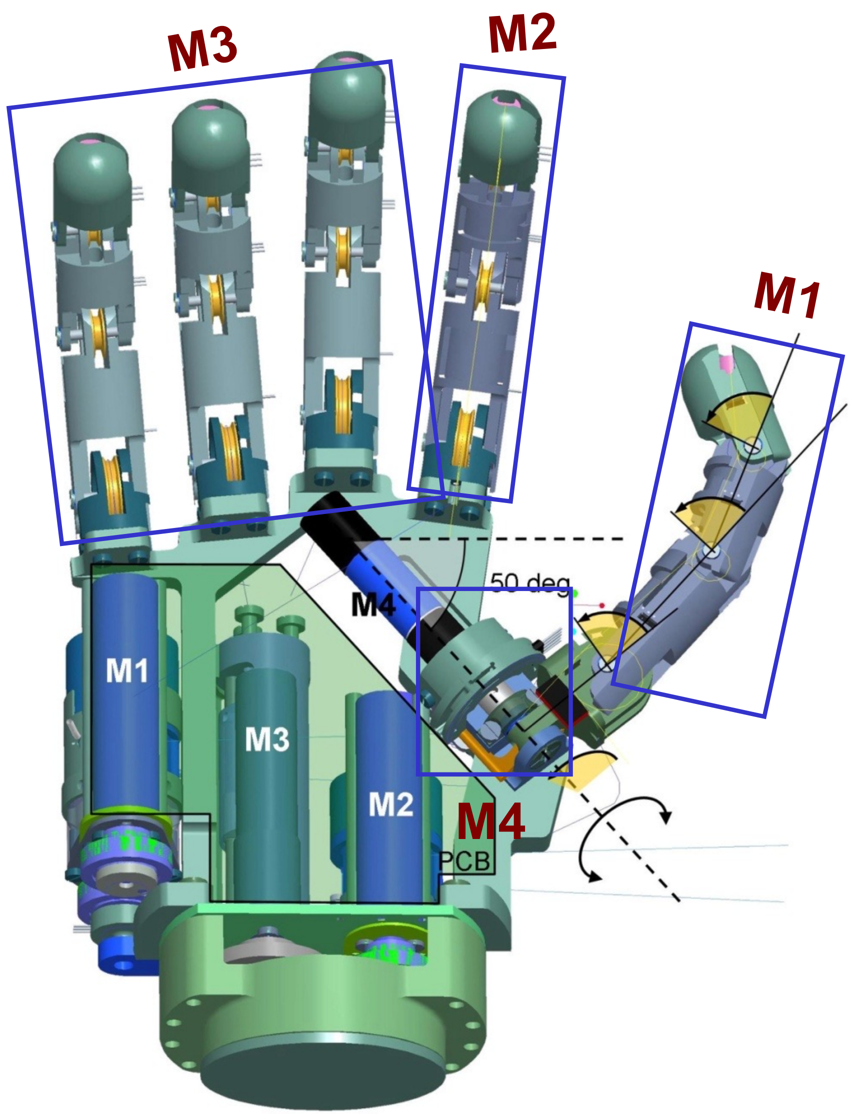

The SmartHand at glance

Mechanical Spec

Weight	600 gr
Size	Human inspired
Degrees of freedom	16
Degrees of actuation	4
Full flexion speed	<1.5 s
Tendon max active force	45 N
Grasp force (Cyl, Lat, Lift)	<30,<5,100 N

Sensory System

Position (digital encoder)	4
Position (Joint Hall sensors)	15
Position (Potentiometer)	2
Tension Sensors (strain gauges)	5
Limit switch (digital)	8

Electrical Spec

Power req.	12V /3A
Control loops	Position and tension (1 kHz)
Reading delays	< 1 ms
Total preset grasps	10 (programmable)
Communication	RS232 / USB

Case Study

The OpenHand prototype

Human finger-tips play a fundamental role during the action of fine manipulation and precision grasping of objects

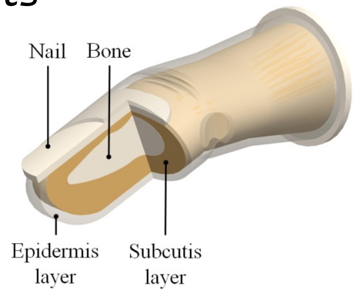

Multi-layers structure with different proprieties:

- Epidermis and subcutis layers - **Compliant materials**
- Nail and inner bone - **Stiff materials**

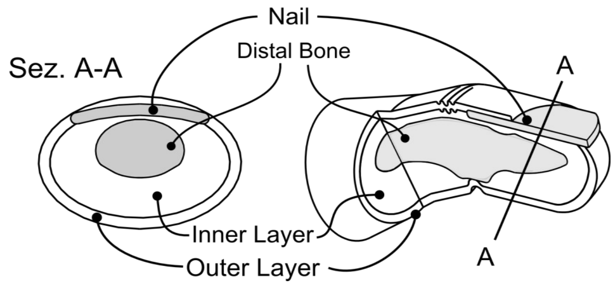

Non-linear & time-dependent characteristic:

- Low forces – Large displacements (**Compliant behavior**)
- High forces – Small displacements (**Stiff behavior**)
- Energy dissipation (**Visco-elastic behavior**)

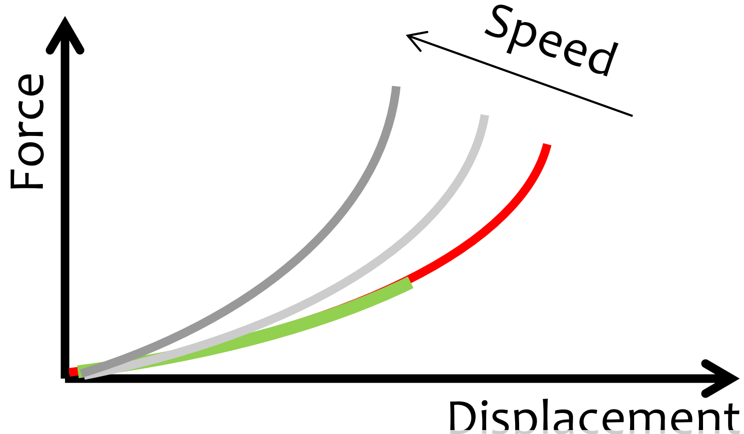

Benefits of grasping and manipulation:

- Conformability;
- Large contact areas;
- Energy dissipation;

1. M. Controzzi, M. D'Alonzo, C. Peccia, C. Cipriani Design, simulation and development of a human inspired fingertip for robotic hand, to be submitted to the Journal o Bioispiration and Biomimetics
2. M. Controzzi, C. Cipriani, M. D'Alonzo, C. Peccia and M. C. Carrozza Design of an Anthropomorphic Robotic Hand with Intrinsic Actuation and Compliant Fingers, GNB 2012, Rome, Italy, June, 2012.
3. M. D'Alonzo, M. Controzzi, C. Peccia, C. Cipriani and M C. Carrozza. ``Design of biomimetic artificial fingertips and analysis of stiffness at the contact,'' GNB 2012, Rome, Italy, June, 2012.

Hand prosthesis – Proportional control

- N antagonist muscles are used to control 1 degree of freedom of the prosthesis (hand opening/closing). Often biceps/triceps or wrist extension/flexion
- An increased number of required movements makes very difficult to use this approach

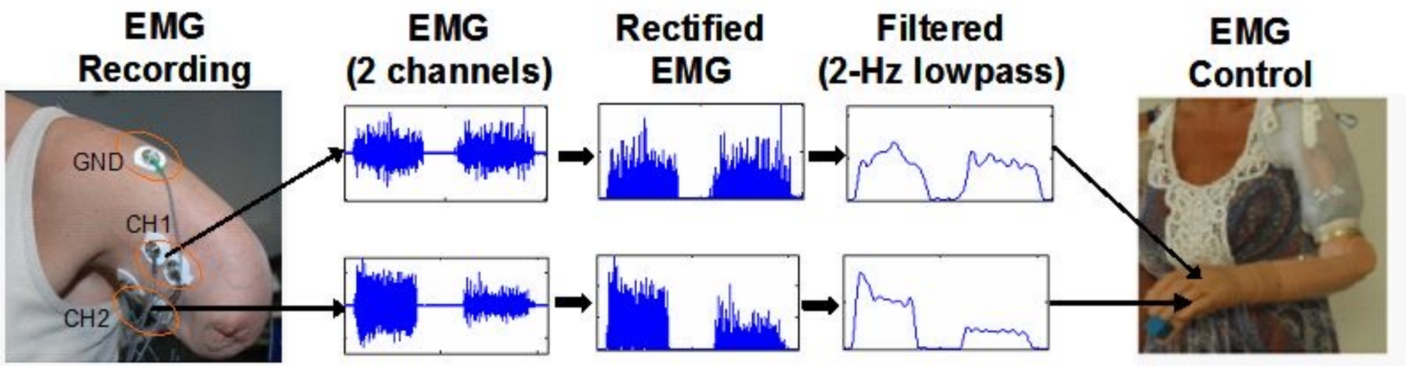

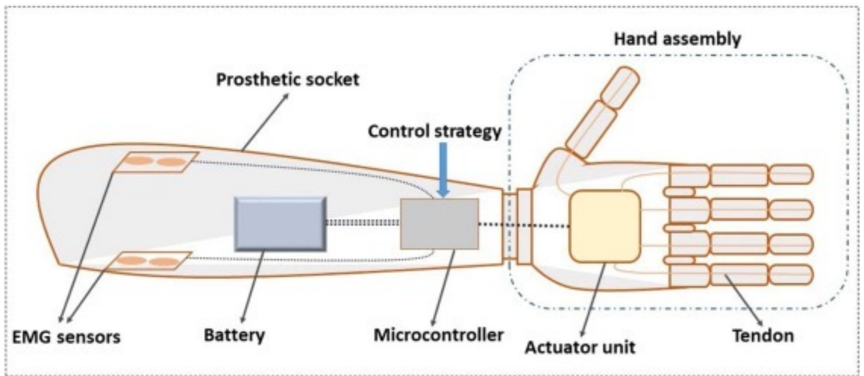

Hand prosthesis – Pattern recognition

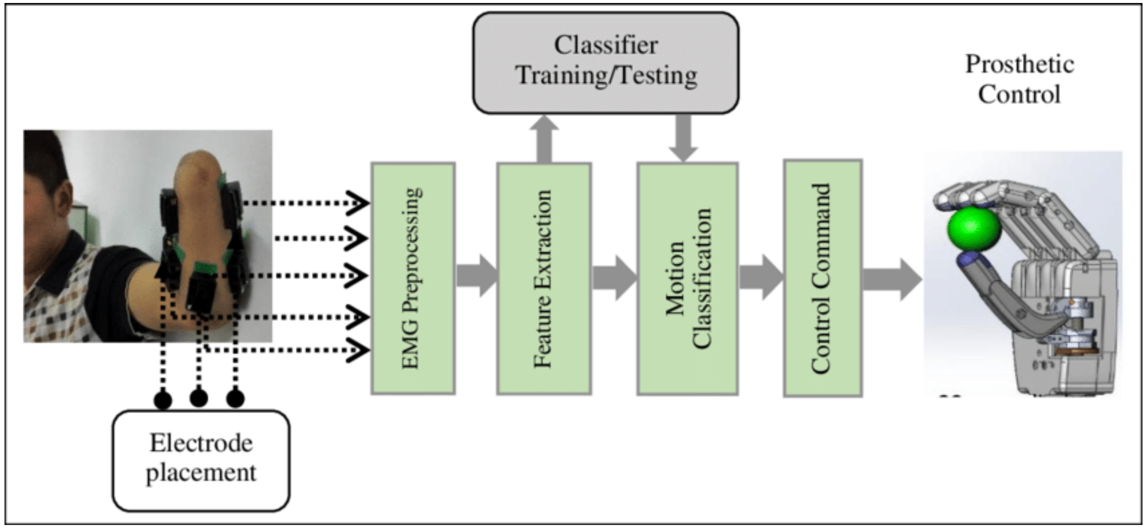

- In this case, the muscles naturally involved in the specific movement (e.g. ECR for the extension of the wrist) are no more available
- For this reason, “not- homologous” voluntary movements of the subject have to be coded as prosthesis movements (e.g. extension of the elbow for the extension of the wrist)
- This approach requires a quite long training phase and makes very difficult for the subject to easily control more than two degrees of freedom

EMG control – Muscle and feature selection

TD Feature	**Definition**	**References**
Mean absolute value	$MAV_i = \frac{1}{N}\sum_{k=1}^{N}\lvert x_i(k)\rvert$	[46], [50], [52]
Integrated absolute value	$IAV_i = MAV_i * N$	[53]
Variance	$VAR_i = \frac{1}{N}\sum_{k=1}^{N}(x_i(k) - \overline{x_i})^2$	[52], [54]
Mean absolute value slope	$MAVS_i = MAV_{i+1} - MAV_i$	[46]
Willison amplitude	$WAMP_i = \sum_{k=1}^{N} f(\lvert x_i(k) - x_i(k+1)\rvert)$ with $f(x) = 1\ if x > x_{th}$, 0 otherwise	[54]
Zero crossing	$ZC_i = \sum_{k=1}^{N} f(k)$ with $f(k) = 1\ if\ x_i(k) * x_i(k+1) < 0$ and $\lvert x_i(k) - x_i(k+1)\rvert > x_{th}$	[46]
Slope sign changes	$SSC_i = \sum_{k=2}^{N-1} f[(x_i(k) - x_i(k-1)) * (x_i(k) - x_i(k+1))]$ with $f(x) = 1\ if x > x_{th}$, 0 otherwise	[55]
Waveform length	$WL_i = \sum_{k=1}^{N-1}(\lvert x_i(k) - x_i(k+1)\rvert)$	[46], [55]
TSD Feature	**Definition**	**References**
Autoregressive coefficients	$x_i(k) = \sum_{j=1}^{N} a_j x_i(k-j)$, n^{th} order AR model	[53], [56]–[58]
Cepstral coefficients	$c_1 = -a_1;\ \ c_i = -a_i - \sum_{k=1}^{i-1}(1 - \frac{k}{i})a_n c_{i-k}$ $1 \leq k \leq n$ and a_i are the AR coefficients	[52]
FD Feature	**Definition**	**References**
Mean of signal frequencies	$FMN_i = \sum_{j=1}^{M}(f_j p_j)\ / \sum_{j=1}^{M}(p_j)$	[7]
Frequency ratio	$FR_i = \frac{min(FFT(x_i))}{max(FFT(x_i))}$	[7]
TSC or TF Feature	**Definition**	**References**
Short-time Fourier transform	$STFT[k,m] = \sum_{r=1}^{N-1} x[r]g[r-k]e^{-j2\pi mi/N}$ where g, k, and m are the window function, the time sample, and frequency bins, respectively.	[7]
Wavelet transform	Continuous WT (CWT) produces a good frequency resolution Δf in long time windows (low frequencies) and a good time localization Δt at high frequencies $CWT_x(\tau, a) = \frac{1}{\sqrt{a}}\int x(t)\Psi(\frac{t-\tau}{a})dt$ where t and a are the translation and scale parameters and Ψ is the mother wavelet function	[47], [51]
Wavelet packet transform	WPT is a generalized version of the continuous and discrete WT.	[47], [51], [59]

PCA or similar could be necessary to select few more information muscles

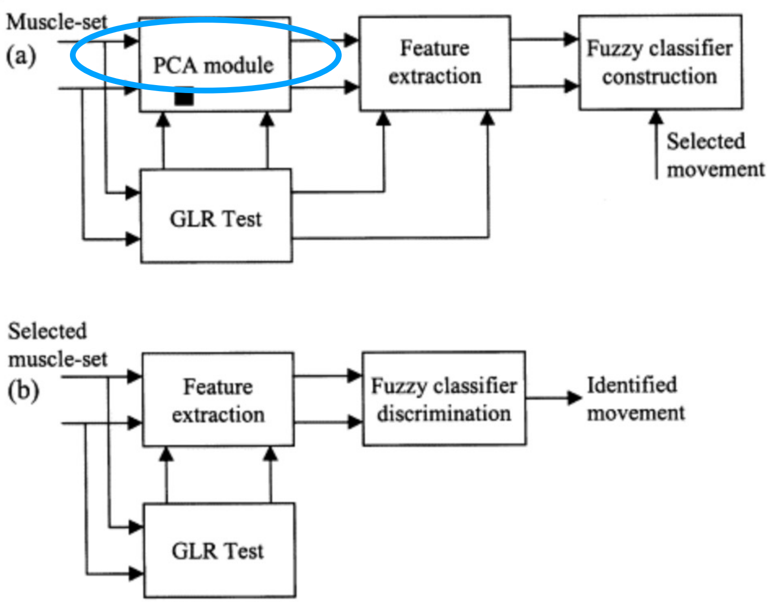

EMG control – Classifier selection

- Supervised learning classifier to link EMG signals (features) to desired hand movements
- More or less anything has been tried (including majority voting)
- Make a fair comparison!!

TABLE IV
SOME PATTERN RECOGNITION BASED CONTROL OF UPPER LIMB PROSTHESIS.
A = amputee subjects, H = healthy subjects, LD = limb deficiency subjects

Classifier	EMG channels	Classes	Features	Subjects involved	References
MLP	2	4	MAV, MAVS, ZC, SSC, WL	9H+6A	Hudgins et al [46]
Fuzzy	2	6	IAV,VAR,AR, CC, adaptive CC	6H	Park and Lee [52]
LDA,MLP	2	4	-	16H	Englehart et al [51]
Fuzzy	2	4	MAV, MAVS, ZC, WL	4H	Chan et al [65]
PCA,LDA	2,4	4,6	-	11H	Englehart et al [47]
PCA,LDA	4	6	STFT, WT, WPT	12H	Englehart et al [12]
-	3,4	3,4	Fuzzy	3H+1A+1LD	Ajiboye and Weir [67]
HMM,MLP	4	6	-	12H	Chan and Englehart [66]
GMM,LDA,MLP	4	6	TD, RMS, AR	12H	Huang et al [68]
LDA,MLP	4	8	WPT	10H	Chu et al [64]
SVm,GDA	3	8	AR, histogram	1H+2A	Liu et al [70]
SVM,LDA,MLP	4	5	single and multi TD/FD	11H	Oskoei and Hu [49]
SVM	7	8	RMS	3H	Shenoy et al [71]
HMM,bayes	4	9	-	10H	Chu and Lee [69]
MLP	12/32	12	MAV, VAR, WL, W	5H+1A	Tenore et al [54]
LDA	12	10	MAV, ZC, WL, SSC	5A	Li et al [72]

EMG control – A little help?

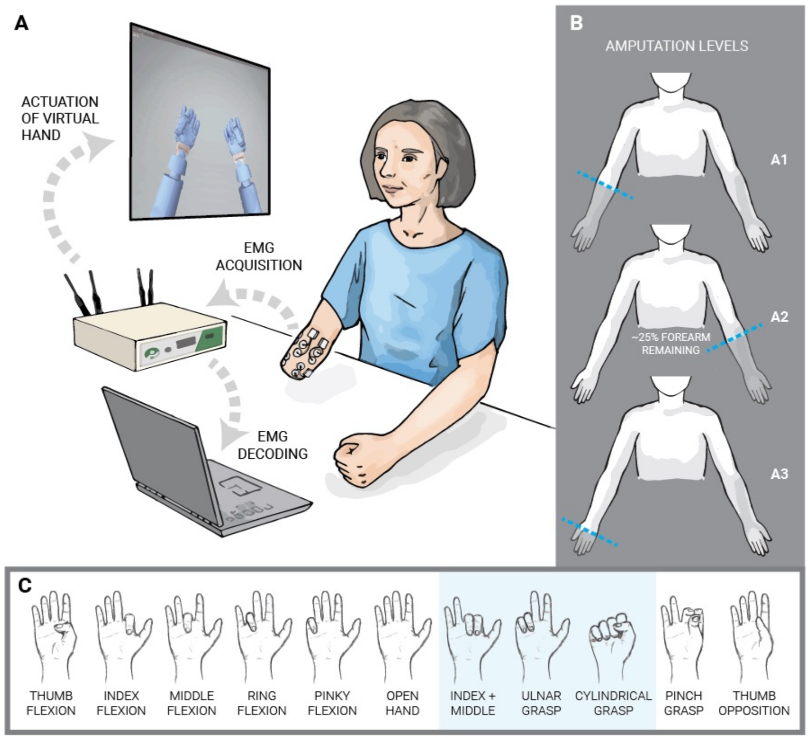

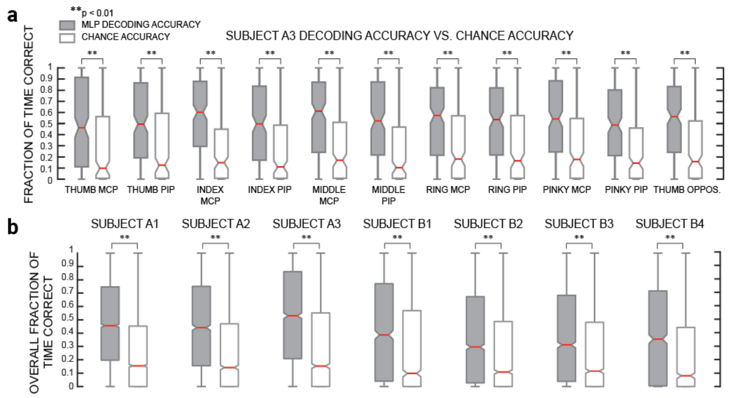

- Single finger decoding using EMG signals
- One implanted patient from UCSC - Loretana
- Two patients from collaboration with hospitals Chuv (Lausanne, CH) and Villa Beretta (Lecco, Italy)

EMG shared control

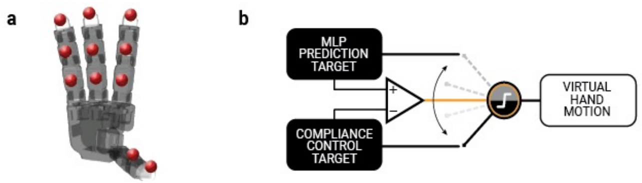

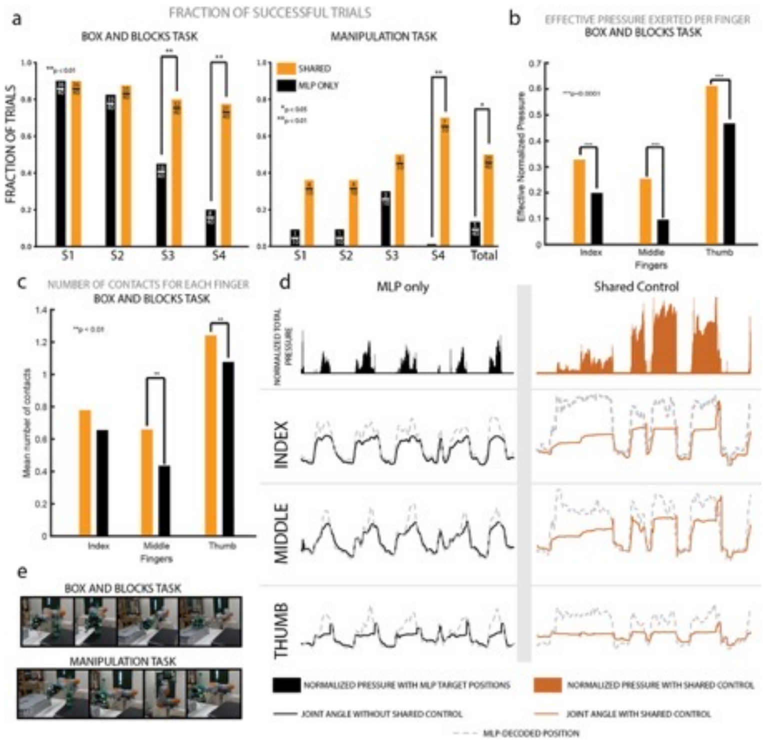

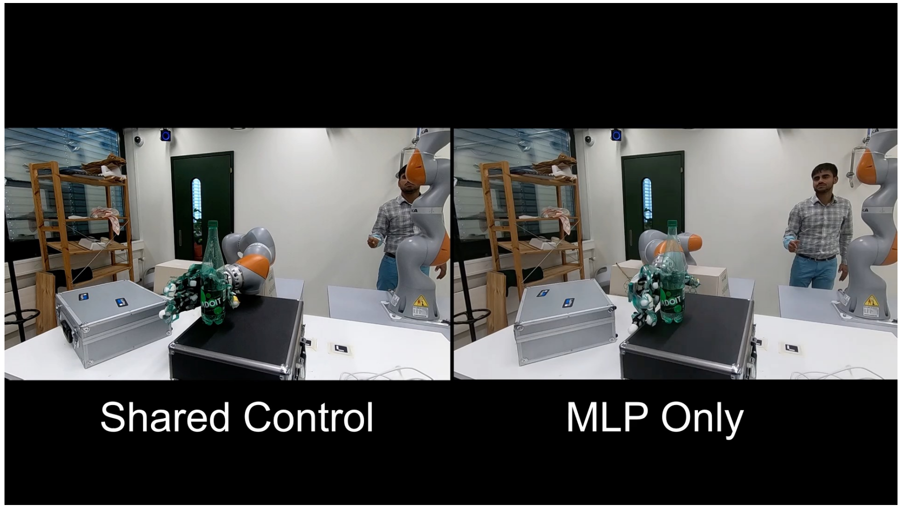

When a hand is not contacting an object, the user controls the robotic hand with the output of EMG decoding

When the hand makes contact with an object, the compliance controller automates hand conformation around the object, allowing a high degree of grasp stability

Intramuscular EMG (iEMG) control

- Clinically available myoelectric control strategies do not allow simultaneous movement of multiple degrees of freedom (DOFs)
- The use of implantable devices that record intramuscular EMG signals could overcome this constraint
- Intramuscular EMG signals can be recorded using percutaneous fine wire electrodes inserted using needles
- The use of iEMG can allow to use proportional control (but of course also pattern recognition)

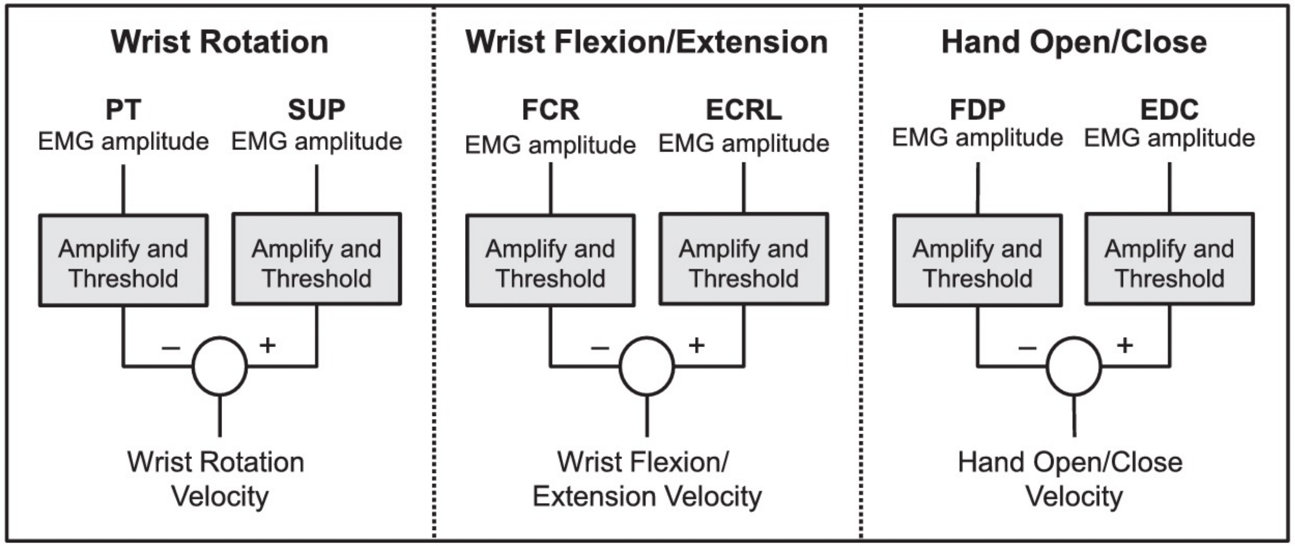

Smith et al., 2014

Intramuscular EMG (iEMG) control

- Sense myoelectric signal at its source, so it acts as an amplifier of the neural command.
- Use inductive coupling to pass power into devices and signal out of device w/o breaking the skin

Multifunction Prosthesis Control Using Implanted MyoElectric Sensors (IMES)

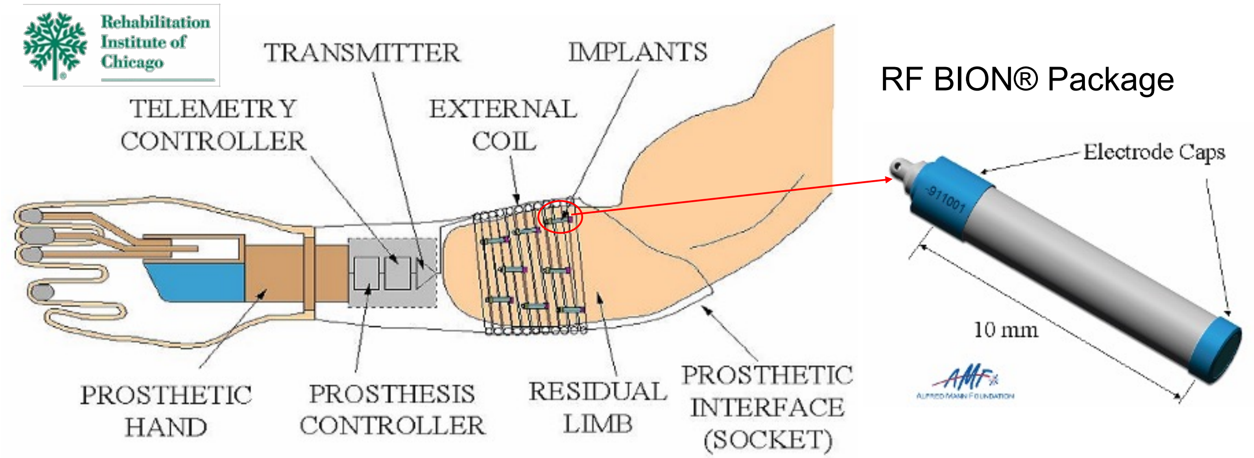

Smith et al., 2014

Targeted muscle reinnervation (TMR)

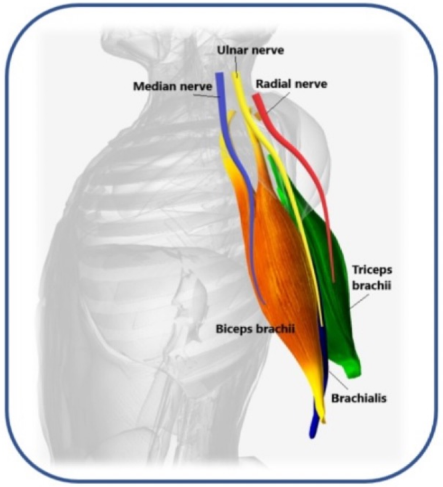

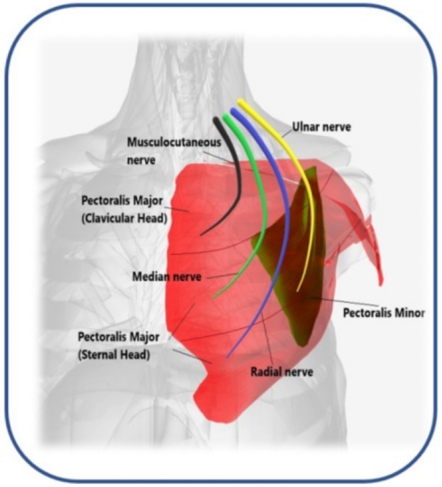

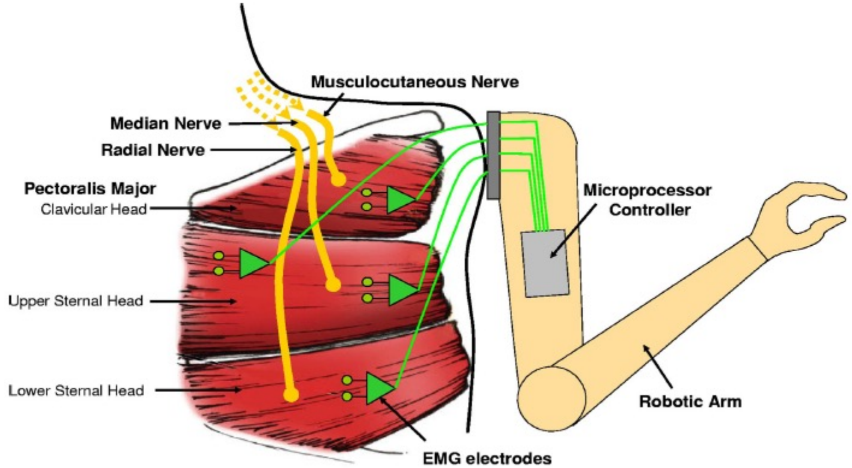

- A surgical technique called targeted muscle reinnervation (TMR) transfers residual arm nerves to alternative muscle sites
- After reinnervation, these target muscles produce electromyogram (EMG) signals on the surface of the skin that can be measured and used to control prosthetic arms

Kuiken et al., 2007

Targeted muscle reinnervation (TMR)

- Subjects showed statistically better performance in the Southampton Hand Assessment Procedure (p=0.04) and the Clothespin relocation task (p=0.02)
- Notably, these tests required movements along 3 degrees of freedom.
- Seven of 8 subjects preferred pattern recognition control over direct control
- Results demonstrate that pattern recognition is a viable option and has functional advantages over direct control.

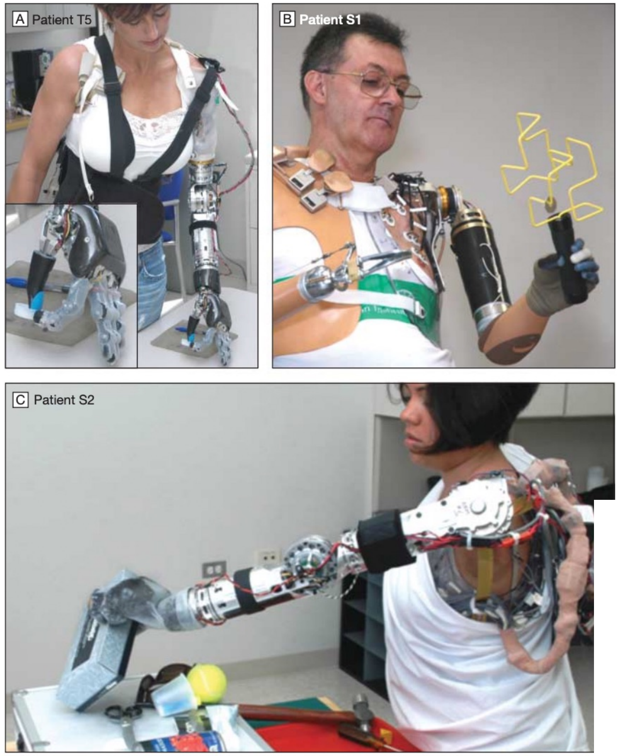

Hargrove et al., 2017

Subject	Direct Control Wear Time (hrs)	Pattern Recognition Wear time (hrs)	Number of Recalibrations	Preference of Control
S1	41	15	7	PR
S2	280.1	301.6	39	PR
S3	196.8	183.6	73	PR
S4	254.6	366.9	56	PR
S5	91.4	85.1	10	PR
S6	54.9	27.9	20	DC
S7	157.7	128.5	18	PR
S8	33.2	73.0	38	PR

Table 2. Wear time, recalibration and control preference.

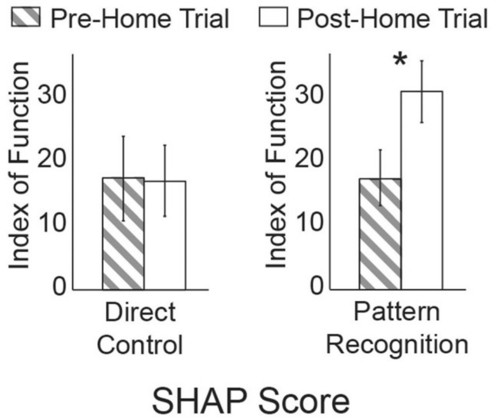

High density electrodes

- The identification of action potentials belonging to individual motor units provides information about the motor output from the spinal cord because of the one-to-one association between the action potentials generated in the axon and those in the innervated muscle fibers
- Intramuscular recordings have been used for about 80 years and are the classic means for investigating the properties of individual motor units
- The possibility to achieve similar results with surface EMG electrodes would be quite interesting
- The recording of surface EMG in multiple locations (spatial sampling) enhances the capacity to discriminate the action potentials of separate motor units)
- This is accomplished by multi-channel systems providing many recordings of motor unit activity along the length of a muscle or over its surface area

High density electrodes

- During voluntary contractions, the action potentials from several motor units superimpose to form a complex interference pattern
- The characteristics of the multi-channel interference pattern can be associated to the level of muscle activation using topographical EMG representations, i.e. maps of electric potential
- The number of identifiable motor units increases substantially with the number of channels used for the discrimination

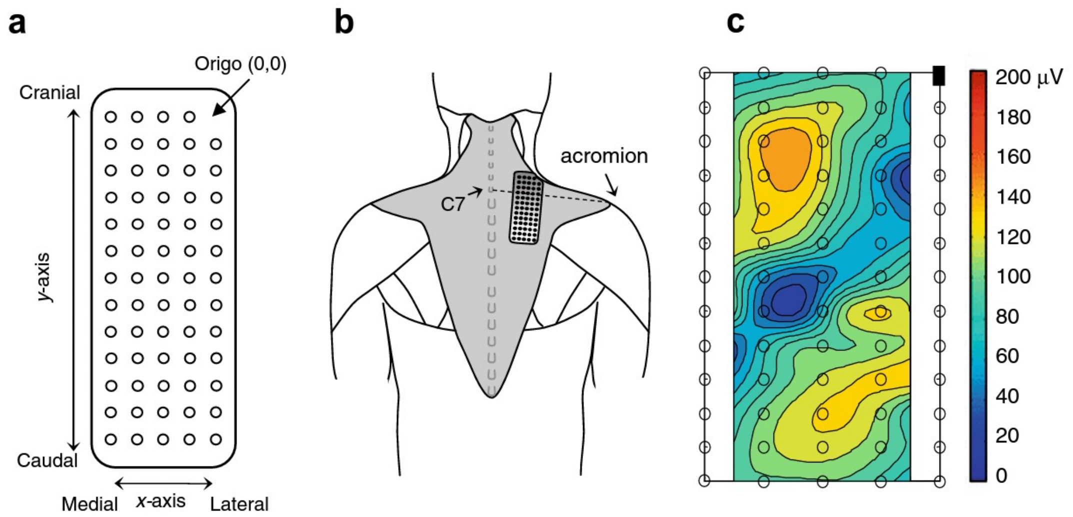

Wearable HD-EMG interface

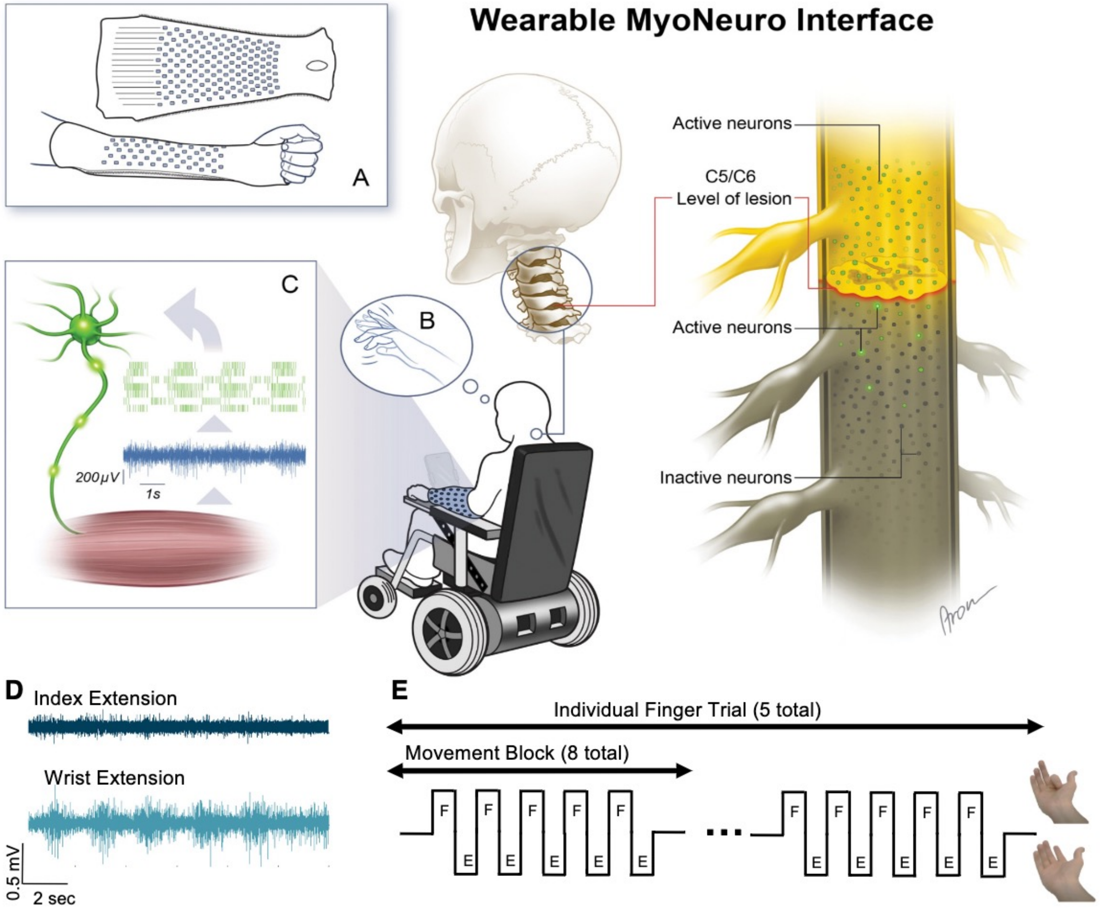

A wearable electrode array and machine learning methods were used to record and decode EMG signals and motor unit firing in paralyzed muscles of a person with motor complete tetraplegia

The myoelectric activity and motor unit firing rates were task specific, even in the absence of visible motion, enabling accurate classification of attempted sigle digit movements

This wearable system has the potential to enable people with tetraplegia to control assistive devices through movement intent.

Ting et al., 2021

Wearable HD-EMG interface

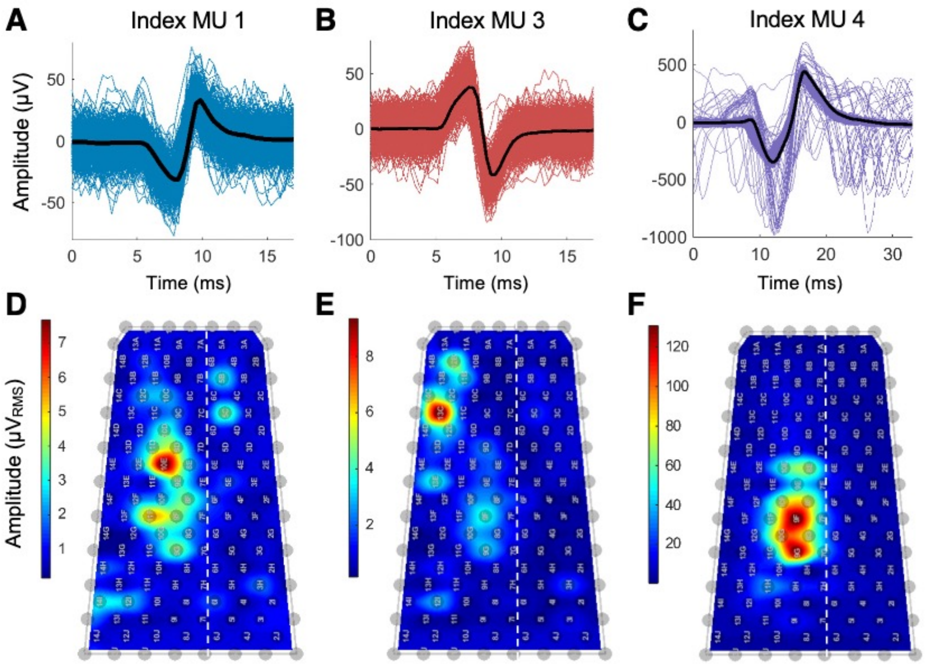

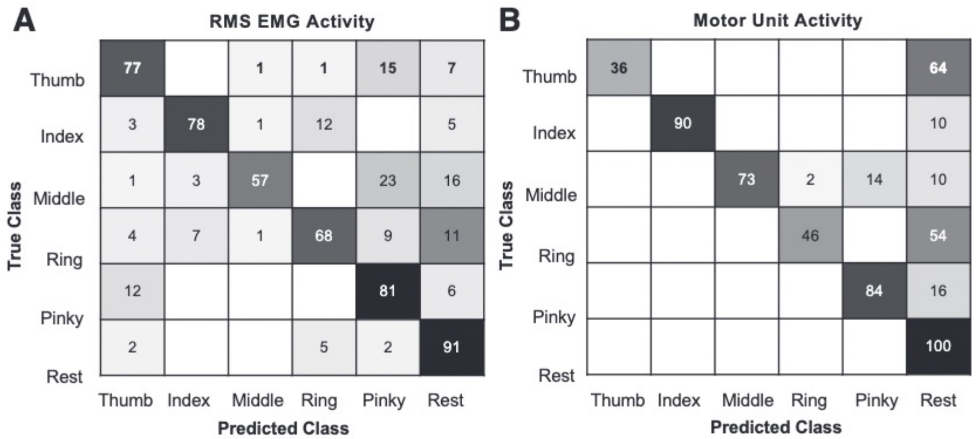

New technologies for HD-EMG interface

- Soft bioelectronic interfaces for mapping and modulating excitable networks at high resolution and at large scale can enable paradigm-shifting diagnostics, monitoring, and treatment strategies

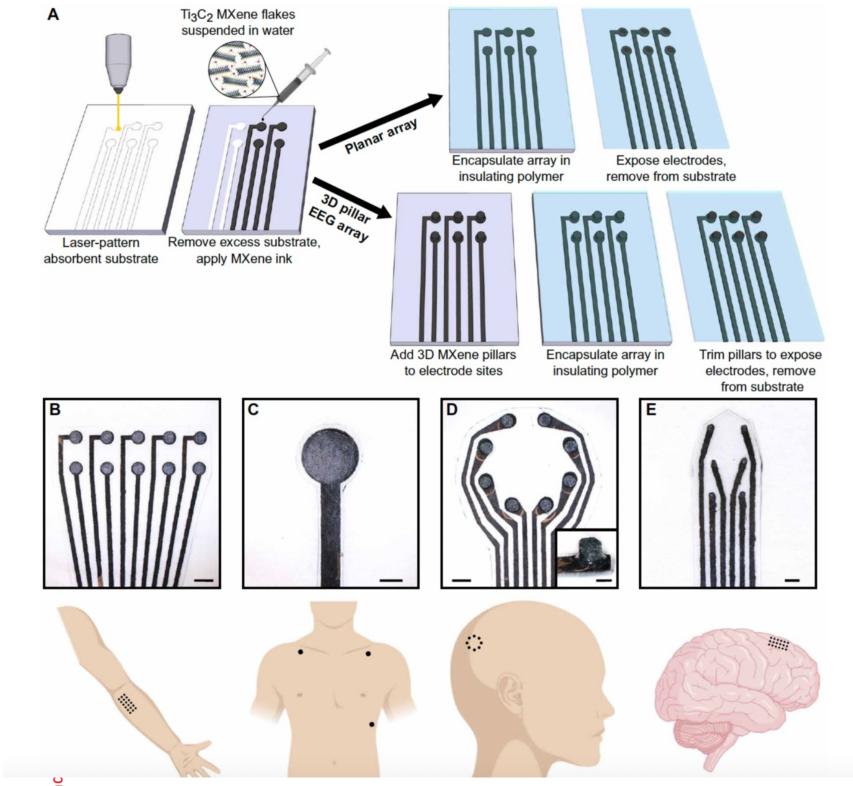

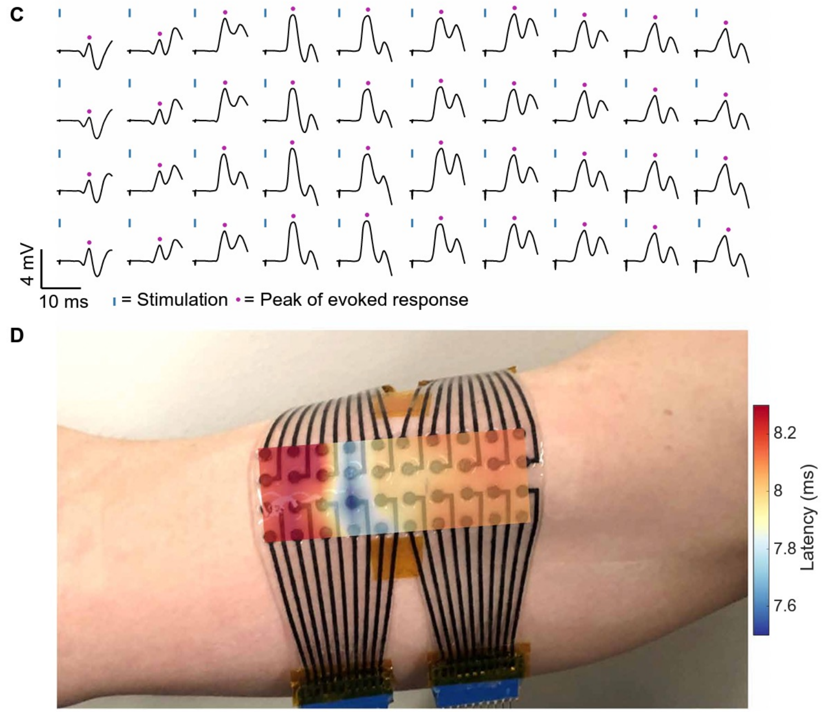

Driscoll et al., 2021

TMR and HD-EMG

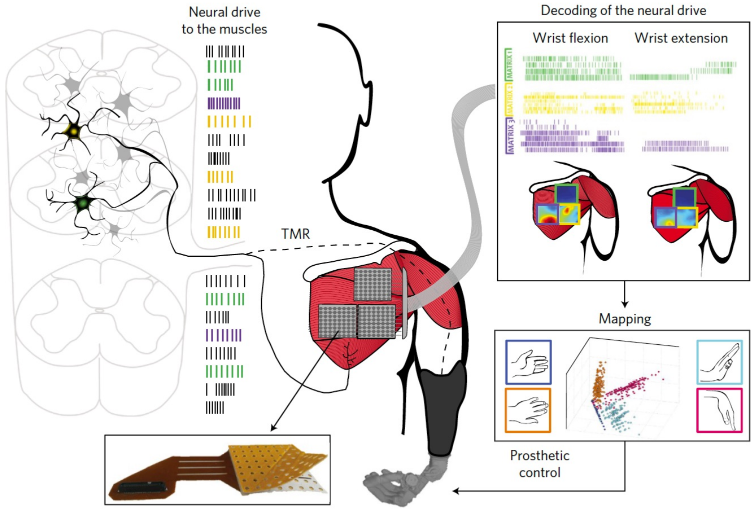

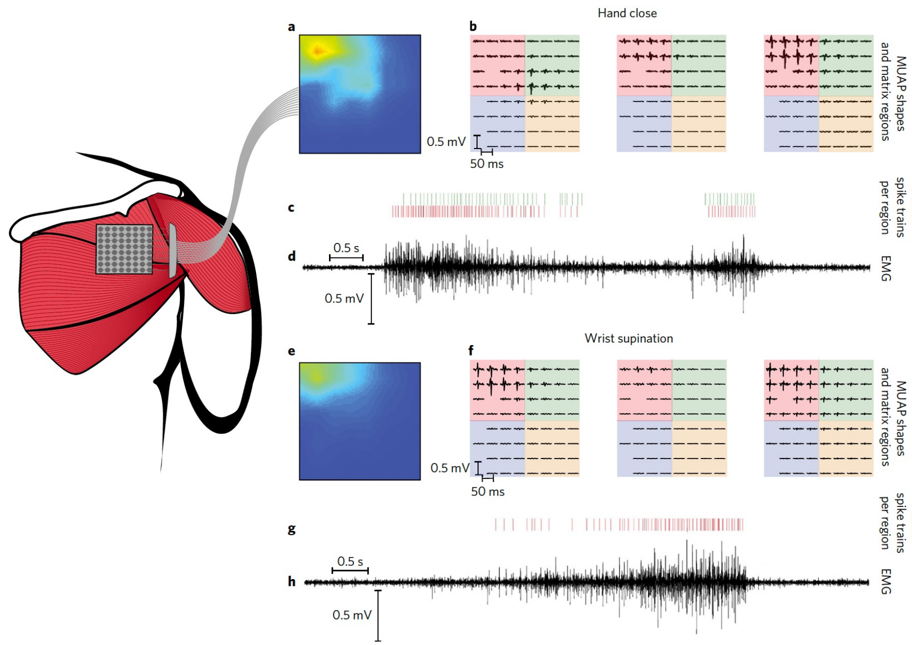

- The motor-neuron behaviour is identified by deconvolution of the electrical activity of muscles reinnervated by nerves of a missing limb in patients with amputation at the shoulder or humeral level
- We mapped the series of motor-neuron discharges into control commands across multiple degrees of freedom via the offline application of direct proportional control, pattern recognition and musculoskeletal modelling
- A series of experiments performed on six patients reveal that the man/machine interface has superior offline performance compared with conventional direct electromyographic control applied after targeted muscle innervation

Farina et al., 2017

Peripheral implantable electrodes

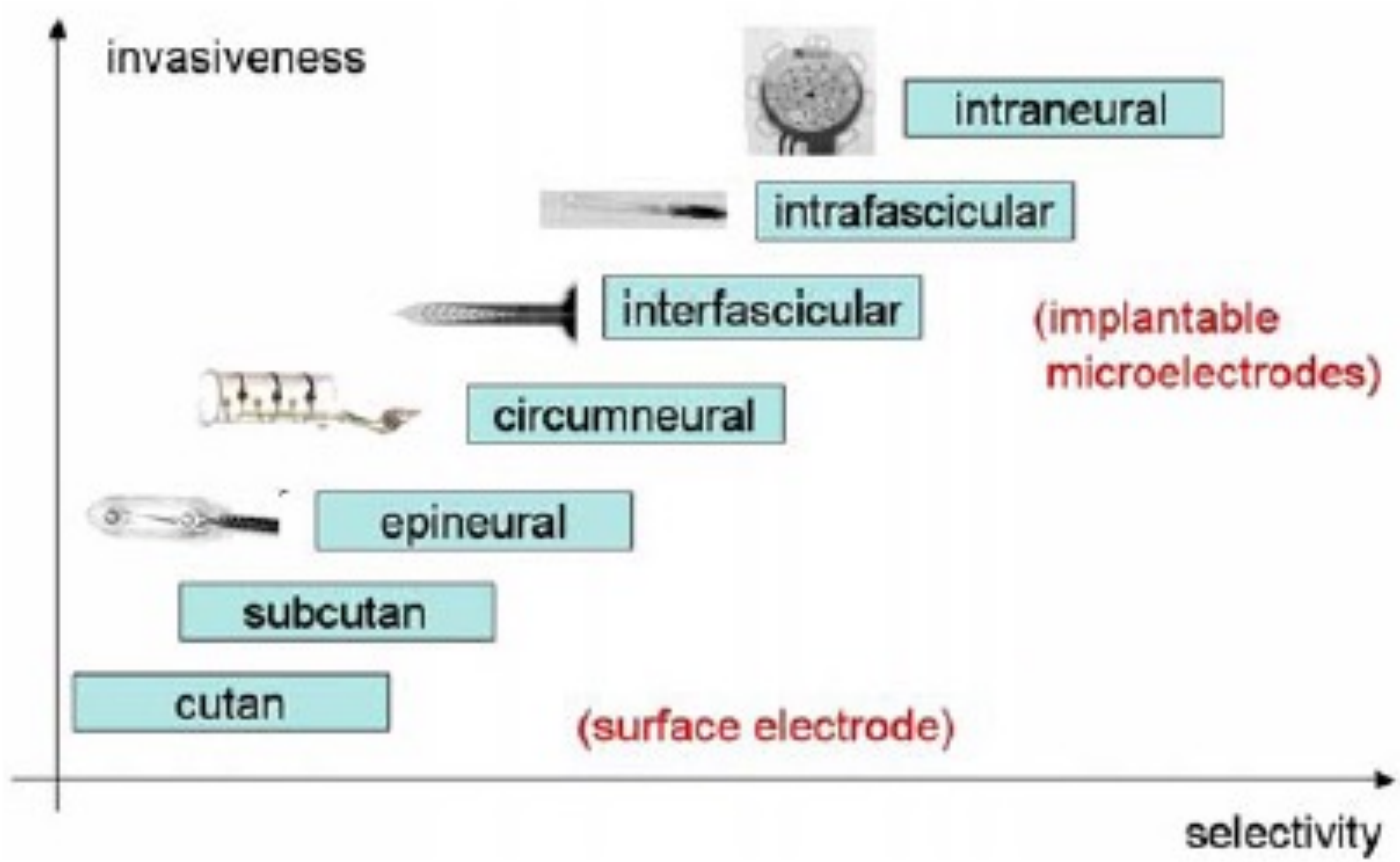

Micera et al., IEEE T-NSRE, 2008

Sensory feedback

Real-time, and natural feedback from the hand prosthesis to the user is essential in order to enhance the control and functional impact of prosthetic hands in daily activities, prompting their full acceptance by the users

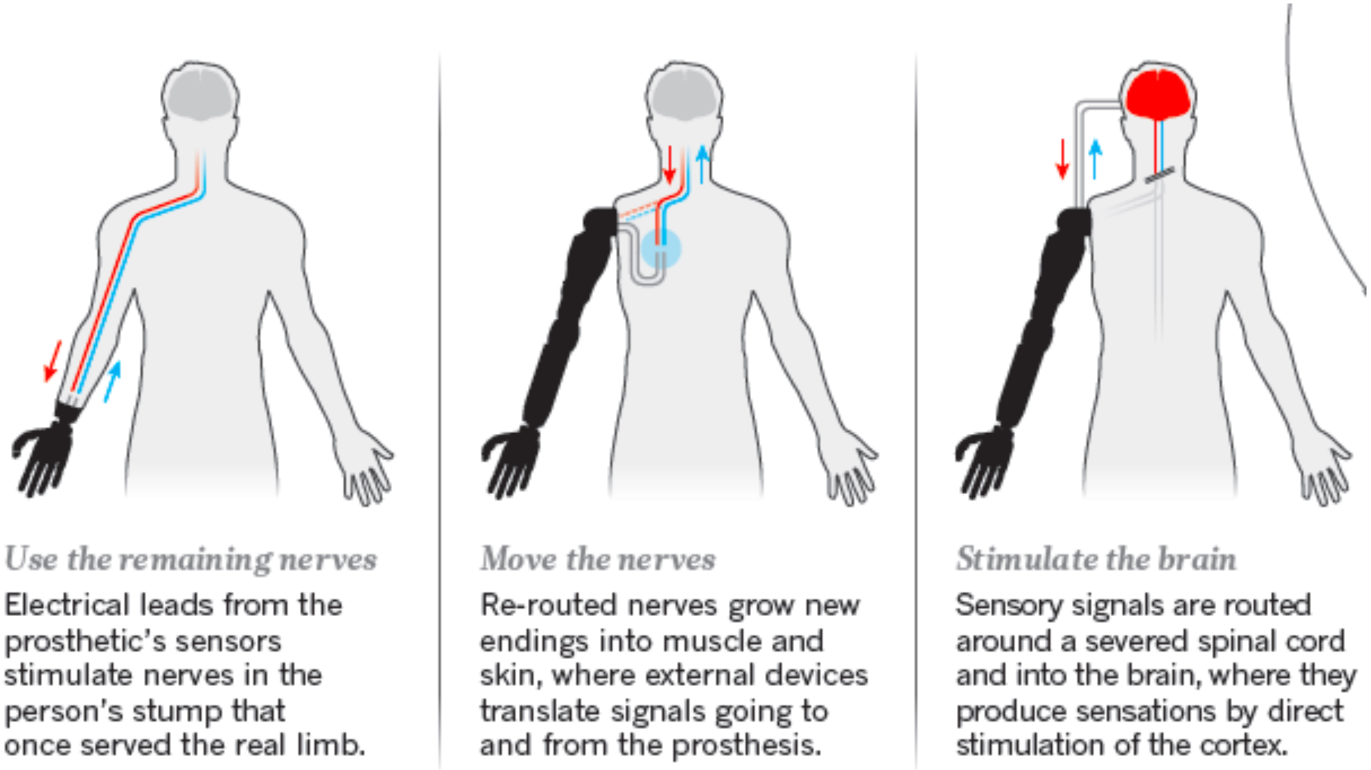

Kwok, Nature, 2013

Targeted Muscle Reinnervation

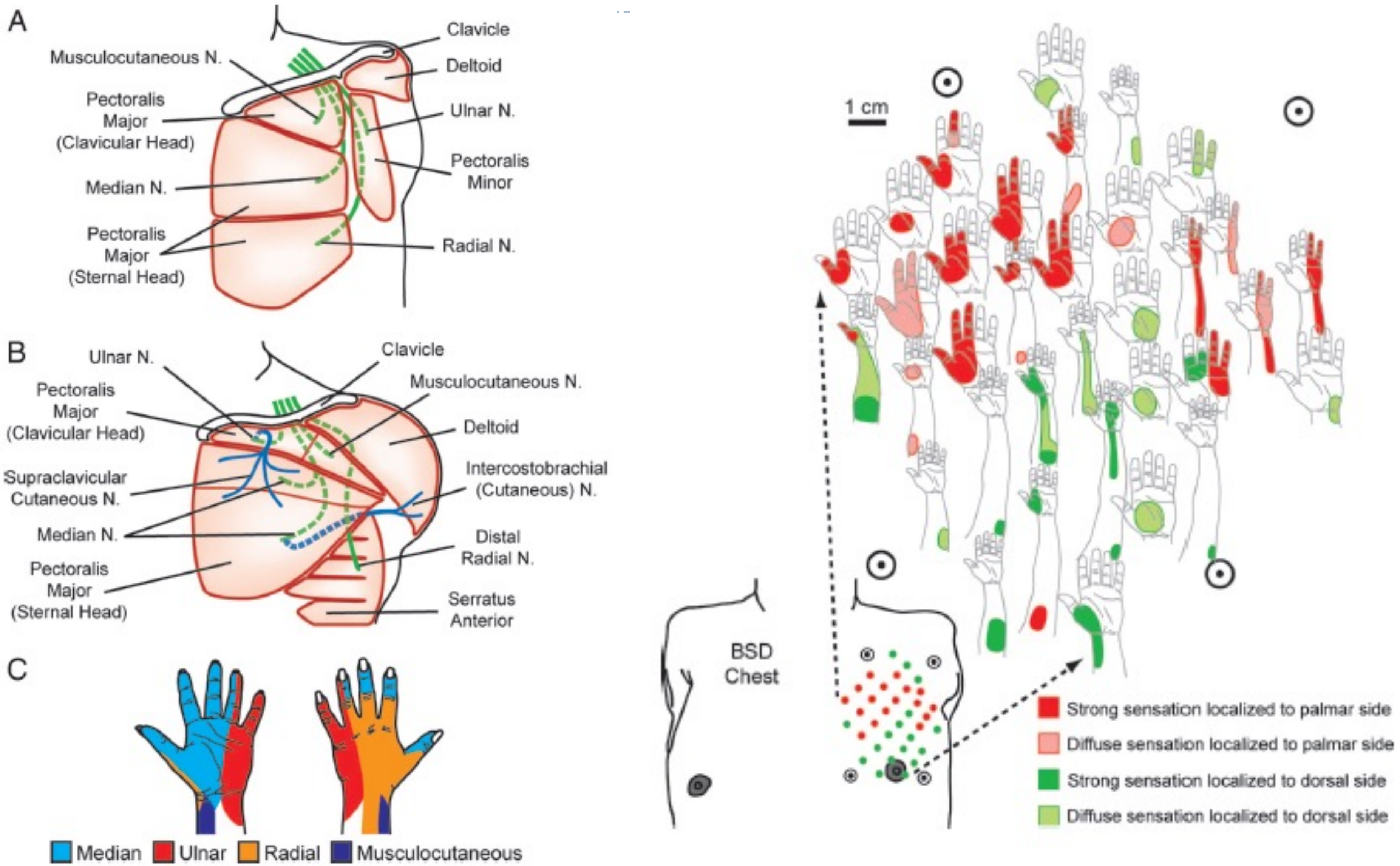

Kuiken et al., 2007, 2008

Targeted Muscle Reinnervation

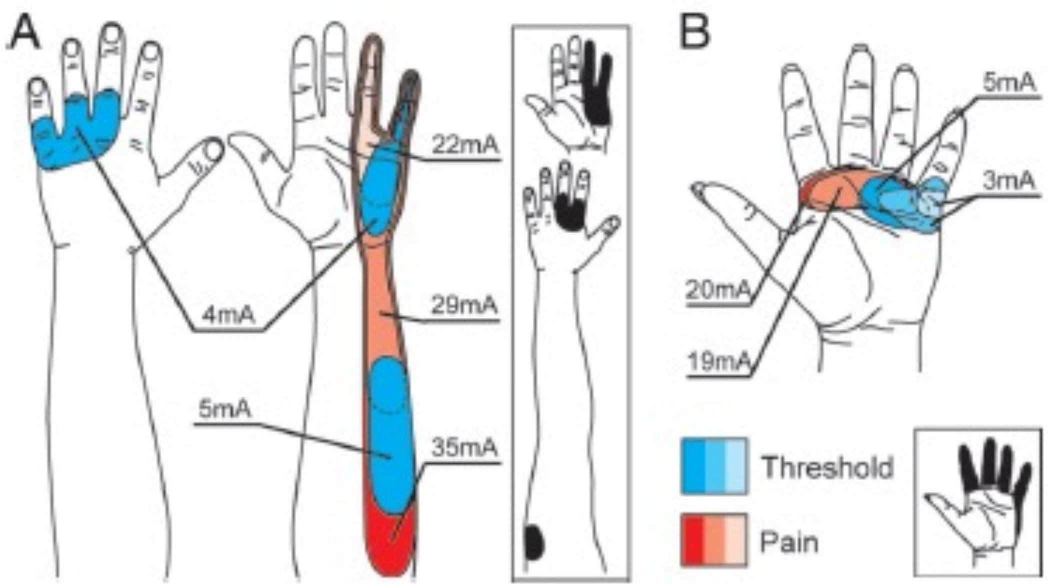

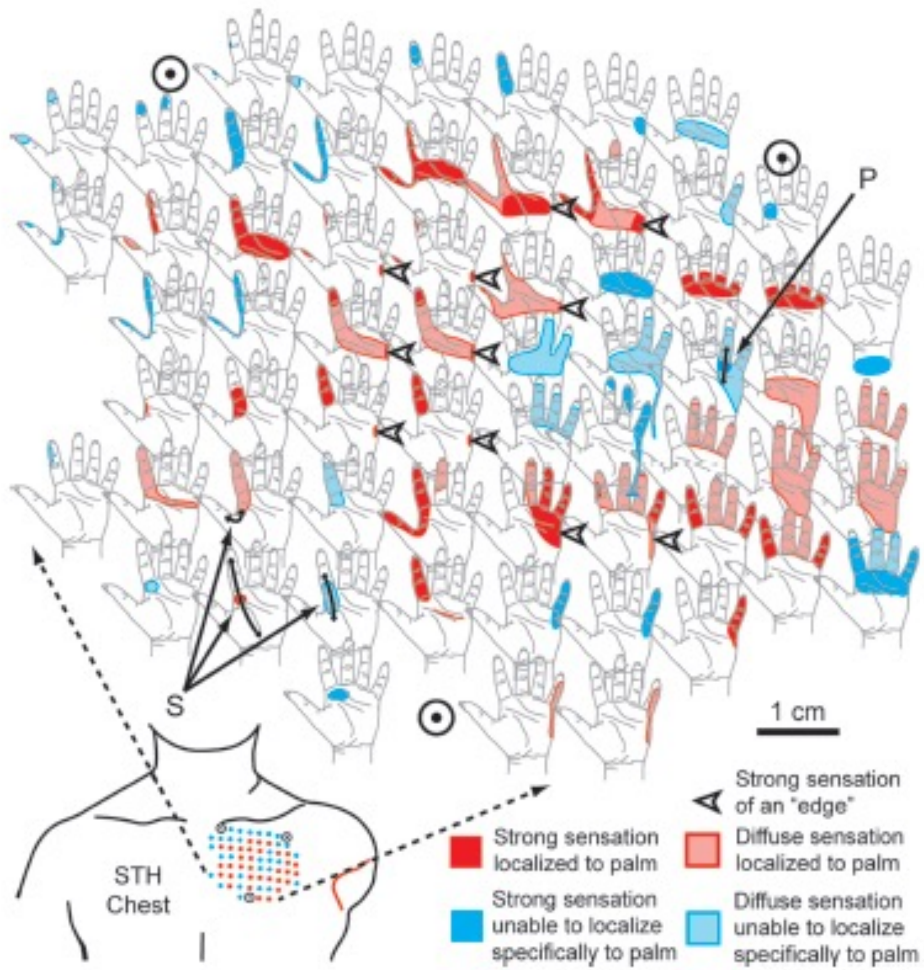

- Very interesting solution but more suitable for proximal (shoulder) amputations
- **Sensory feedback is possible but difficult to be daily usable**

Sensory feedback

Real-time, and natural feedback from the hand prosthesis to the user is essential in order to enhance the control and functional impact of prosthetic hands in daily activities, prompting their full acceptance by the users

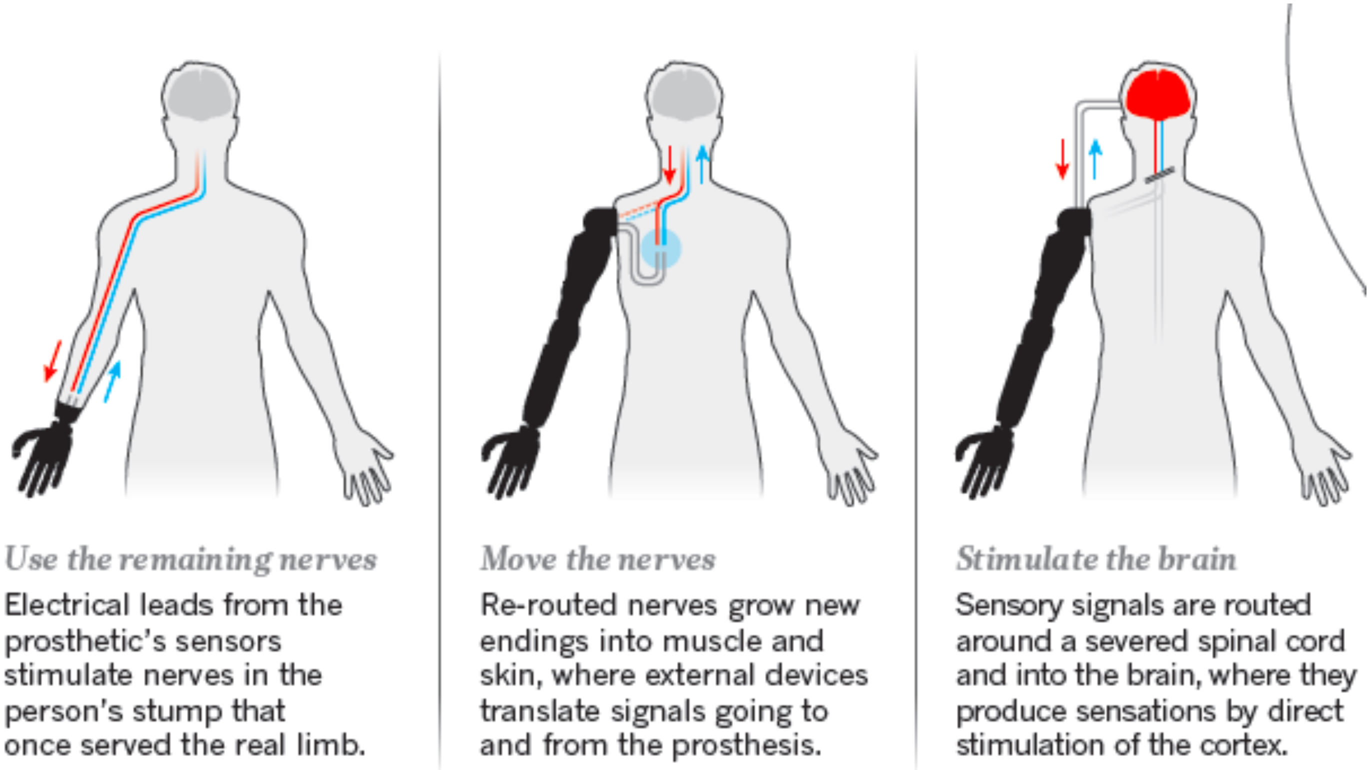

Kwok, Nature, 2013

First intraneural experiment

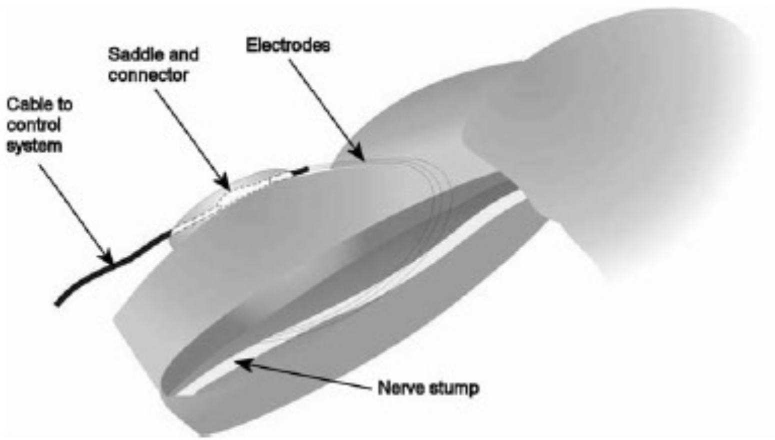

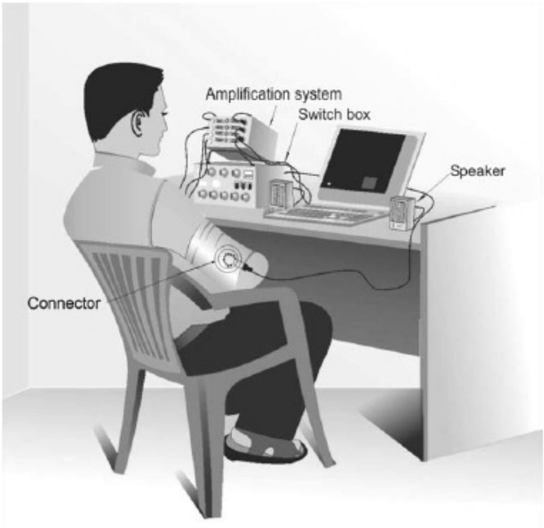

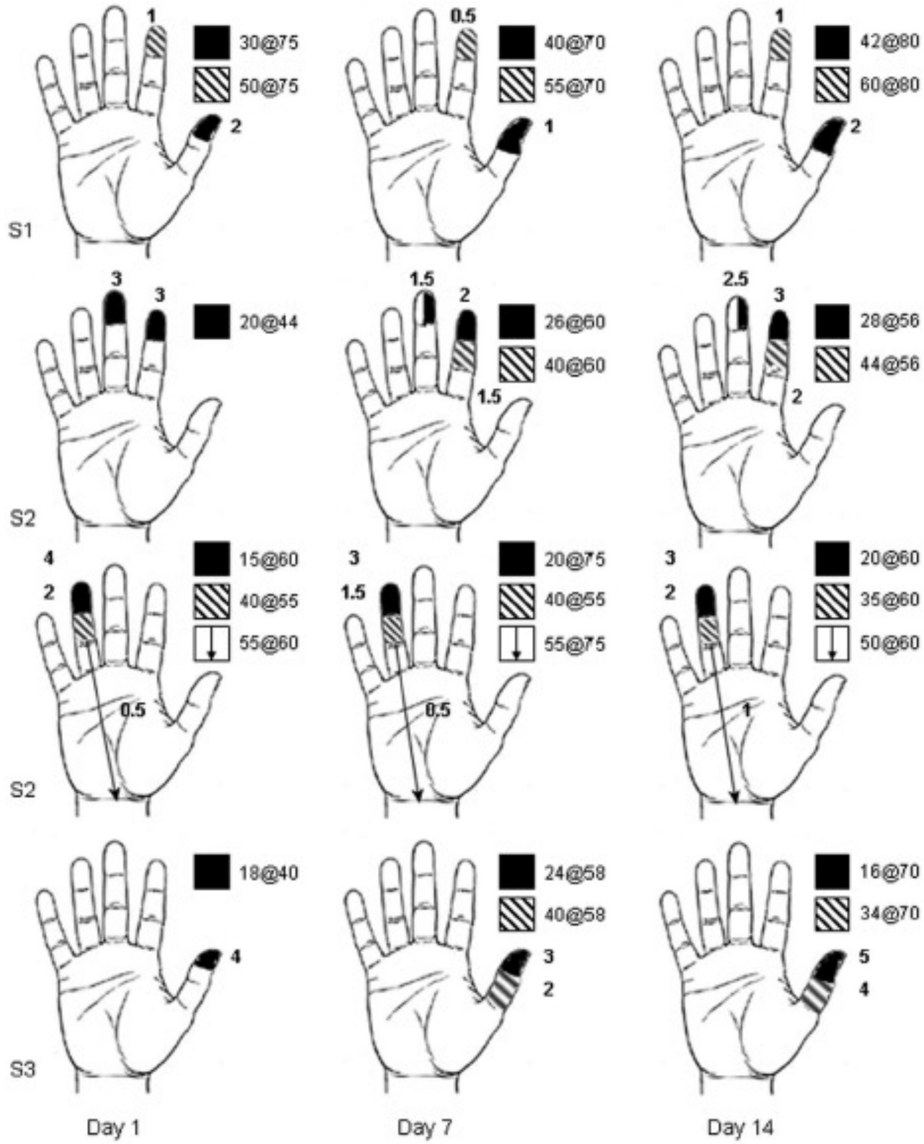

First intraneural experiment

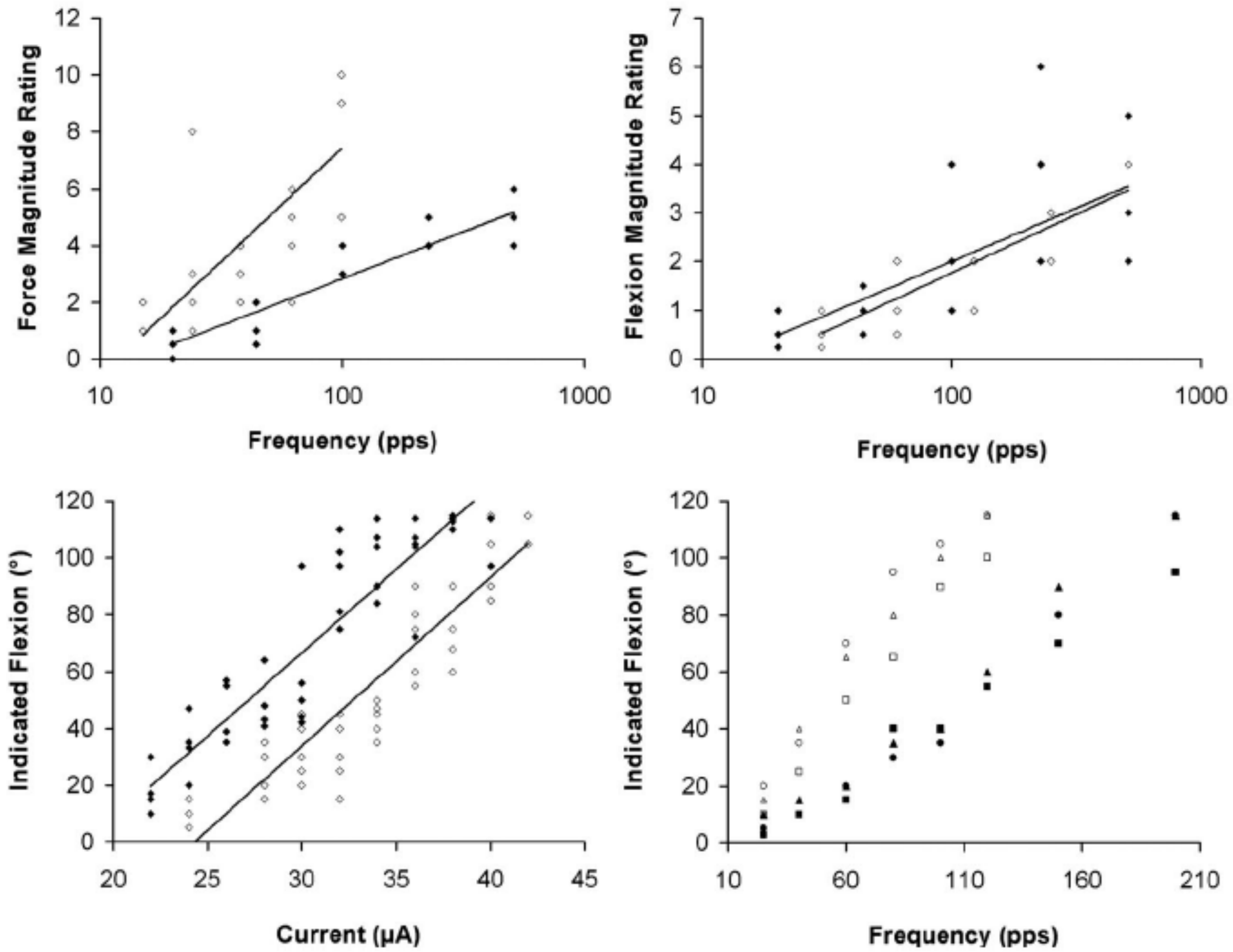

Sensory feedback using FINE electrodes

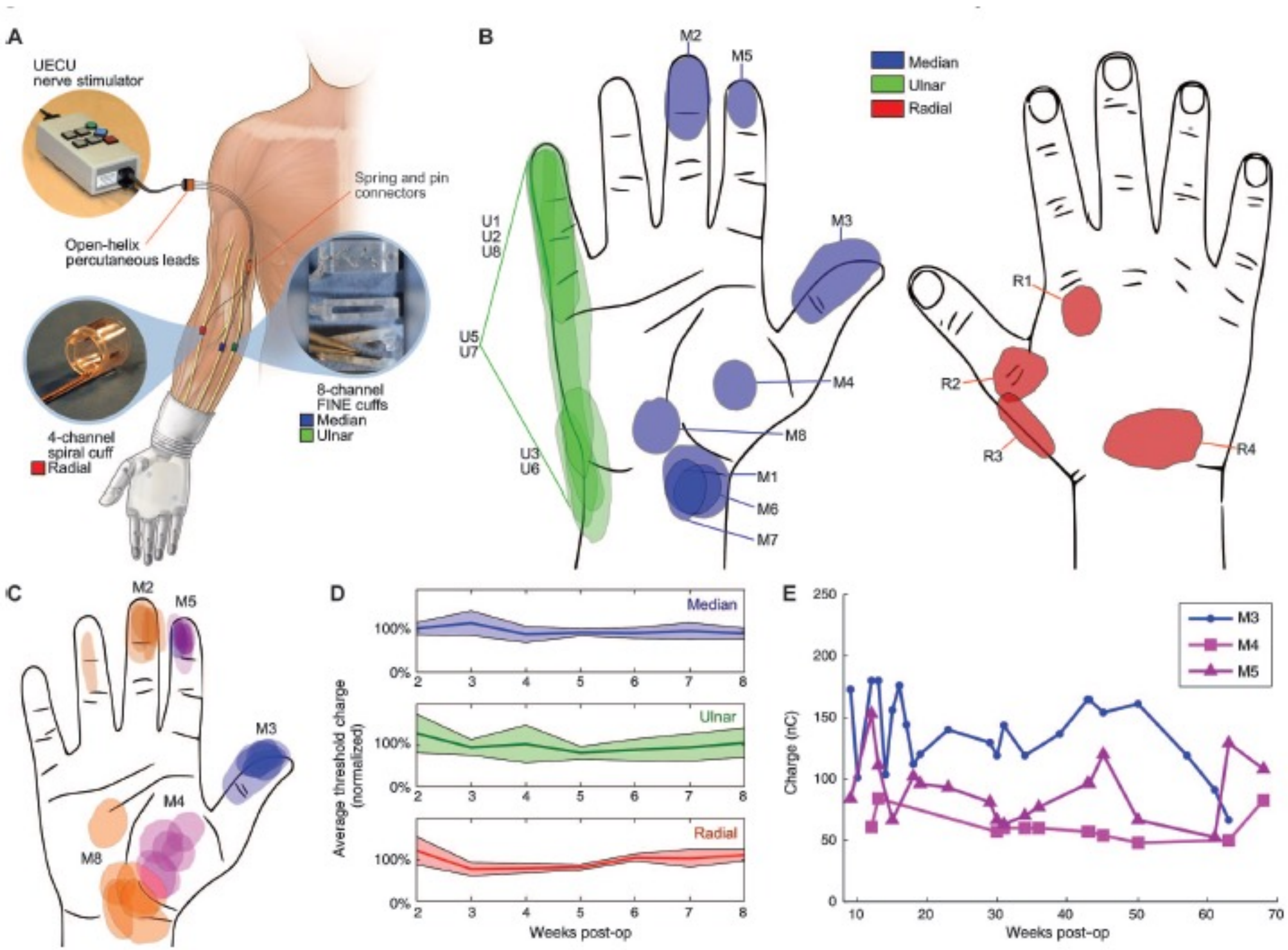

Sensory feedback using FINE electrodes

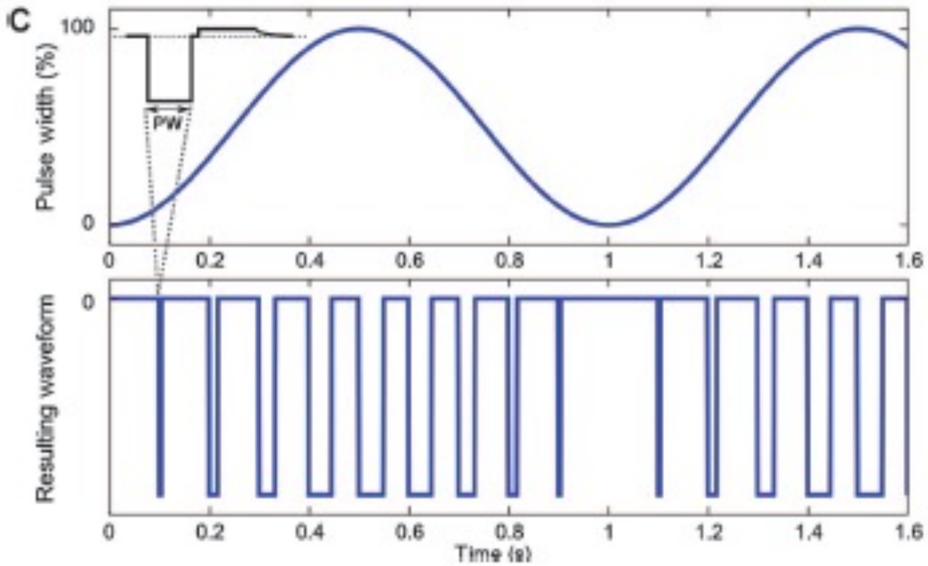

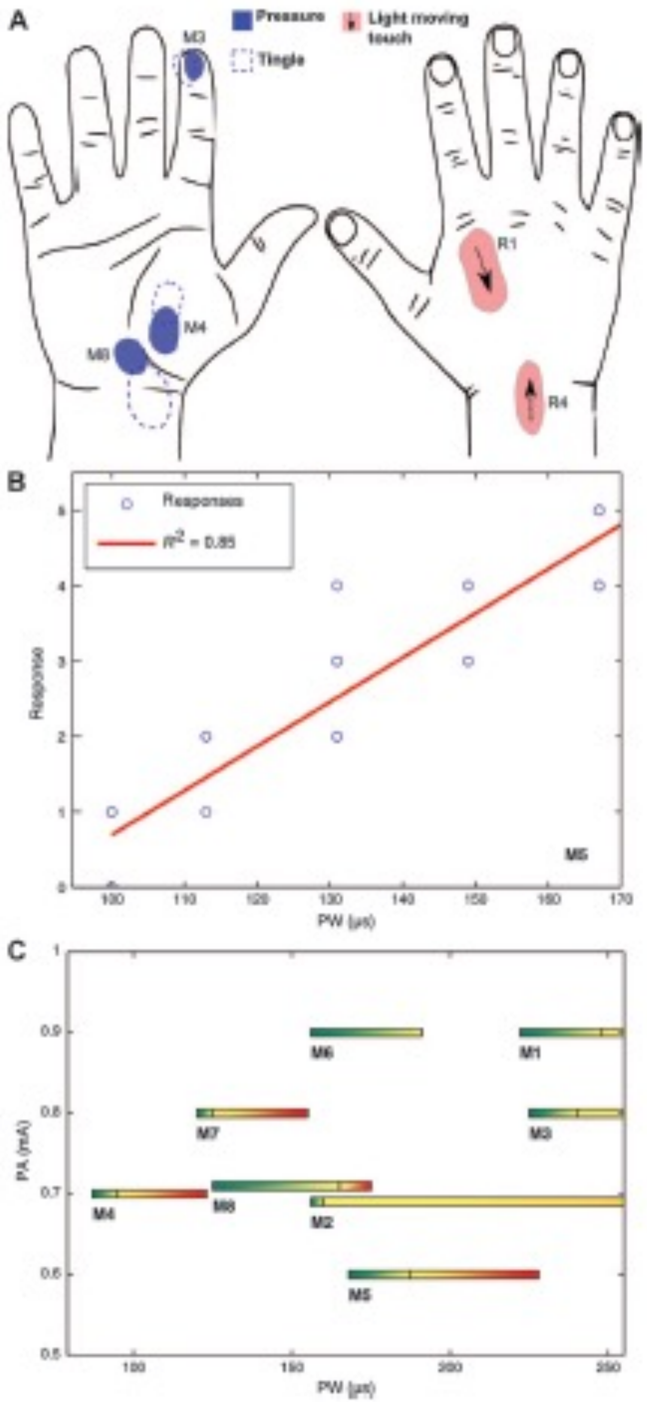

Sensory feedback

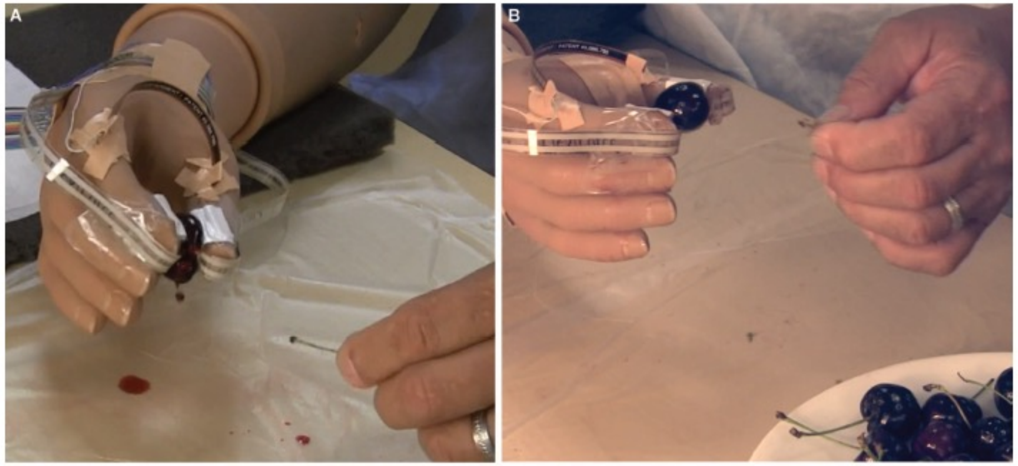

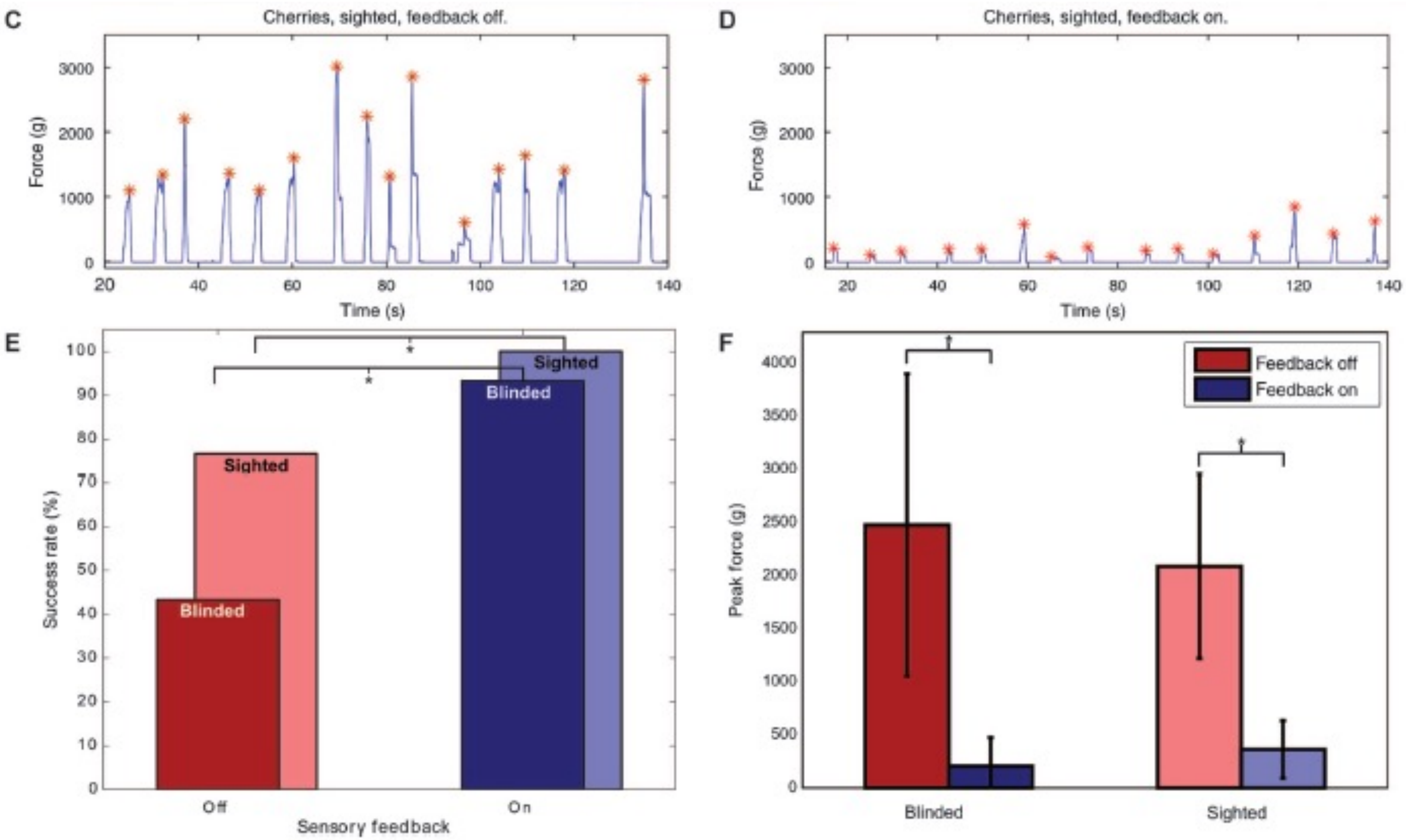

Short-term implant of TIMEs in an amputee

P.M. Rossini

S. Raspopovic

M. Capogrosso

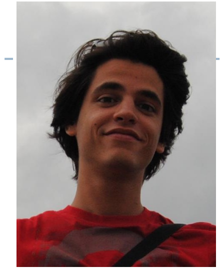

M. Bonizzato

- 35 year old man, from Denmark
- trans-radial amputation in 2004 (fireworks accident during family celebration)

- Subjects resistant to pharmacological therapy and with no neuropathies (evaluated by Electroneurography) or other systemic diseases affecting brain/spinal cord/nerves

- Subjects with no neuropsychiatric disorders, evaluated by neuropsychological and psychiatric tests (WAIS-R, CES-D, MMPI-2)

- FOUR week implant

TIME implant

- **Nerves to implant:**
  - ✓ Median nerve
  - ✓ Ulnar nerve

- **Number of electrodes:**
  - ✓ 2 for each nerve

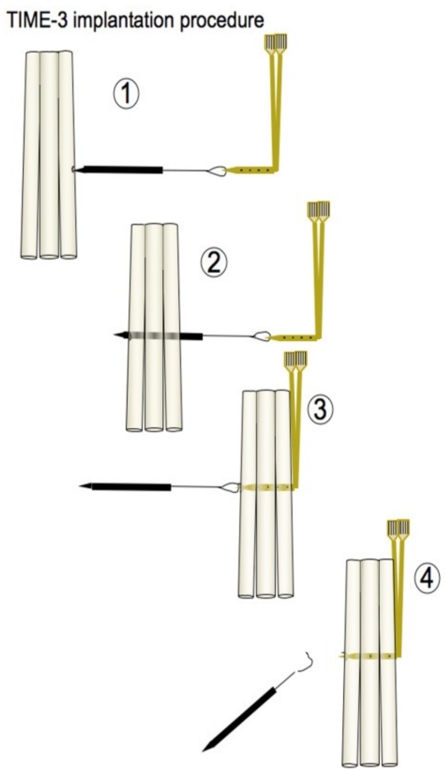

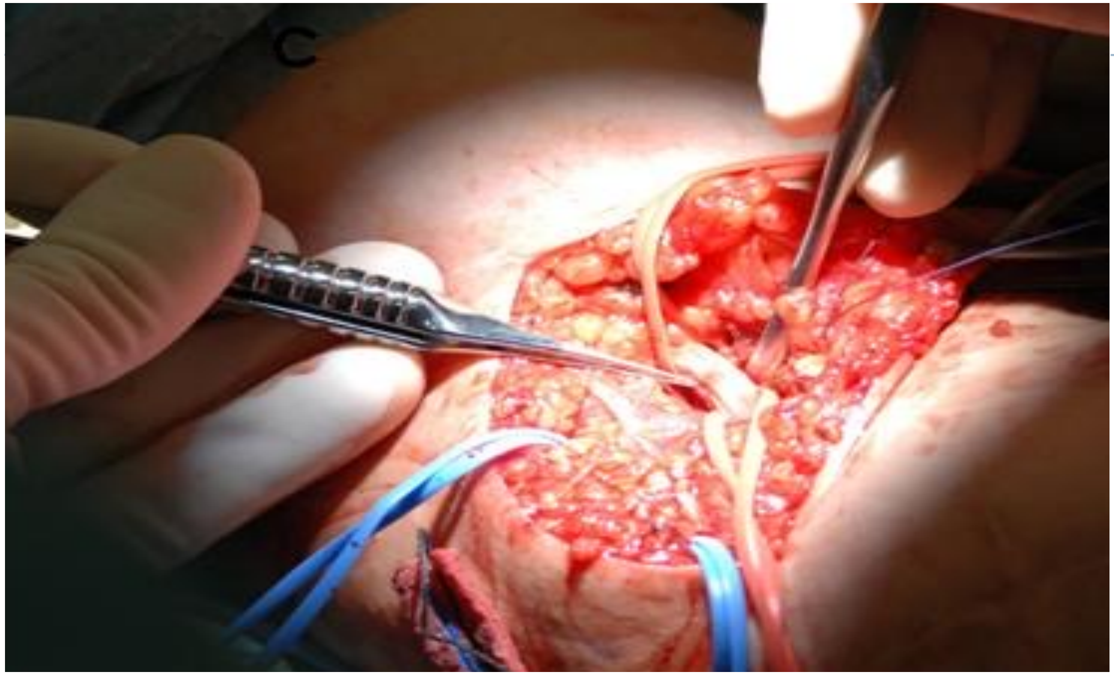

- **Surgical technique:**

✓General anesthesia
✓skin incision (medial edge of the biceps muscle-15 cm)
✓Exposition of the ulnar and median nerves
✓epineural microdissection
✓TIME electrodes inserted under surgical microscope using a guiding needle
✓8-0 suture used to fix the electrodes to the epineurium
✓Subcutaneous pockets

Closed-loop control based on sensory feedback

- Test the possibility for the subject to use the sensory information during closed-loop control and manipulation experiments

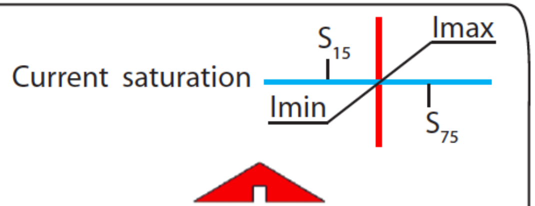

$$\mathbf{I} = (\mathbf{I}_{\mathbf{max}} - \mathbf{I}_{\mathbf{min}}) \cdot \frac{(S - S_{15})}{(S_{75} - S_{15})} + \mathbf{I}_{\mathbf{min}}$$

Current/Sensor relationship

Azzurra dexterous hand (Prensilia srl)

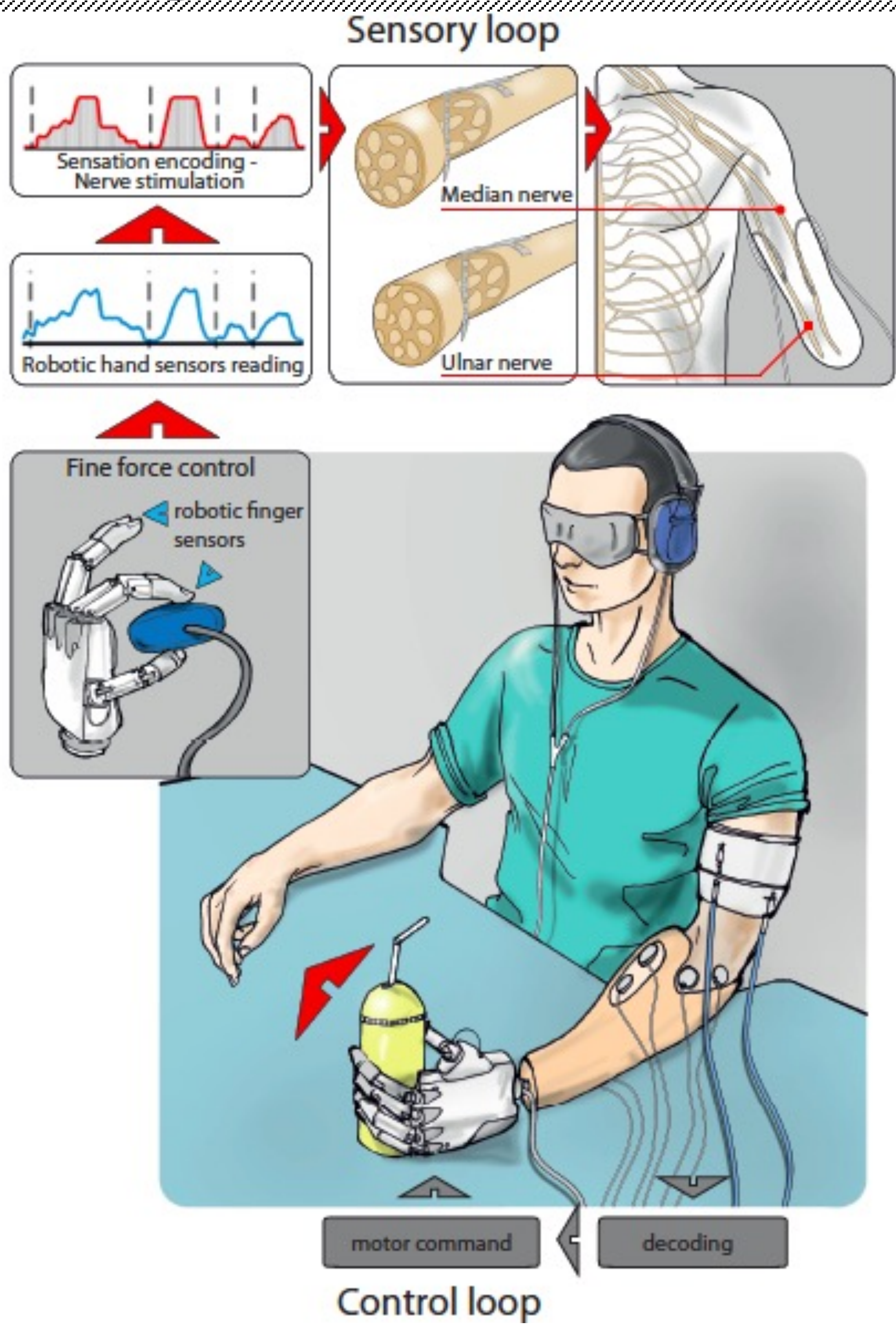

EMG-based control of the hand prosthesis

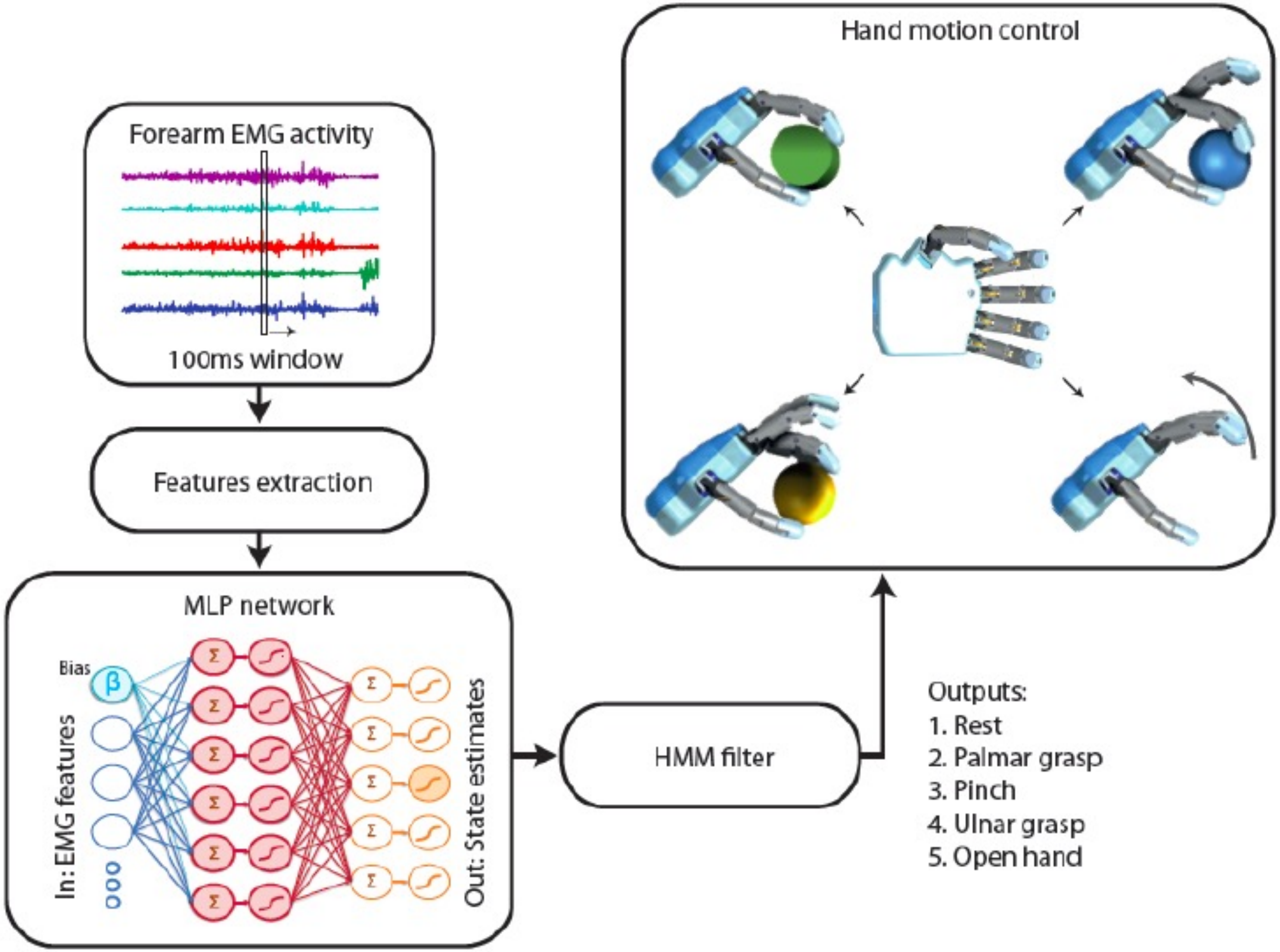

Selection of grasping force levels

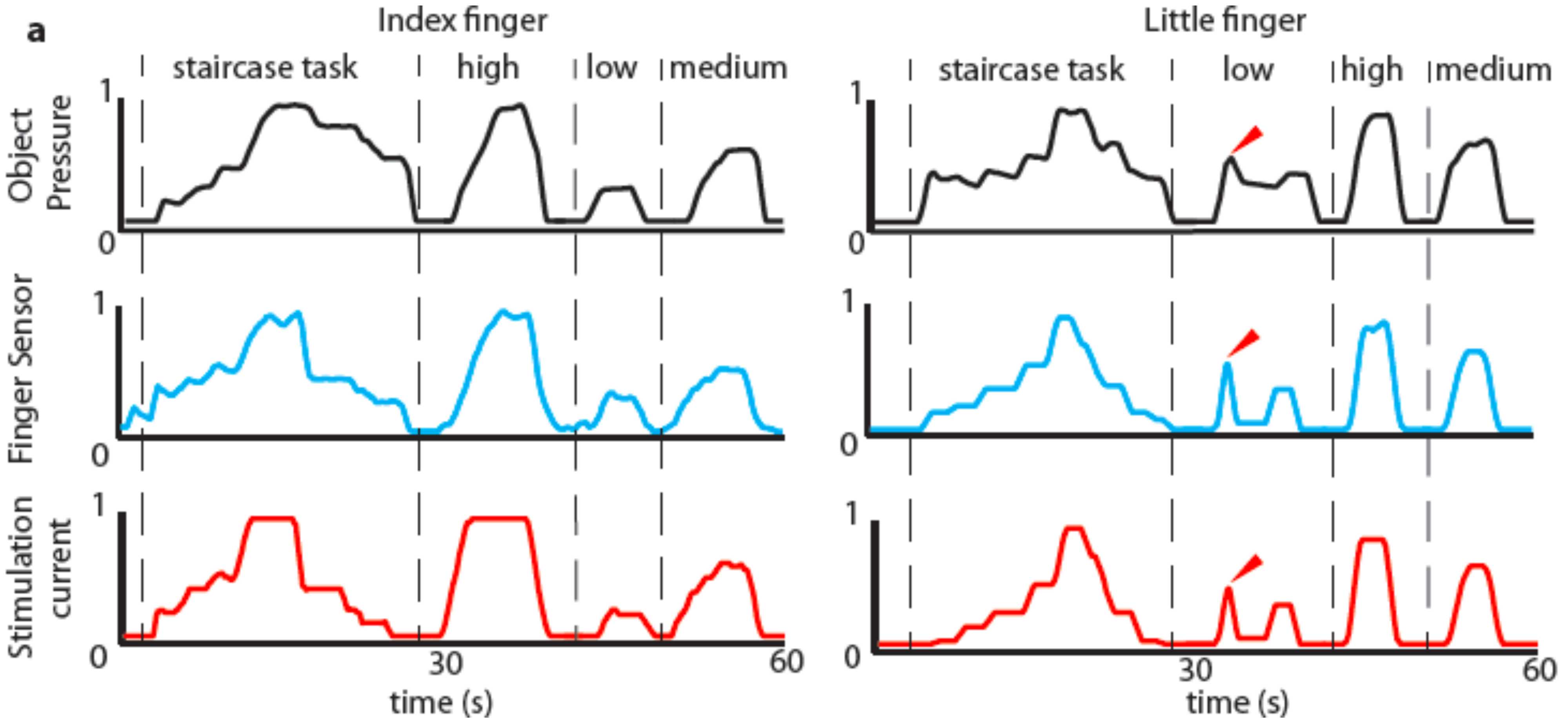

Modulation of grasping force

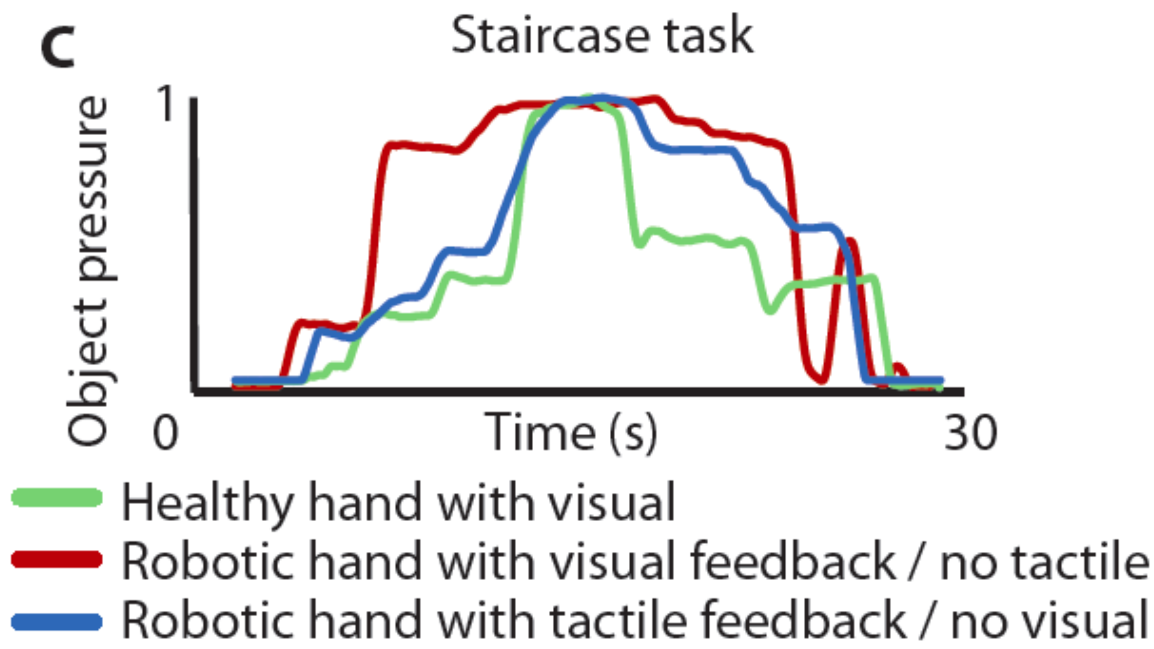

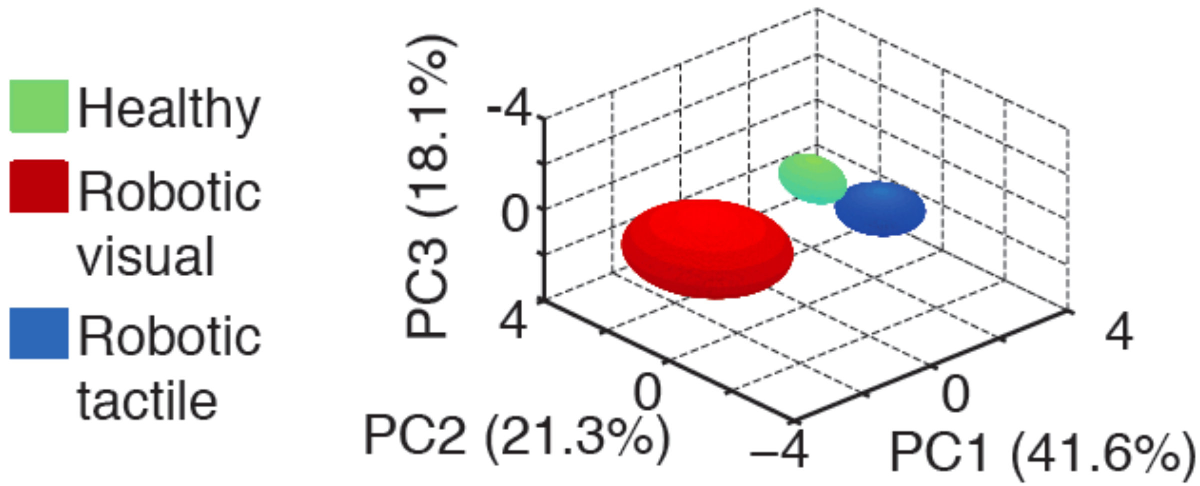

The artificial sensory feedback allowed the user to achieve performance close to the natural ones

Compliance recognition

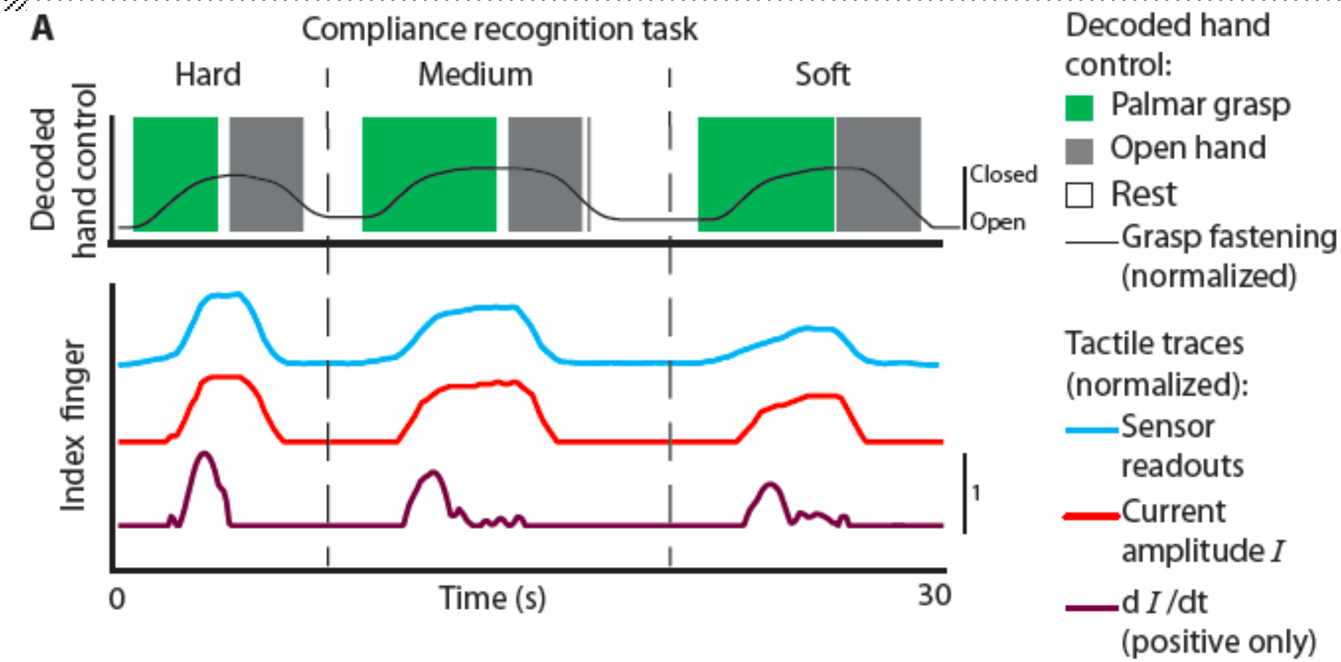

Three objects with different stiffness properties

Quite good performance and interesting learning ability

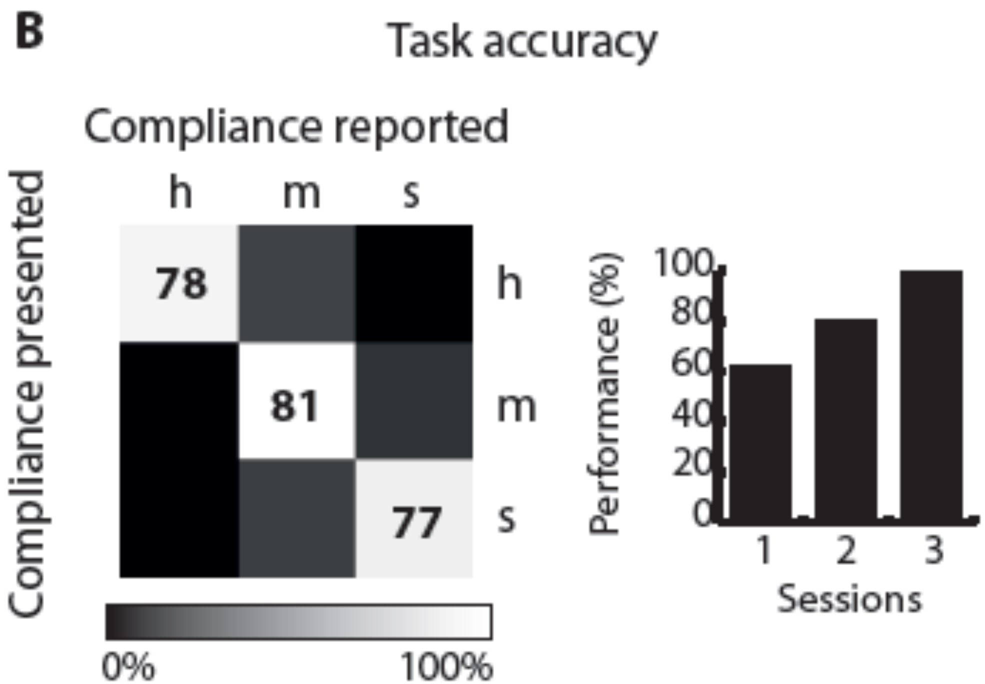

Shape recognition

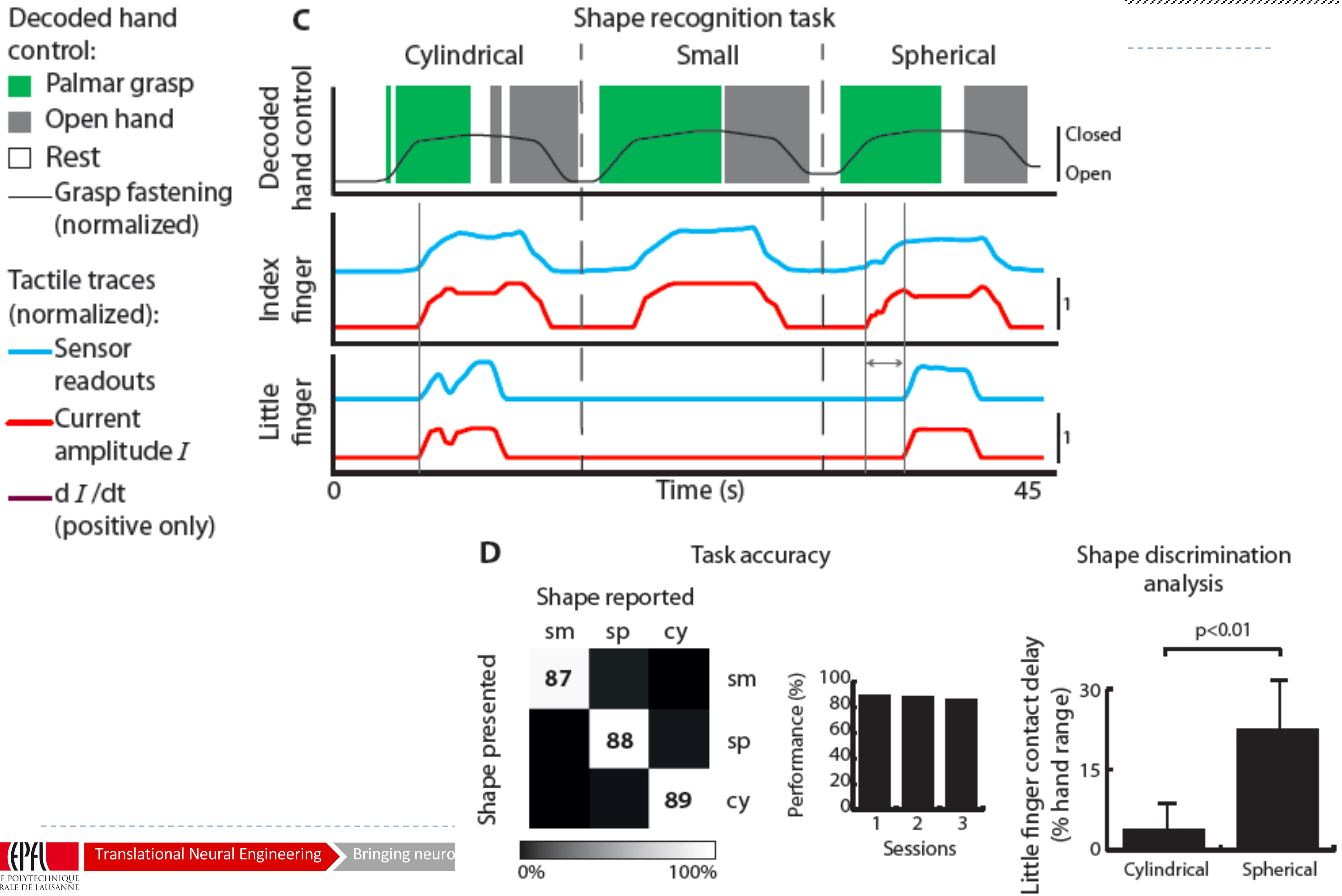

Why this is possible?

Shape recognition

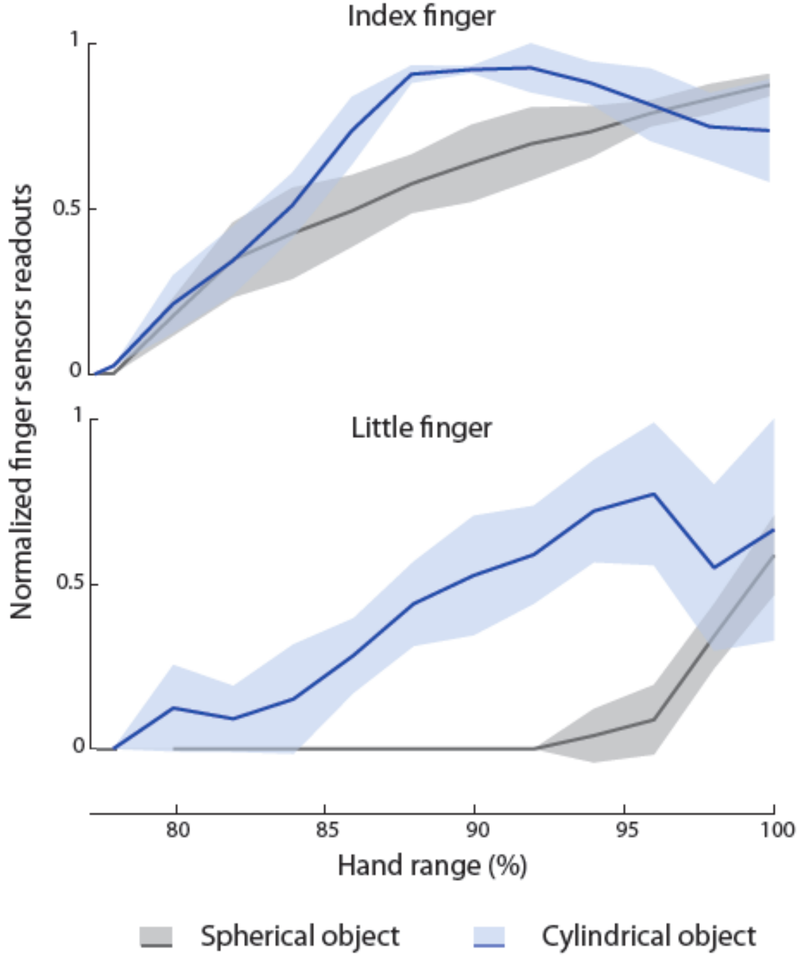

Compliance recognition

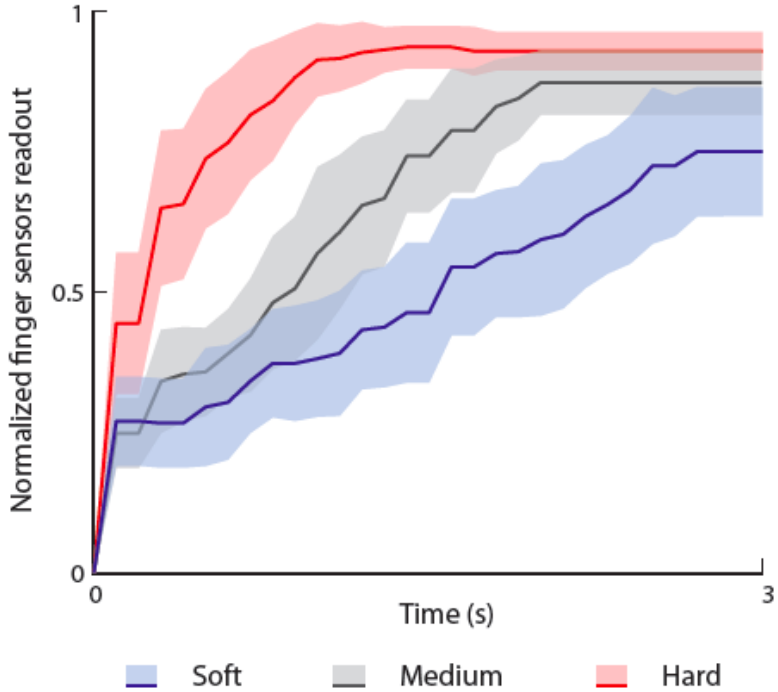

Different force profiles were provided to the users using the afferent stimulation

→ this is **NOT** on-off sensation!

Restoration of proprioception and tactile feedback

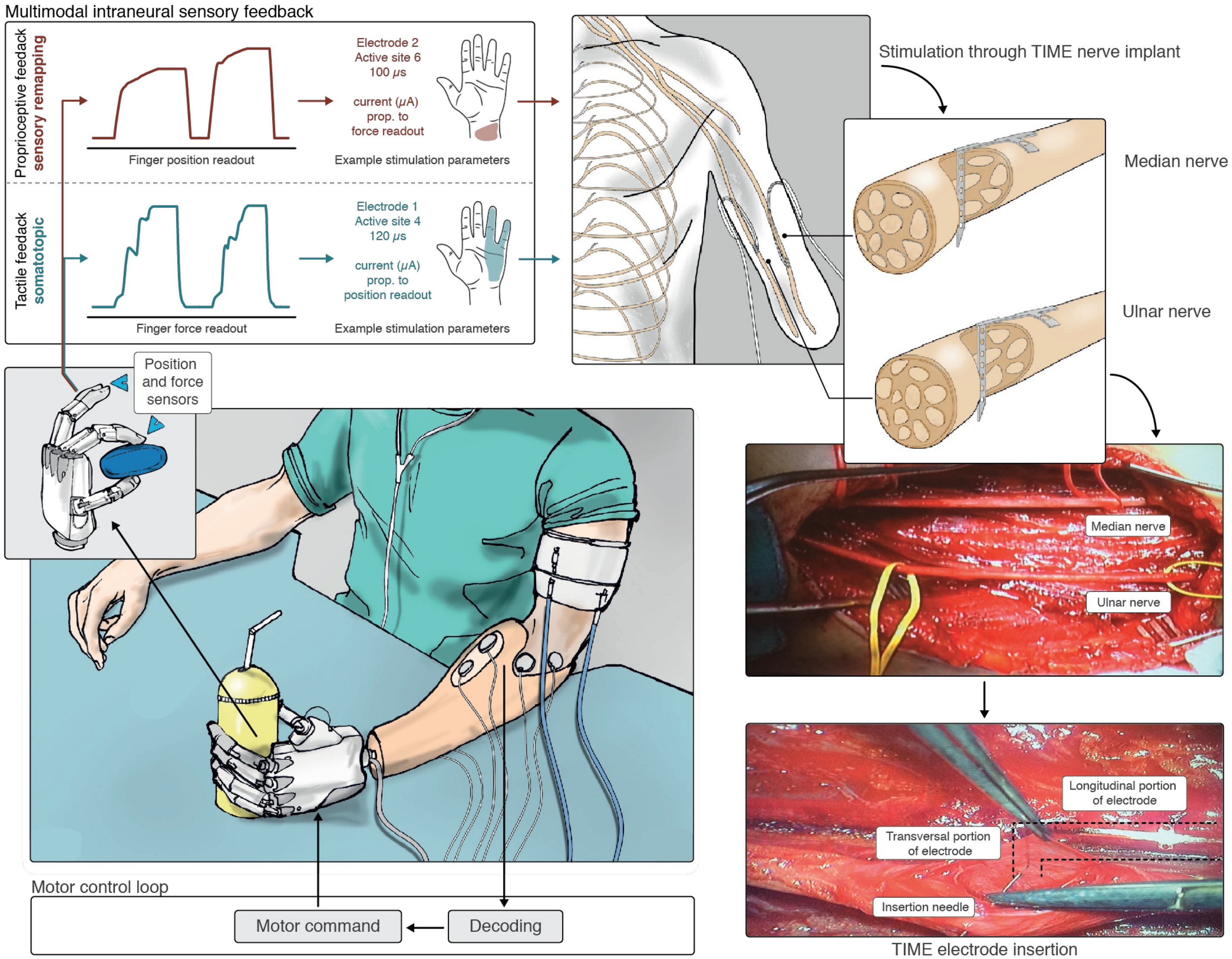

Restoration of proprioception and tactile feedback

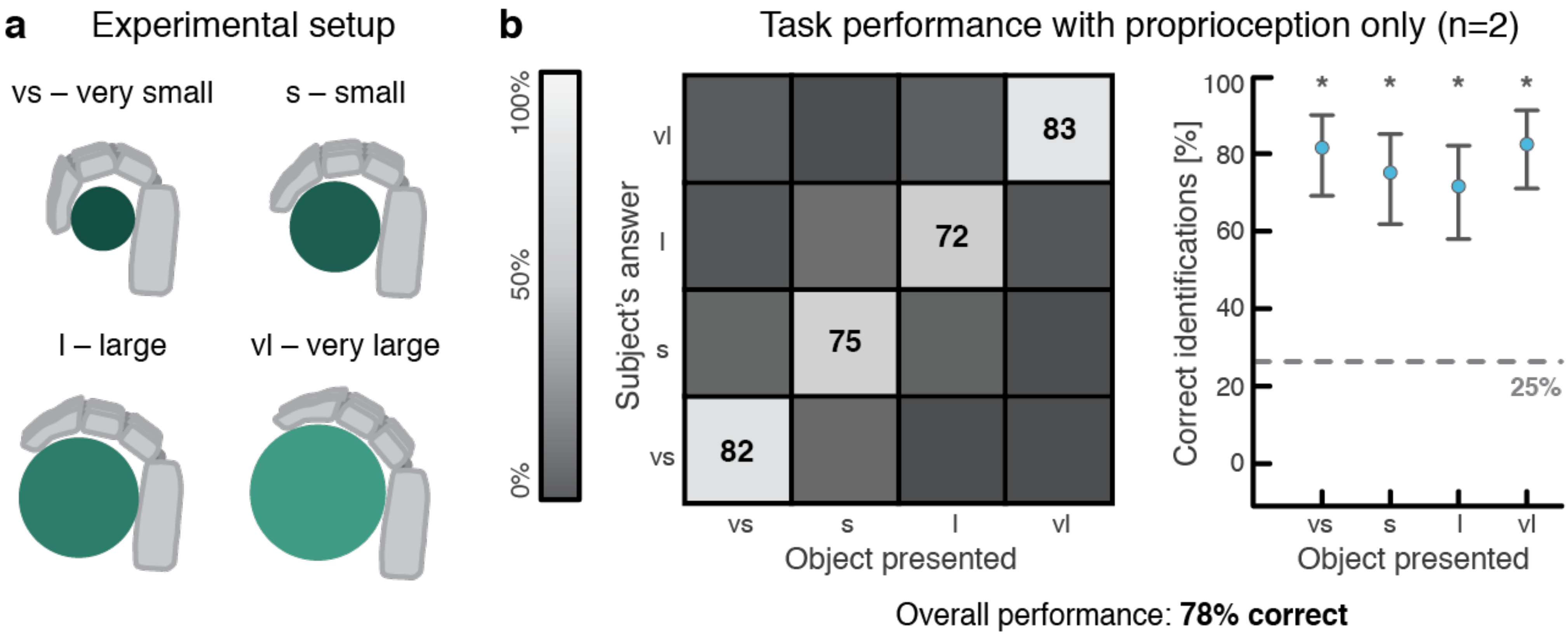

Restoration of proprioception and tactile feedback

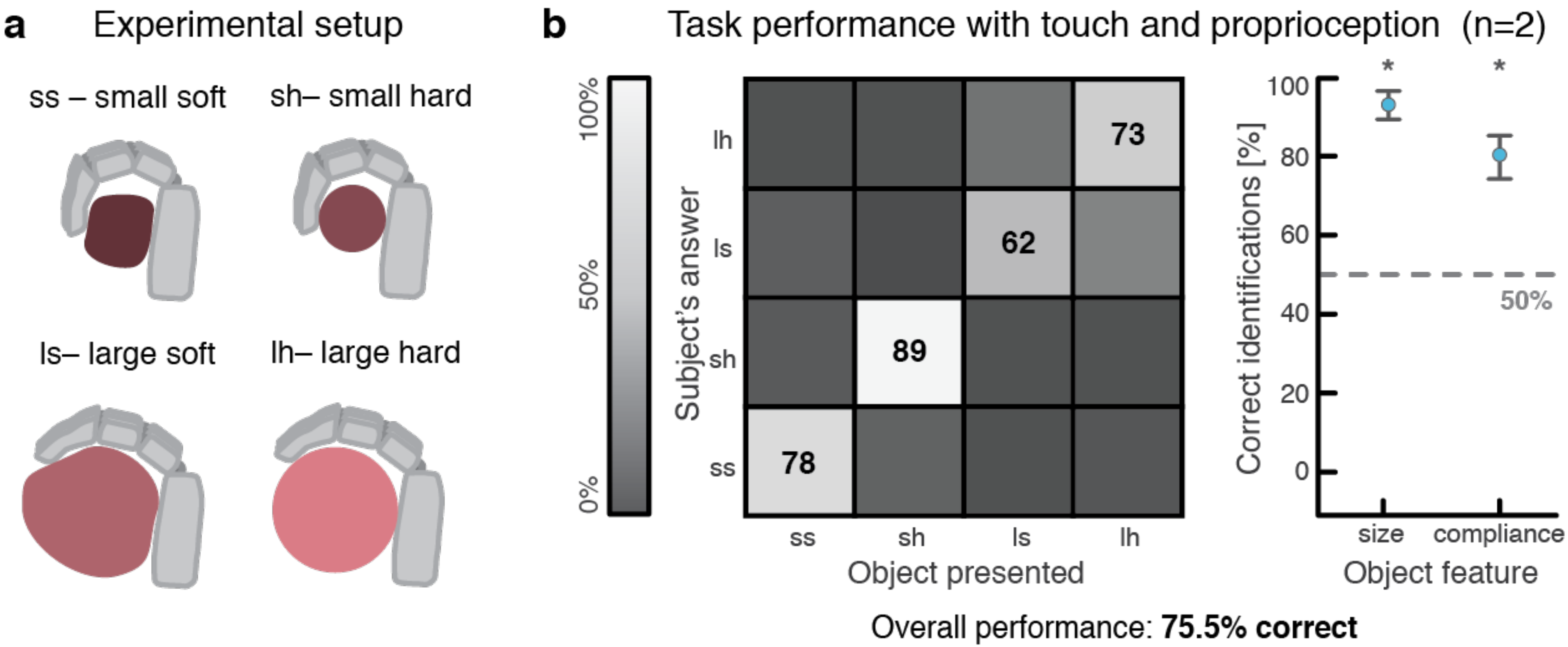

Restoration of proprioception and tactile feedback

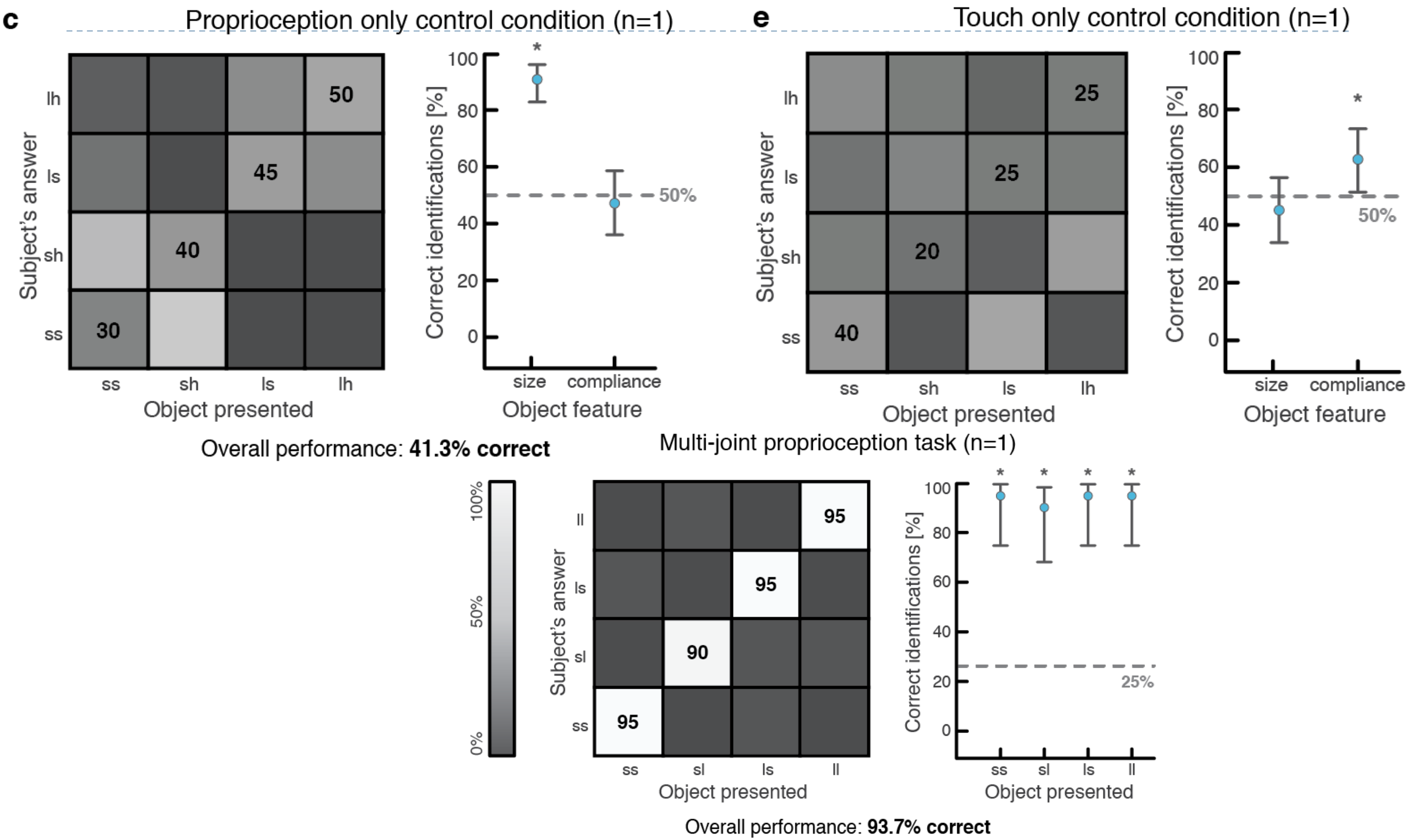

Restoration of proprioception and tactile feedback

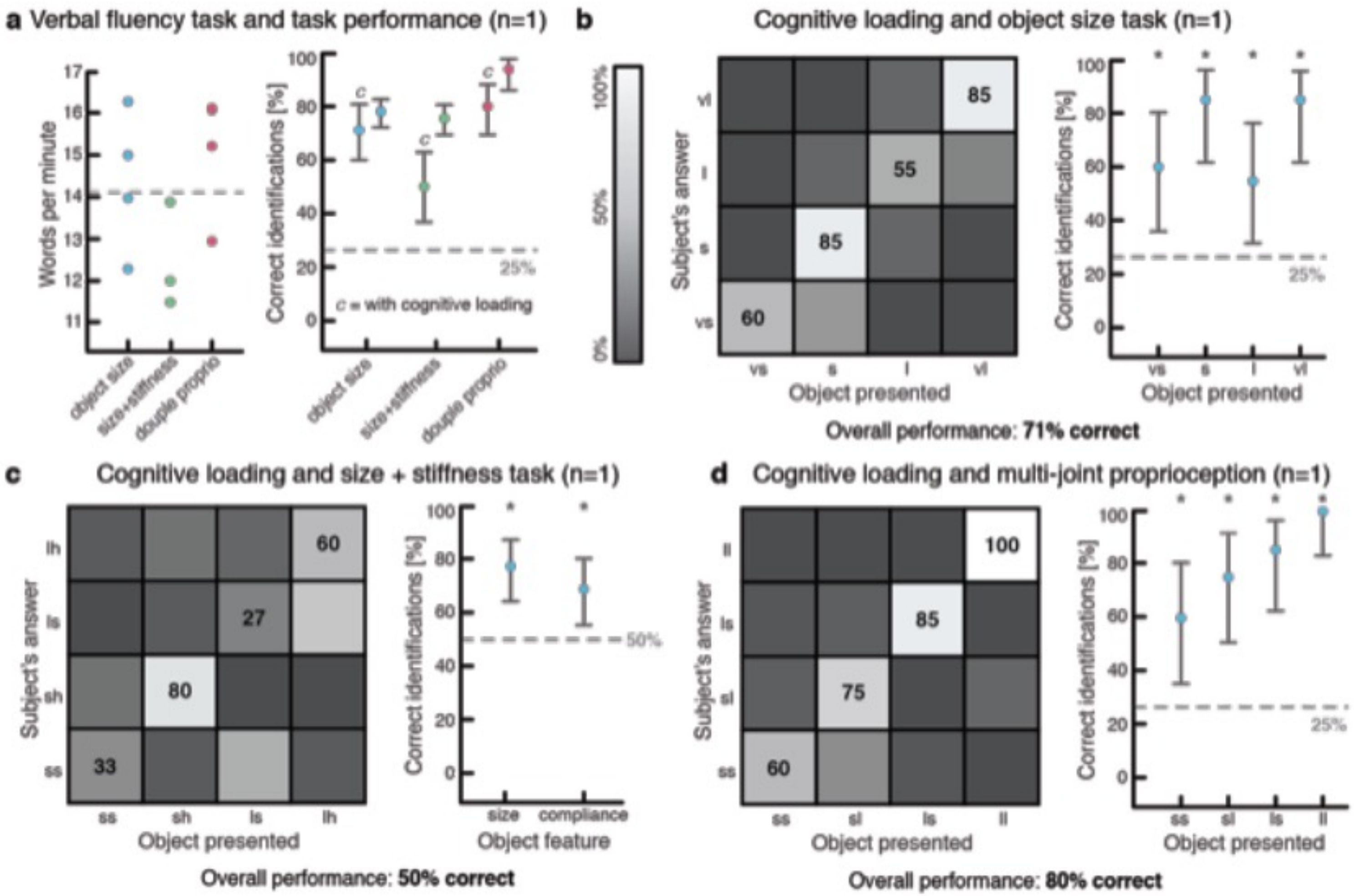

Embodiment

O. Blanke

G. Rognini

Illumination and virtual stimuli as shown on HMD

Neurotactile stimulation

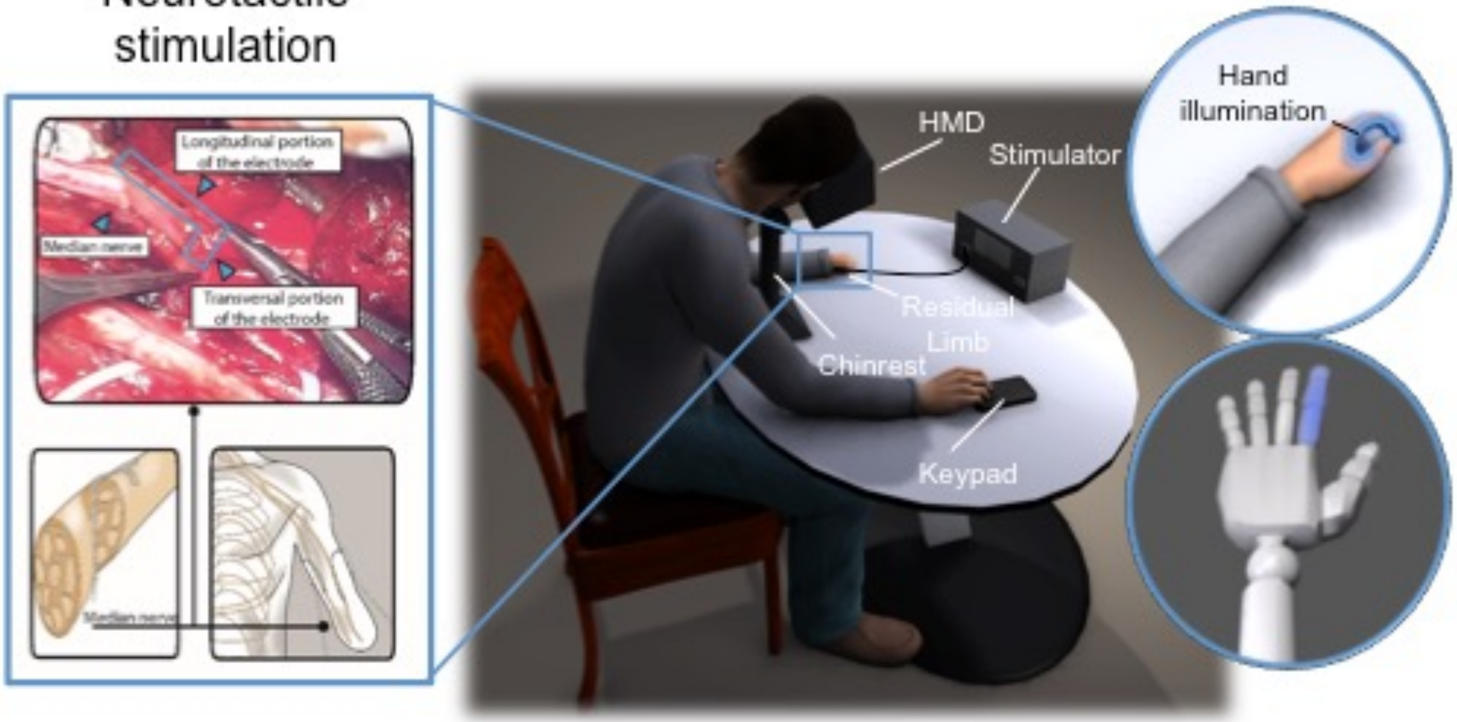

Patient 1 (artificial hand)

Patient 2 (prosthetic hand)

Embodiment

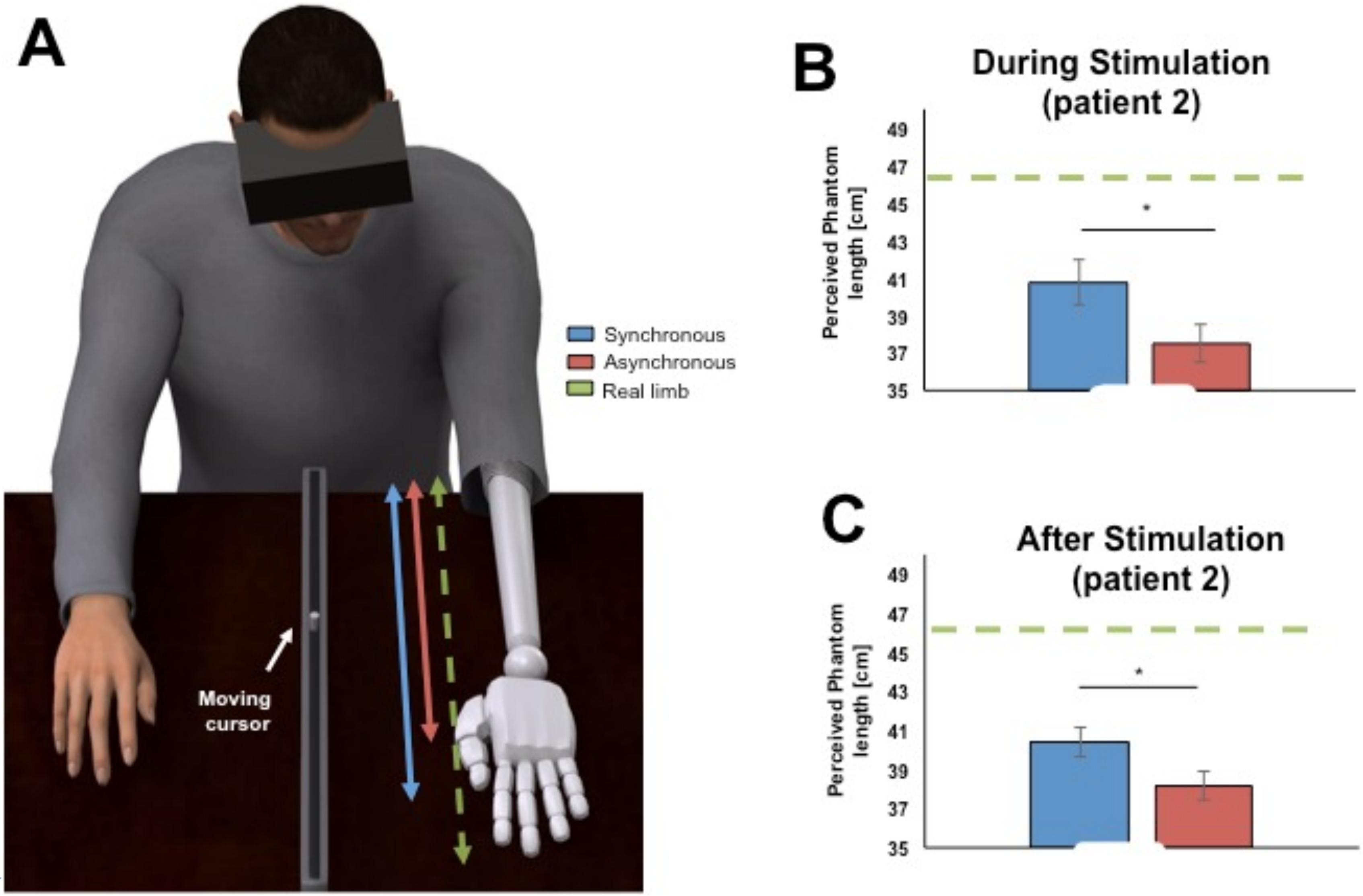

A
Moving cursor
Synchronous
Asynchronous
Real limb
B
During Stimulation (patient 2)
Perceived Phantom length [cm]
49
47
45
43
41
39
37
35
*
C
After Stimulation (patient 2)
Perceived Phantom length [cm]
49
47
45
43
41
39
37
35
*

Biomimetic encoding strategy

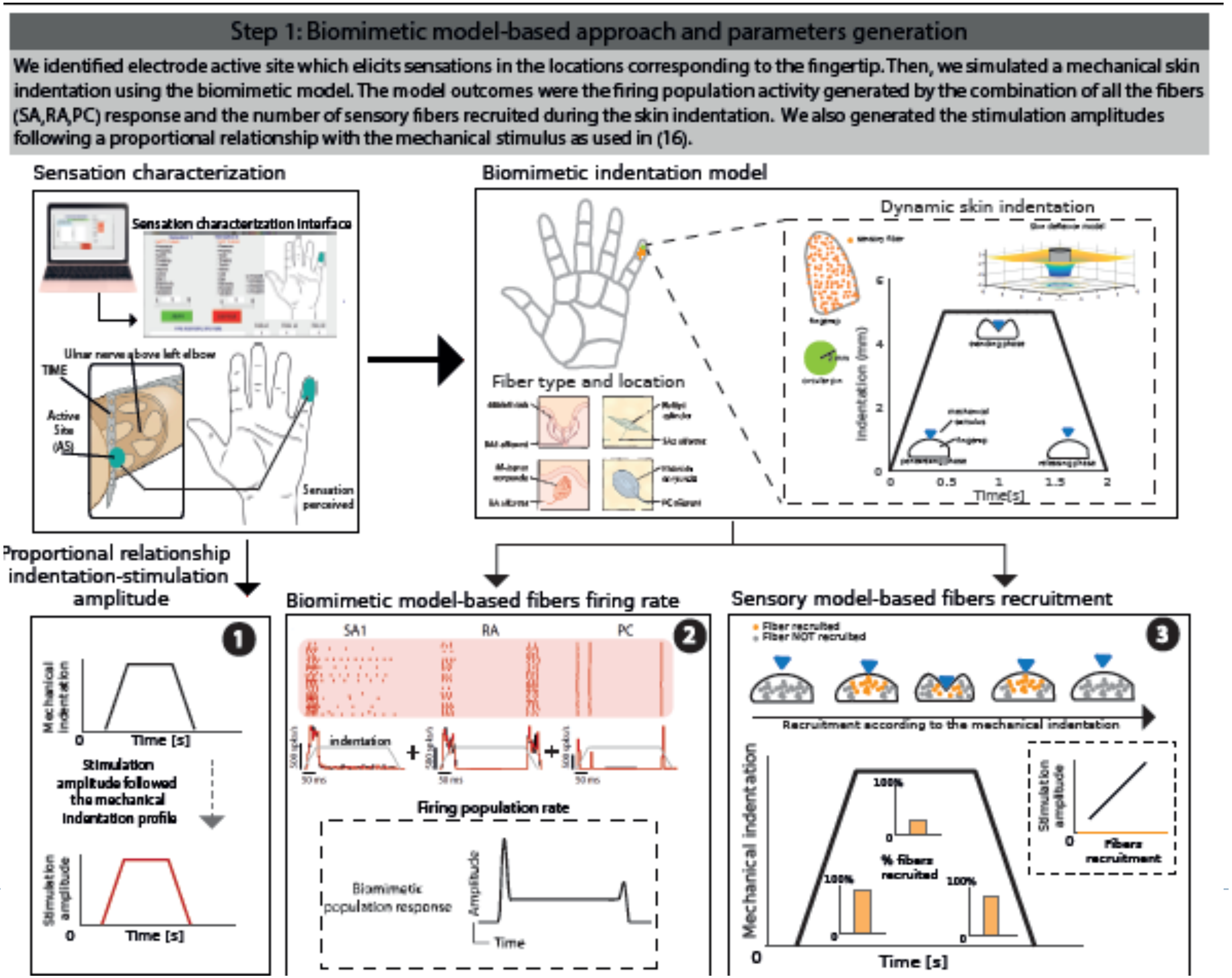

Biomimetic encoding strategy

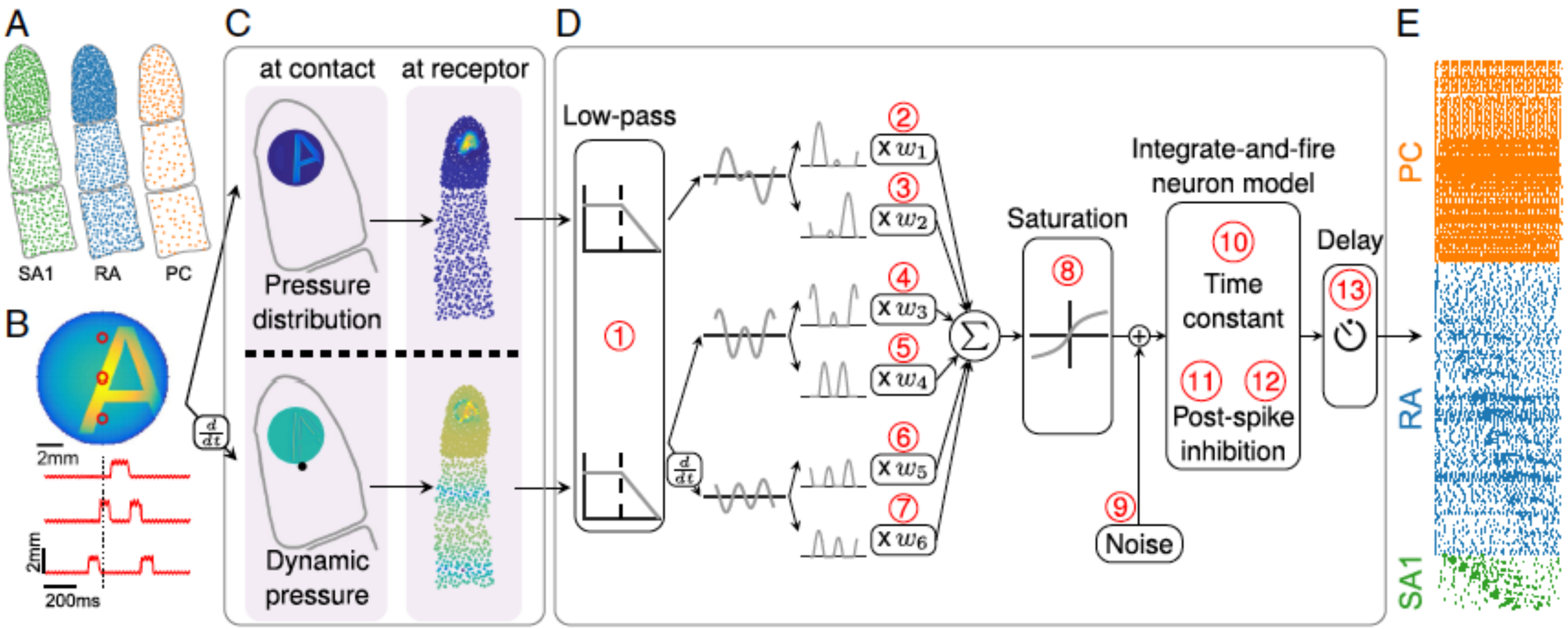

Fig. 1. Overview of the model. (*A*) Receptors are distributed across the skin given the known innervation densities of SA1, RA, and PC afferents. (*B*) The stimulus—in this case, a vibrating embossed letter A scanned across the skin—is defined as the time-varying depth at which each small patch of skin (here dubbed a pin) is indented (with a spatial resolution of 0.1 mm). The traces in *Lower* show the time-varying depth at the three locations on the skin indicated by the red dots in *Upper*. (*C*) The mechanics model relies on two parts: (*Upper*) modeling the distribution of stresses using a quasistatic elastic model and (*Lower*) modeling dynamic pressure and surface wave propagation. *Left* shows the surface deformation of the skin, and *Right* shows the resulting pattern of stresses at the location of the receptors. (*D*) The spiking responses are determined by leaky IF models using different sets of up to 13 parameters (marked in red numbers) for individual SA1, RA, and PC afferents fit based on peripheral recordings to skin vibrations. Adapted from ref. 71. (*E*) The output of the model is the spike train of each afferent in the population. Raster of the response of the afferent population sampled as in *A* to the stimulus shown in *B* (only active afferents are included). Note that the SA1s (in contact) only encode the spatial aspect of the stimulus, that the PCs encode from the whole finger phase-lock with the 200-Hz vibration, and that the RAs show mixed spatial and vibration responses.

Biomimetic encoding strategy

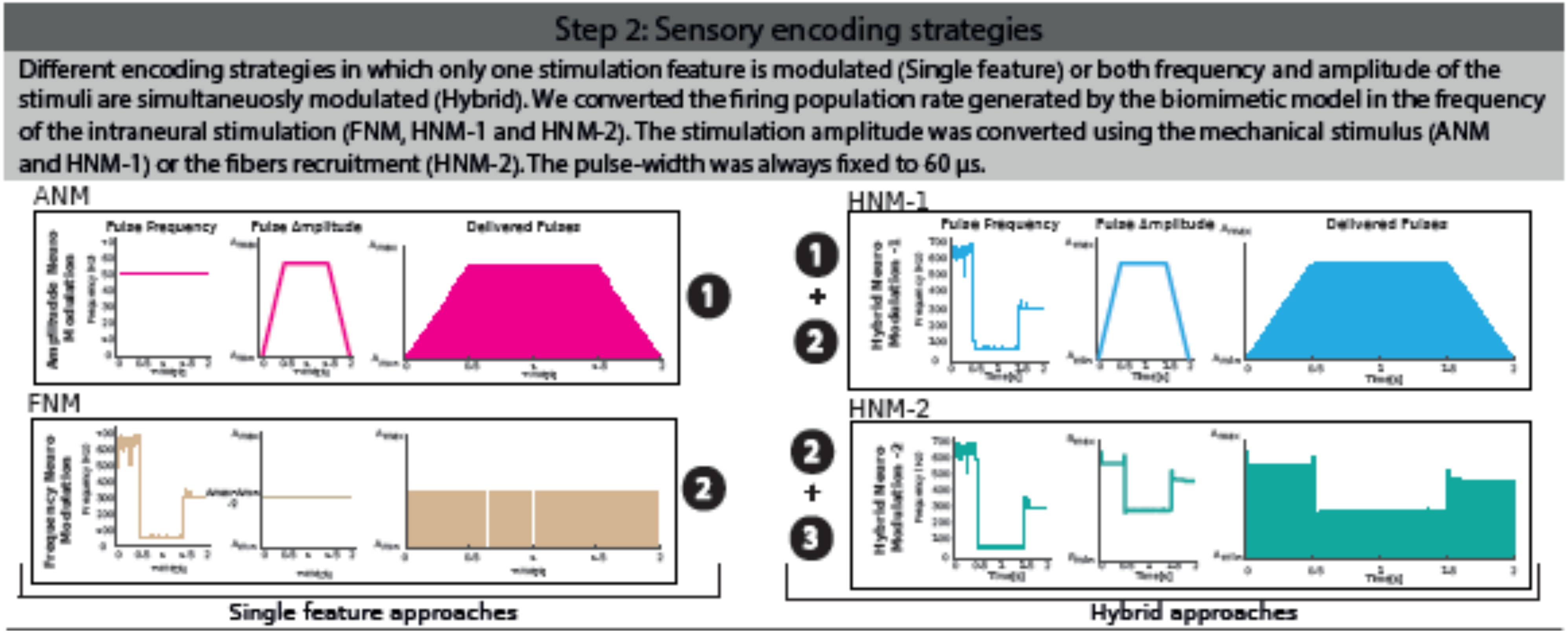

Biomimetic encoding strategy

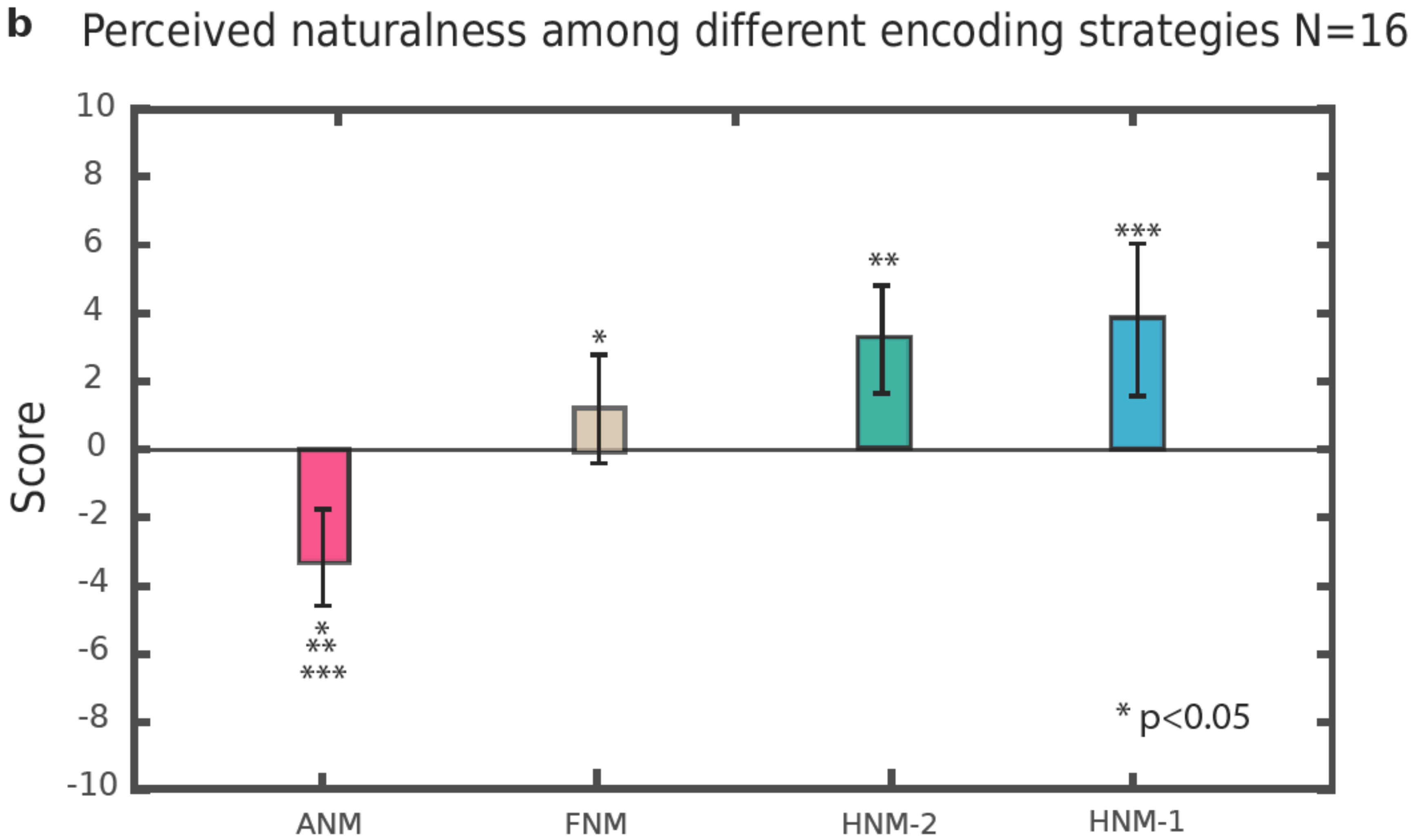

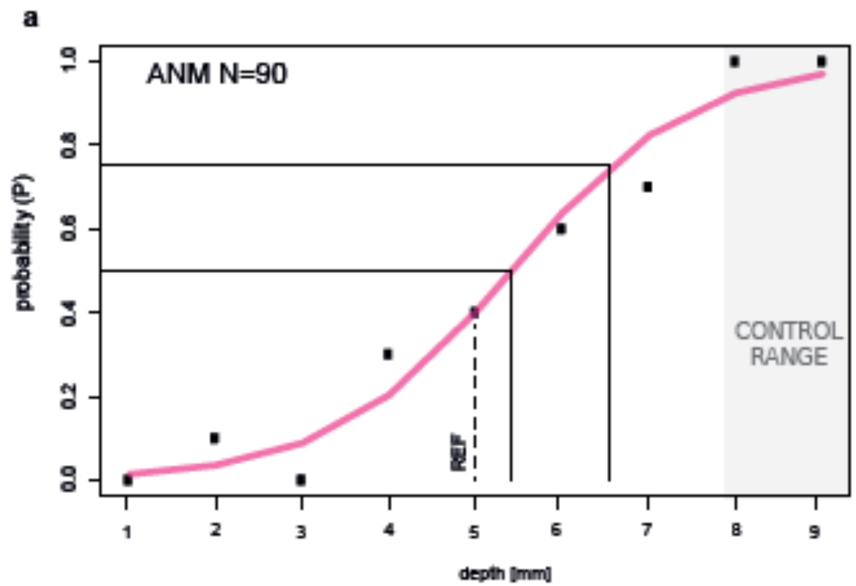

Point of Subjective Equality (PSE): **5.51** mm

Just-Noticeable Difference (JND): **1.01** mm

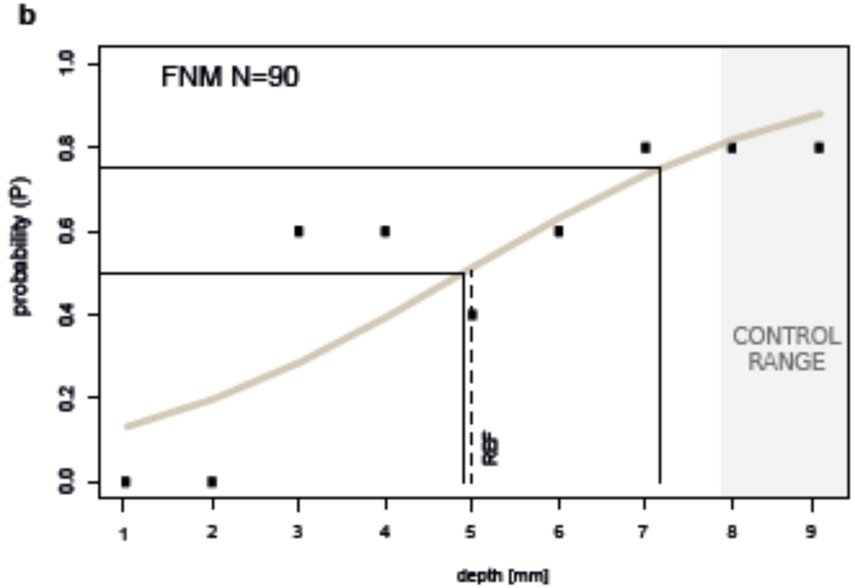

Point of Subjective Equality (PSE): **4.87** mm

Just-Noticeable Difference (JND): **2.26** mm

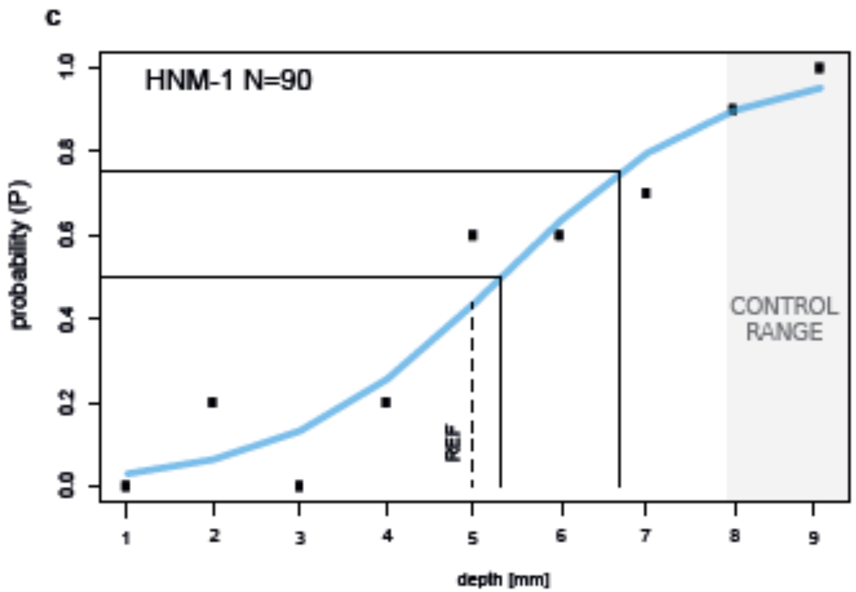

Point of Subjective Equality (PSE): **5.31** mm

Just-Noticeable Difference (JND): **1.35** mm

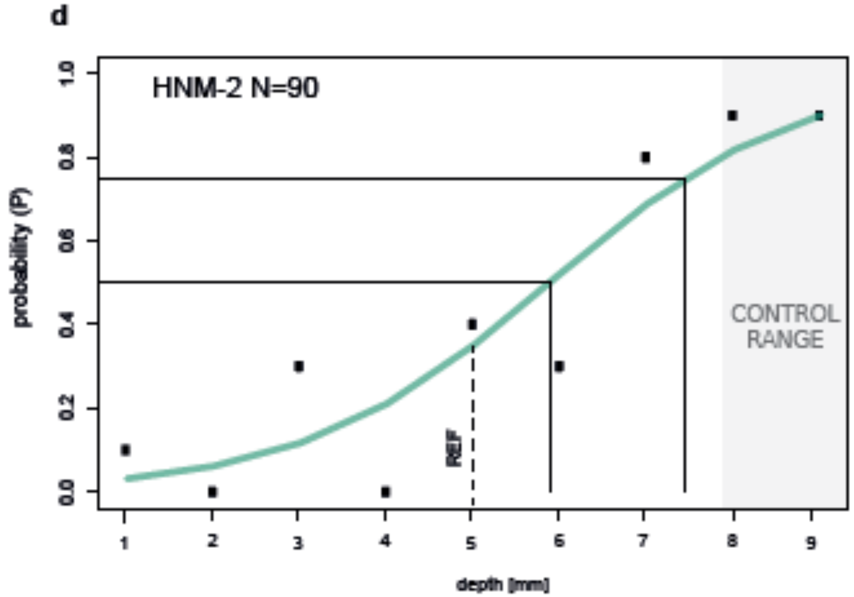

Point of Subjective Equality (PSE): **5.87** mm

Just-Noticeable Difference (JND): **1.55** mm

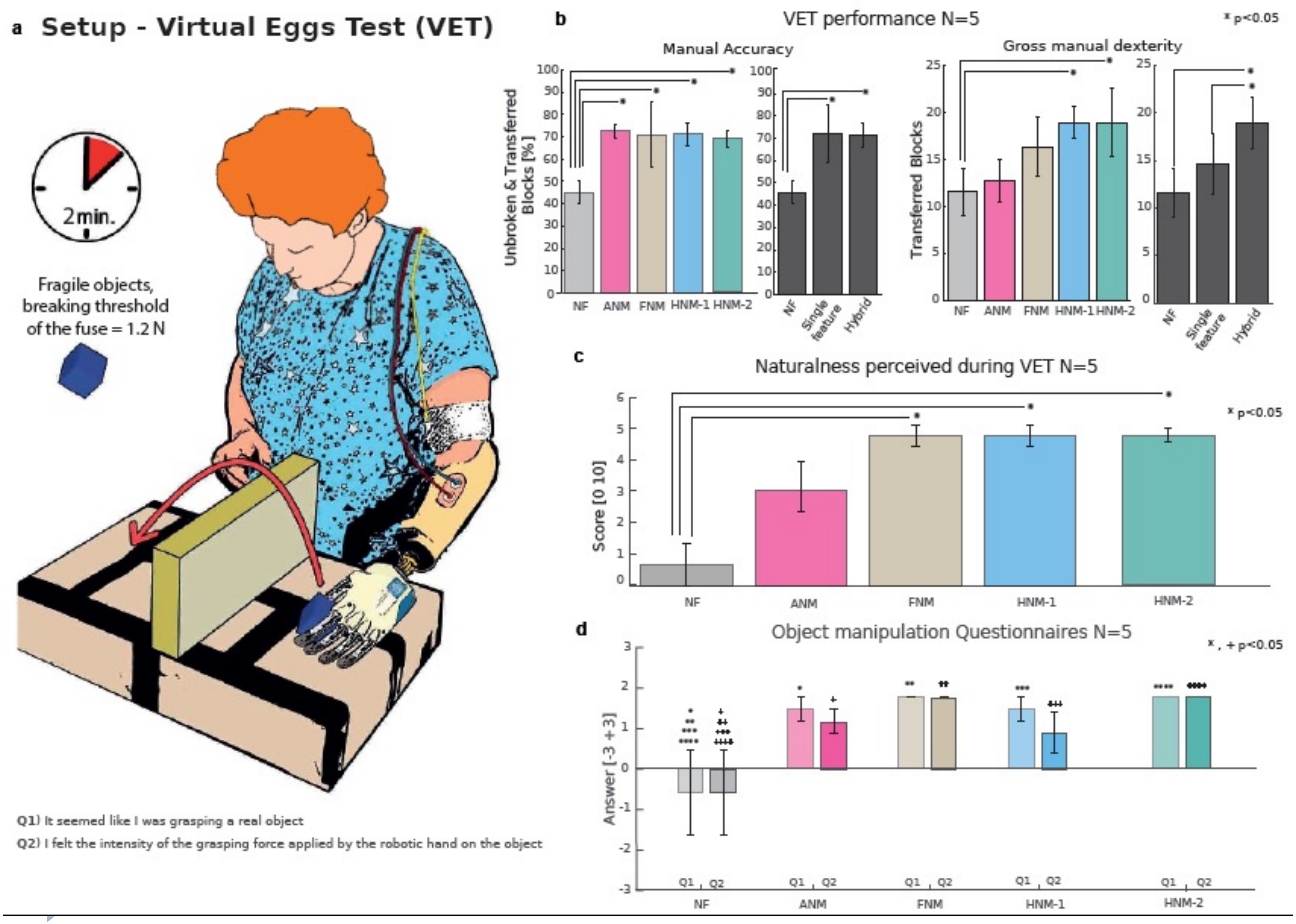

a Setup - Virtual Eggs Test (VET)
2min.
Fragile objects, breaking threshold of the fuse = 1.2 N
Q1) It seemed like I was grasping a real object
Q2) I felt the intensity of the grasping force applied by the robotic hand on the object
b
VET performance N=5
* p<0.05
Manual Accuracy
Unbroken & Transferred Blocks [%]
NF ANM FNM HNM-1 HNM-2
NF Single feature Hybrid
Gross manual dexterity
Transferred Blocks
c
Naturalness perceived during VET N=5
Score [0 10]
d
Object manipulation Questionnaires N=5
*, + p<0.05
Answer [-3 +3]
Q1 Q2

Biomimetic encoding strategy

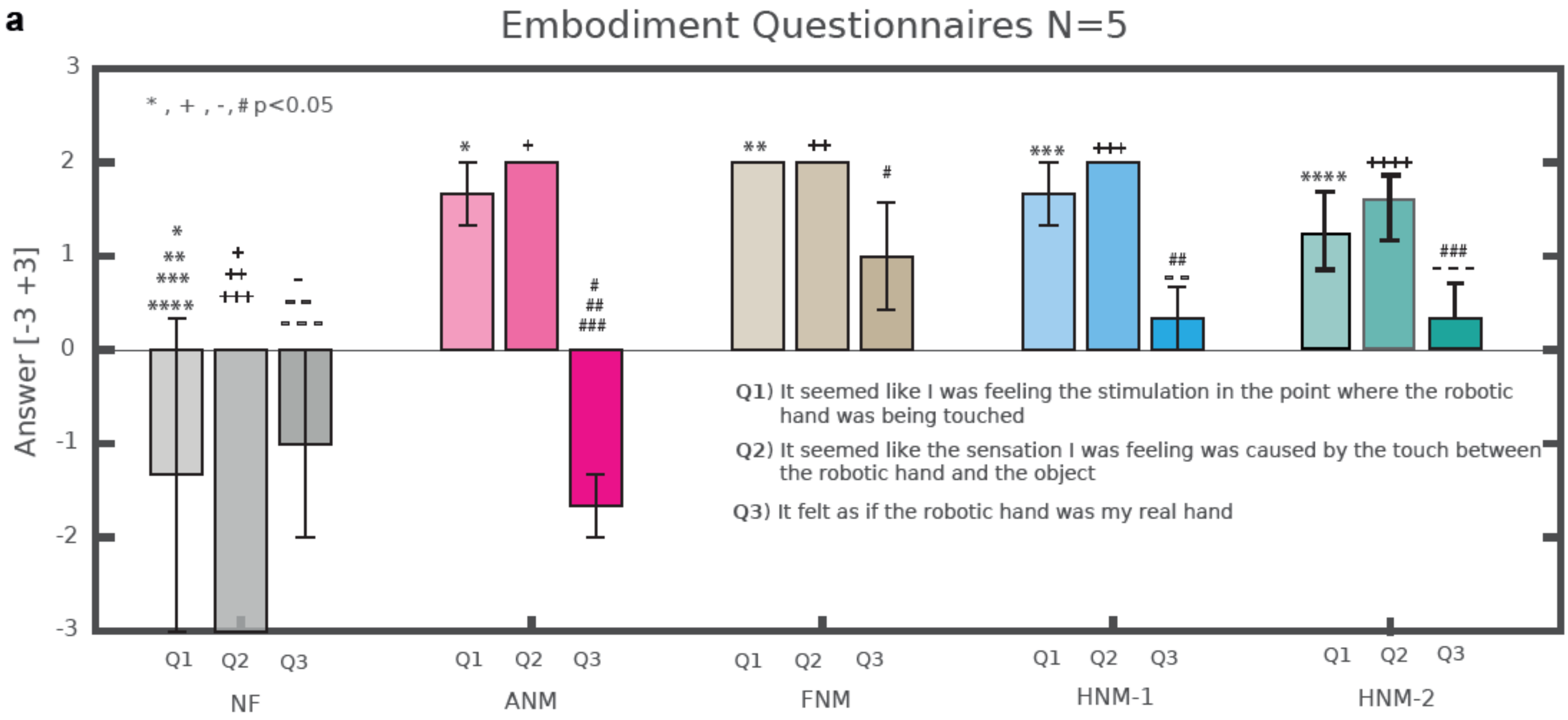

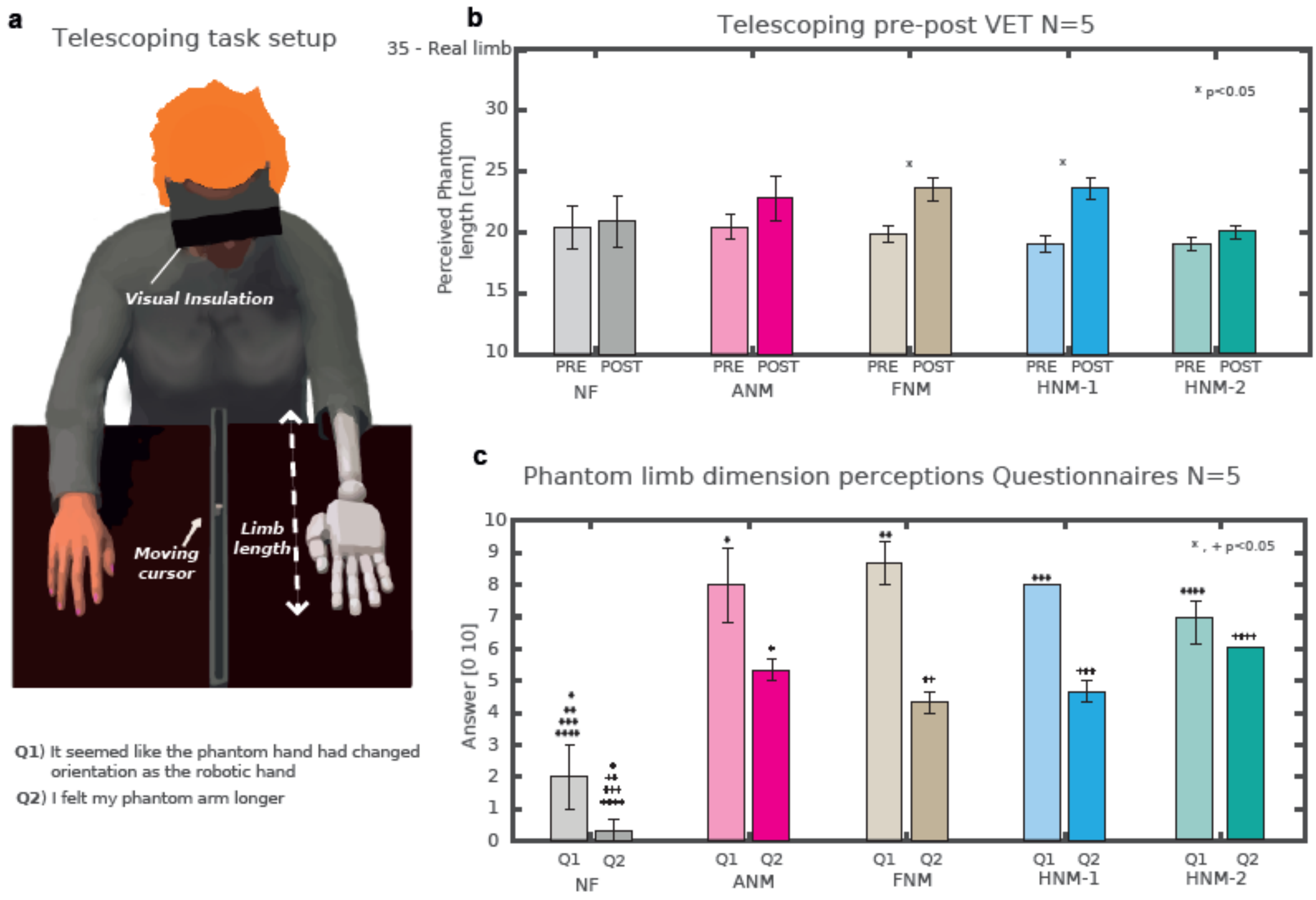
a
Telescoping task setup
Visual Insulation
Moving cursor
Limb length
Q1) It seemed like the phantom hand had changed orientation as the robotic hand
Q2) I felt my phantom arm longer
b
Telescoping pre-post VET N=5
35 - Real limb
Perceived Phantom length [cm]
x p<0.05
PRE POST
NF
ANM
FNM
HNM-1
HNM-2
c
Phantom limb dimension perceptions Questionnaires N=5
Answer [0 10]
x , + p<0.05
Q1 Q2
NF
ANM
FNM
HNM-1
HNM-2

Restoring perception of real textures

C. Oddo

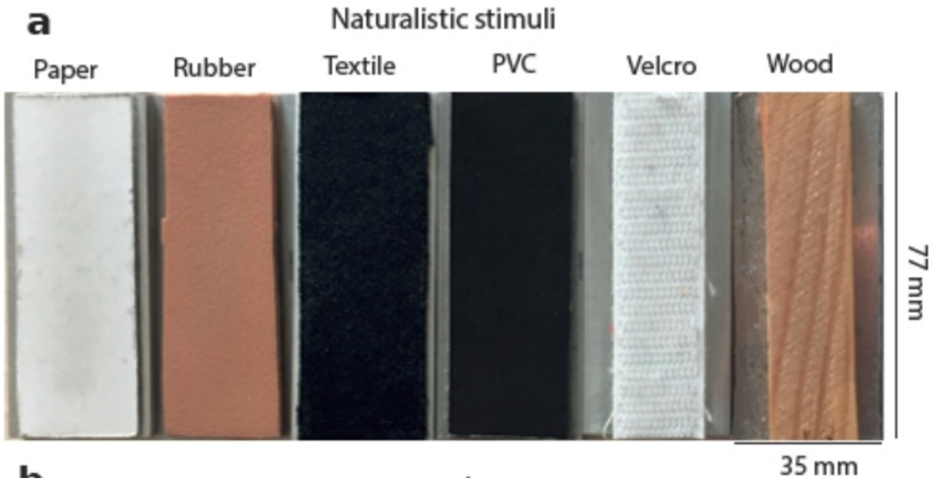

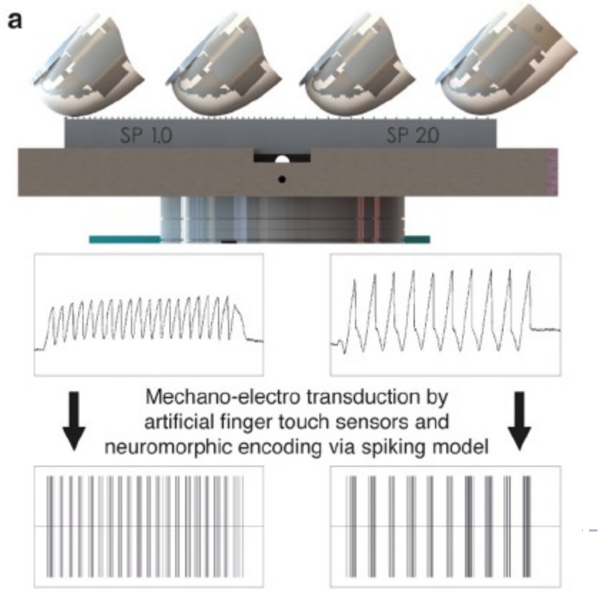

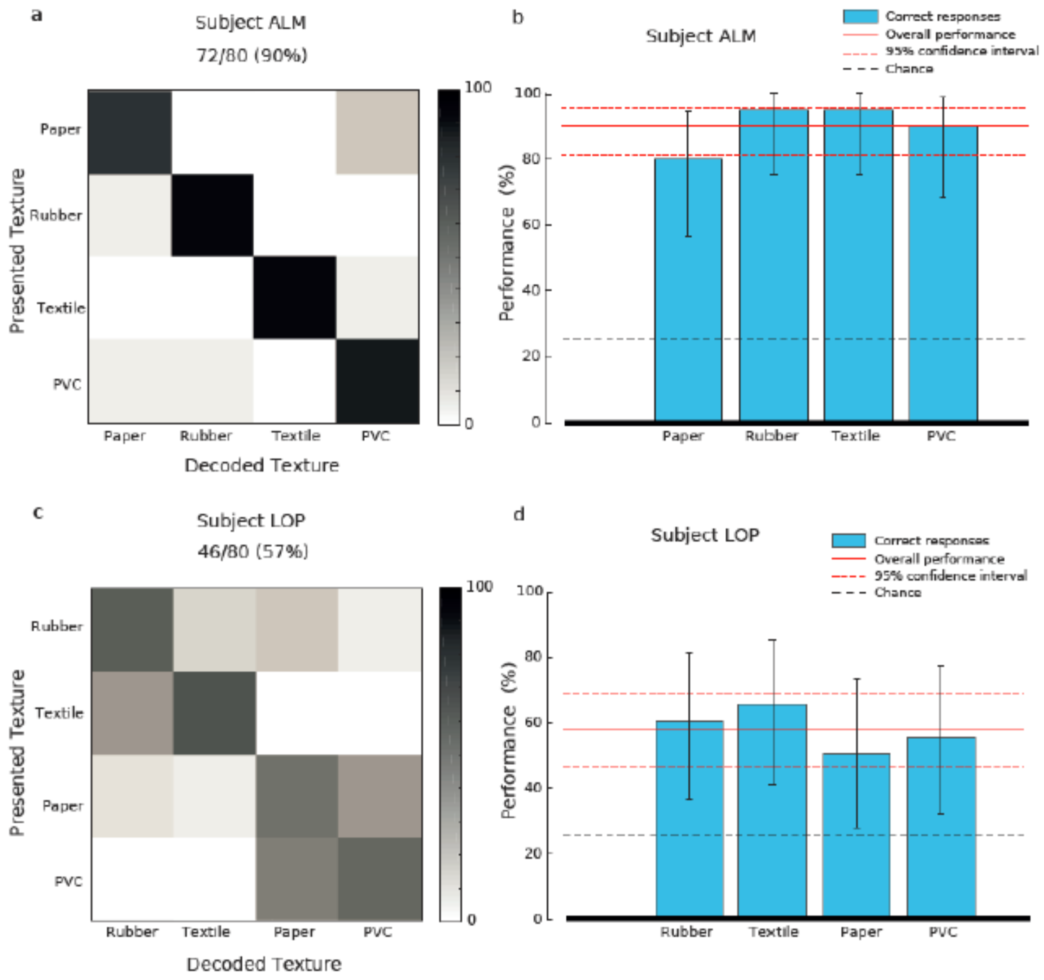

Restoring perception of real textures

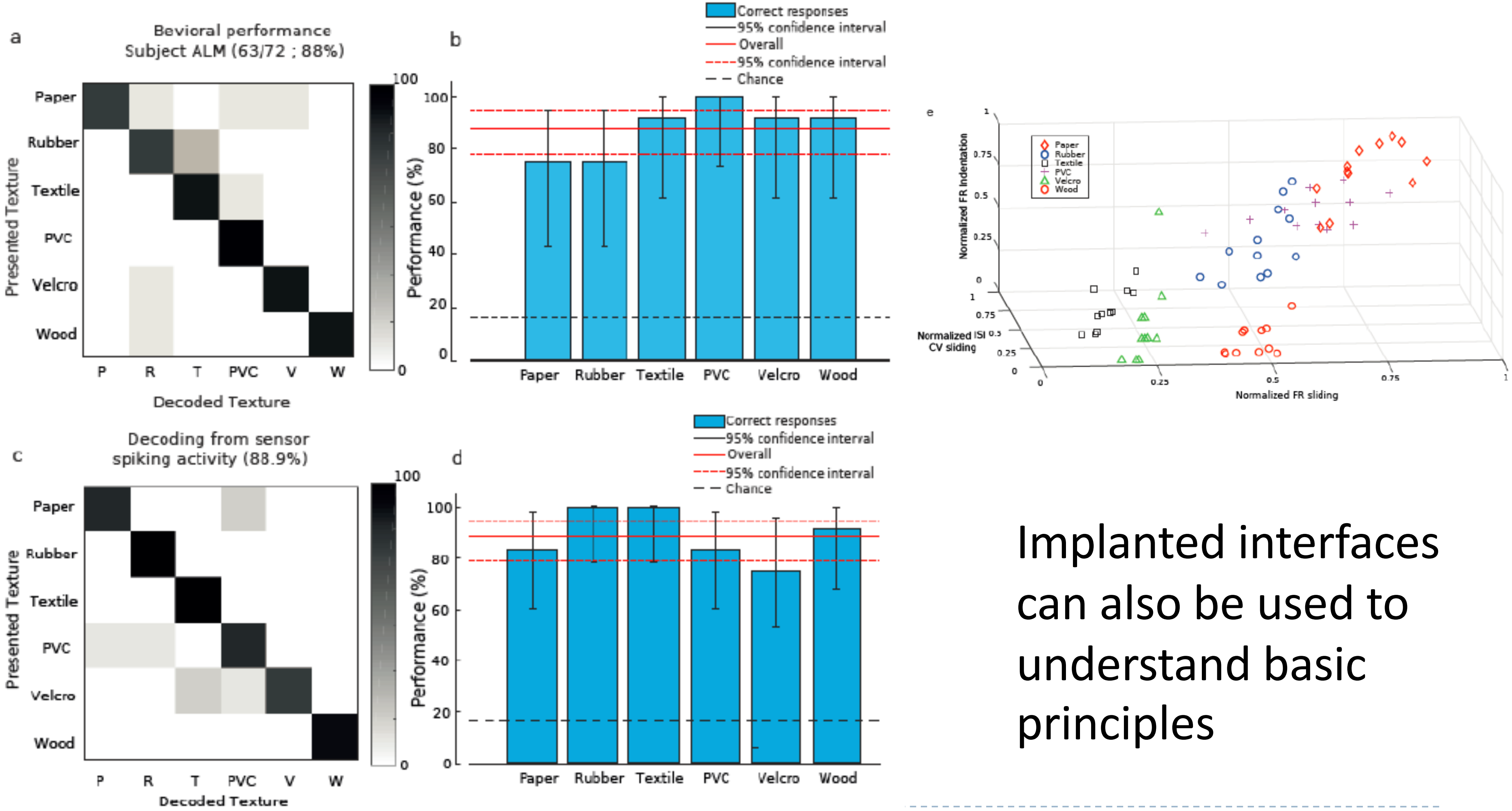

Implanted interfaces can also be used to understand basic principles

Effects of cognitive load

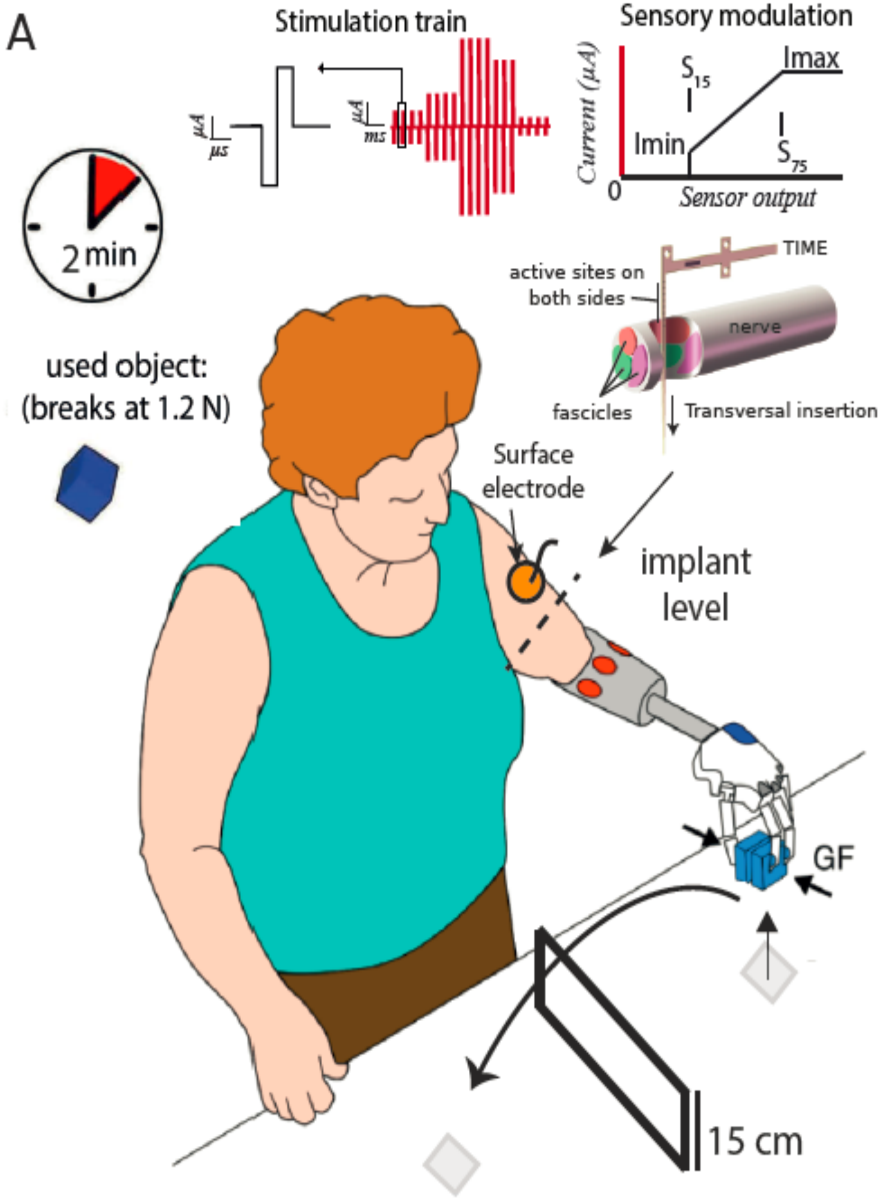

B

Induced sensations & stimulation parameters

Intraneural sensory Feedback (IF)

sensation type	vibration
sensation intensity	$S_{min} = 1$, $S_{max} = 8$
electrode position	proximal part of ulnar nerve above elbow
amplitude	$A_{min} = 200$ μA, $A_{max} = 300$ μA
pulse-width	80 μs
frequency	50 Hz

Superficial sensory Feedback (SF)

sensation type	electricity
sensation intensity	$S_{min} = 1$, $S_{max} = 8$
electrode position	on the skin of the left arm
amplitude	$A_{min} = 100$ μA, $A_{max} = 500$ μA
pulse-width	200 μs
frequency	50 Hz

Effects of cognitive load